



**Calhoun: The NPS Institutional Archive**  
**DSpace Repository**

---

Theses and Dissertations

1. Thesis and Dissertation Collection, all items

---

2018-12

**BIOPHOTON EMISSION FROM PLANTS: A  
CONTRIBUTION TO THE UNDERSTANDING OF  
PLANT SIGNALING**

Oros, Carl L.

Monterey, CA; Naval Postgraduate School

---

<http://hdl.handle.net/10945/61235>

---

This publication is a work of the U.S. Government as defined in Title 17, United States Code, Section 101. Copyright protection is not available for this work in the United States.

*Downloaded from NPS Archive: Calhoun*



Calhoun is the Naval Postgraduate School's public access digital repository for research materials and institutional publications created by the NPS community. Calhoun is named for Professor of Mathematics Guy K. Calhoun, NPS's first appointed -- and published -- scholarly author.

**Dudley Knox Library / Naval Postgraduate School**  
**411 Dyer Road / 1 University Circle**  
**Monterey, California USA 93943**

<http://www.nps.edu/library>



**NAVAL  
POSTGRADUATE  
SCHOOL**

**MONTEREY, CALIFORNIA**

**DISSERTATION**

**BIOPHOTON EMISSION FROM PLANTS:  
A CONTRIBUTION TO THE UNDERSTANDING OF  
PLANT SIGNALING**

by

Carl L. Oros

December 2018

Dissertation Supervisors:

Dan C. Boger  
Gamani Karunasiri

**Approved for public release. Distribution is unlimited.**

THIS PAGE INTENTIONALLY LEFT BLANK

<b>REPORT DOCUMENTATION PAGE</b>			<i>Form Approved OMB No. 0704-0188</i>	
Public reporting burden for this collection of information is estimated to average 1 hour per response, including the time for reviewing instruction, searching existing data sources, gathering and maintaining the data needed, and completing and reviewing the collection of information. Send comments regarding this burden estimate or any other aspect of this collection of information, including suggestions for reducing this burden, to Washington headquarters Services, Directorate for Information Operations and Reports, 1215 Jefferson Davis Highway, Suite 1204, Arlington, VA 22202-4302, and to the Office of Management and Budget, Paperwork Reduction Project (0704-0188) Washington, DC 20503.				
<b>1. AGENCY USE ONLY (Leave blank)</b>		<b>2. REPORT DATE</b> December 2018	<b>3. REPORT TYPE AND DATES COVERED</b> Dissertation	
<b>4. TITLE AND SUBTITLE</b> BIOPHOTON EMISSION FROM PLANTS: A CONTRIBUTION TO THE UNDERSTANDING OF PLANT SIGNALING			<b>5. FUNDING NUMBERS</b>	
<b>6. AUTHOR(S)</b> Carl L. Oros				
<b>7. PERFORMING ORGANIZATION NAME(S) AND ADDRESS(ES)</b> Naval Postgraduate School Monterey, CA 93943-5000			<b>8. PERFORMING ORGANIZATION REPORT NUMBER</b>	
<b>9. SPONSORING / MONITORING AGENCY NAME(S) AND ADDRESS(ES)</b> N/A			<b>10. SPONSORING / MONITORING AGENCY REPORT NUMBER</b>	
<b>11. SUPPLEMENTARY NOTES</b> The views expressed in this thesis are those of the author and do not reflect the official policy or position of the Department of Defense or the U.S. Government.				
<b>12a. DISTRIBUTION / AVAILABILITY STATEMENT</b> Approved for public release. Distribution is unlimited.			<b>12b. DISTRIBUTION CODE</b> A	
<b>13. ABSTRACT (maximum 200 words)</b> The intriguing discovery that all living systems continuously emit endogenous, ultraweak photons has inspired numerous researchers to consider the information-bearing potential of biological photons as carriers of inter- and intracellular communication. In 1923, Alexander Gurwitsch first observed that a "morphogenetic field" in the form of ultraviolet light was involved in the regulation of plant cellular division. Over the last half century, the development of increasingly more sensitive photon detection technologies has revealed that a variety of plant, animal, and human cells continuously emit a low-intensity photoemission, which reflects the state of the organism's health. Wounded, stressed, and diseased cells tend to emit more light than healthy ones. It has also been suggested that photon emission and re-absorption in green leafy plants may provide for a dynamic communication feedback process. All of these observations and theoretic conjectures are dependent upon an actual photon emitter, and the primary plant emitters are chlorophyll molecules. In this research, corroborating evidence is provided to support recent research findings that the biophotonic signaling in wounded plant leaves is suppressed when in an oxygen-deficient environment. This novel research contributes to the body of plant wound-induced luminescence research and provides a novel methodology to measure this signaling phenomenon in vivo under both aerobic and anaerobic conditions.				
<b>14. SUBJECT TERMS</b> biophotons, ultraweak photon emission, UPE, plant signaling, wound-induced photon emission			<b>15. NUMBER OF PAGES</b> 113	
			<b>16. PRICE CODE</b>	
<b>17. SECURITY CLASSIFICATION OF REPORT</b> Unclassified	<b>18. SECURITY CLASSIFICATION OF THIS PAGE</b> Unclassified	<b>19. SECURITY CLASSIFICATION OF ABSTRACT</b> Unclassified	<b>20. LIMITATION OF ABSTRACT</b> UU	

THIS PAGE INTENTIONALLY LEFT BLANK

**Approved for public release. Distribution is unlimited.**

**BIOPHOTON EMISSION FROM PLANTS: A CONTRIBUTION TO THE  
UNDERSTANDING OF PLANT SIGNALING**

Carl L. Oros  
Civilian, Department of the Navy  
BA, University of Chicago, 1986  
MMS, Marine Corps University, 2000  
MS, Naval Postgraduate School, 2004

Submitted in partial fulfillment of the  
requirements for the degree of

**DOCTOR OF PHILOSOPHY IN INFORMATION SCIENCES**

from the

**NAVAL POSTGRADUATE SCHOOL  
December 2018**

Approved by: Dan C. Boger  
Department of  
Information Sciences  
Dissertation Supervisor

Gamani Karunasiri  
Department of Physics  
Dissertation Supervisor

Fabio D. Alves  
Department of Physics

Alex Bordetsky  
Department of  
Information Sciences

Raymond R. Buettner  
Department of  
Information Sciences

Approved by: Dan C. Boger, Chair, Department of Information Sciences

Douglas Moses, Vice Provost of Academic Affairs

THIS PAGE INTENTIONALLY LEFT BLANK

## **ABSTRACT**

The intriguing discovery that all living systems continuously emit endogenous, ultraweak photons has inspired numerous researchers to consider the information-bearing potential of biological photons as carriers of inter- and intracellular communication. In 1923, Alexander Gurwitsch first observed that a “morphogenetic field” in the form of ultraviolet light was involved in the regulation of plant cellular division. Over the last half century, the development of increasingly more sensitive photon detection technologies has revealed that a variety of plant, animal, and human cells continuously emit a low-intensity photoemission, which reflects the state of the organism's health. Wounded, stressed, and diseased cells tend to emit more light than healthy ones. It has also been suggested that photon emission and re-absorption in green leafy plants may provide for a dynamic communication feedback process. All of these observations and theoretic conjectures are dependent upon an actual photon emitter, and the primary plant emitters are chlorophyll molecules. In this research, corroborating evidence is provided to support recent research findings that the biophotonic signaling in wounded plant leaves is suppressed when in an oxygen-deficient environment. This novel research contributes to the body of plant wound-induced luminescence research and provides a novel methodology to measure this signaling phenomenon in vivo under both aerobic and anaerobic conditions.



THIS PAGE INTENTIONALLY LEFT BLANK

# TABLE OF CONTENTS

<b>I.</b>	<b>INTRODUCTION.....</b>	<b>1</b>
<b>A.</b>	<b>MOTIVATIONS .....</b>	<b>1</b>
<b>B.</b>	<b>RESEARCH QUESTIONS AND OVERVIEW OF RESEARCH PERFORMED.....</b>	<b>8</b>
<b>II.</b>	<b>BIOPHOTONS AND BIOINFORMATION: MESSAGE, MEDIUM, OR MATTER? .....</b>	<b>13</b>
<b>A.</b>	<b>MAKING SENSE OF THE MANY “SENSES” OF INFORMATION.....</b>	<b>13</b>
<b>B.</b>	<b>BIOLOGICAL INFORMATION.....</b>	<b>17</b>
<b>1.</b>	<b>Philosophical Issues .....</b>	<b>17</b>
<b>2.</b>	<b>Plant Signaling and Communication .....</b>	<b>18</b>
<b>III.</b>	<b>BACKGROUND AND LITERATURE REVIEW .....</b>	<b>19</b>
<b>A.</b>	<b>GENERAL CHARACTERISTICS OF BIOLOGICAL PHOTONS.....</b>	<b>19</b>
<b>B.</b>	<b>EXISTING THEORIES .....</b>	<b>20</b>
<b>1.</b>	<b>Biochemical Theory: Light as Metabolic Byproduct.....</b>	<b>20</b>
<b>2.</b>	<b>Biophoton Theory: Light Results from a Coherent Biological Field .....</b>	<b>21</b>
<b>C.</b>	<b>WOUND-INDUCED BIOPHOTONS.....</b>	<b>22</b>
<b>1.</b>	<b>Plant Photo-Chemical Wounding Responses .....</b>	<b>22</b>
<b>2.</b>	<b>Plant Anaerobic Stress .....</b>	<b>24</b>
<b>IV.</b>	<b>EXPERIMENTAL DESIGN: MATERIALS AND METHODS.....</b>	<b>27</b>
<b>A.</b>	<b>SPATHIPHYLLUM TEST CONDITIONS .....</b>	<b>27</b>
<b>B.</b>	<b>PLANT AND DARK TENT TEST ENCLOSURES .....</b>	<b>29</b>
<b>C.</b>	<b>TESTS INVOLVING NITROGEN (N<sub>2</sub>) GAS .....</b>	<b>30</b>
<b>D.</b>	<b>ULTRAWEAK PHOTON EMISSION MEASUREMENT.....</b>	<b>31</b>
<b>1.</b>	<b>Highly Sensitive PMT .....</b>	<b>31</b>
<b>2.</b>	<b>Software .....</b>	<b>33</b>
<b>E.</b>	<b>SPECTROSCOPY MEASUREMENTS.....</b>	<b>34</b>
<b>V.</b>	<b>EXPERIMENTAL RESULTS AND DISCUSSION .....</b>	<b>39</b>
<b>A.</b>	<b>SPONTANEOUS ULTRAWEAK PHOTON EMISSION FROM SPATHIPHYLLUM LEAVES .....</b>	<b>39</b>
<b>B.</b>	<b>BIOPHOTON PRE-WOUND DARK ADAPTATION ANALYSIS .....</b>	<b>40</b>

C.	BIOPHOTON WOUND ANALYSES.....	42
1.	Wound-Induced Biophoton Emission (Aerobic).....	43
2.	Wound-Induced Biophoton Emission (Anaerobic Conditions).....	46
D.	PHOTON COUNTING STATISTICS (PCS) OF PRE- AND POST-WOUND DATA.....	49
1.	Aerobic PCS .....	50
2.	Anaerobic PCS .....	55
E.	POISSON FITNESS .....	56
F.	SPECTRAL ANALYSIS.....	58
1.	Pre-wounding Dark Adaptation Spectral Analysis .....	58
2.	Wound Spectral Analysis .....	62
VI.	CONTRIBUTIONS.....	65
VII.	SUMMARY .....	67
A.	FINDINGS .....	67
B.	RECOMMENDATIONS FOR FOLLOW-ON RESEARCH.....	73
1.	Expand the Wavelength Measurement Sensitivity .....	73
2.	Improve Spectral Analysis .....	73
3.	Extend Methodology to Human Subjects Research .....	74
	APPENDIX. SUPPORTING FIGURES AND INFORMATION .....	75
	LIST OF REFERENCES .....	83
	INITIAL DISTRIBUTION LIST .....	93

## LIST OF FIGURES

Figure 1.	UPE of palms and eyes .....	3
Figure 2.	UPE of fingertips .....	4
Figure 3.	In vivo triboluminescence induced by rubbing of both palms.....	5
Figure 4.	Leaf heat–induced photon emission.....	6
Figure 5.	Leaf UPE induced as a function of increasing air temperature .....	7
Figure 6.	Biochemical explanations for leaf wound-induced photo-chemical response. Figures and description adapted from Fall et al. (1999) and Prasad et al. (2017). .....	9
Figure 7.	UPE from singlet oxygen and singlet chlorophyll in response to wounding. Adapted from Prasad et al. (2017). .....	10
Figure 8.	Experimental approach. (A, C) source: Oros and Alves (2018). (B) adapted from Prasad et al. (2017). .....	11
Figure 9.	Photon flux in perspective .....	20
Figure 10.	Plant test enclosure. Source: Oros and Alves (2018).....	28
Figure 11.	Experiment layout and test equipment. Source: Oros and Alves (2018).....	30
Figure 12.	Photon counting hardware Source: Hamamatsu Photonics (2018a, 2018b, 2005). .....	32
Figure 13.	Primary photon counting lens and PMT assembly. Source: Oros and Alves (2018).....	33
Figure 14.	Screen shot of Hamamatsu-supplied photon counting software.....	34
Figure 15.	Images of leaf used for filter wheel wound spectrum measurements. Source: Oros and Alves (2018).....	36
Figure 16.	Spathiphyllum dark-adaptation decay plots. Source: Oros and Alves (2018).....	40
Figure 17.	Dark-adaptation decay curve fitting. Source: Oros and Alves (2018).....	42
Figure 18.	Aerobic wounding UPE. Source: Oros and Alves (2018). .....	43

Figure 19.	Aerobic wound decay trends. Source: Oros and Alves (2018).....	44
Figure 20.	Aerobic wounding temperature and humidity data.....	45
Figure 21.	Spathiphyllum wounding UPE while under anoxic stress (nitrogen gas). Source: Oros and Alves (2018).....	47
Figure 22.	Anoxic wounding temperature and humidity data.....	48
Figure 23.	Aerobic pre-wound photocount distributions. Source: Oros and Alves (2018).....	50
Figure 24.	Leaf aerobic wounding photocount comparison. Source: Oros and Alves (2018).....	51
Figure 25.	Aerobic post-wound initial decay analysis (300s). Source: Oros and Alves (2018).....	52
Figure 26.	Aerobic post-wound secondary exponential decay. Source: Oros and Alves (2018).....	53
Figure 27.	Aerobic post-wound secondary decay photocount distributions. Source: Oros and Alves (2018).....	54
Figure 28.	Multiple regression comparison of averaged anaerobic wound data. Source: Oros and Alves (2018).....	55
Figure 29.	Anoxic wounding photocount distributions. Source: Oros and Alves (2018).....	56
Figure 30.	Poisson distribution fitness ( $\delta$ ) of leaf wounding and dark count data. Source: Oros and Alves (2018).....	57
Figure 31.	Secondary photon counting lens and PMT assembly. Source: Oros and Alves (2018).....	59
Figure 32.	Spathiphyllum dark adaptation filter wheel spectral analysis. Source: Oros and Alves (2018).....	61
Figure 33.	Spathiphyllum aerobic wounding filter wheel spectral analysis. Source: Oros and Alves (2018).....	62
Figure 34.	Primary and secondary aerobic wound UPE decay. Adapted from Oros and Alves (2018).....	68
Figure 35.	Anoxic wounding photocounts in resulting from singlet chlorophyll as an indicator of the state of triplet carbonyls. Adapted from Oros and Alves (2018) and Prasad et al. (2017).....	69

Figure 36.	Comparison of aerobic and anoxic Poisson PCS. Adapted from Oros and Alves (2018).....	70
Figure 37.	Summary of aerobic wounding initial decay PCS. Adapted from Oros and Alves (2018).....	71
Figure 38.	Summary of aerobic wounding secondary decay PCS. Adapted from Oros and Alves (2018).....	71
Figure 39.	Spectral comparison of aerobic dark adaptation and wounding. Adapted from Oros and Alves (2018).....	72
Figure 40.	Photocathode radiant sensitivity. Adapted from Hamamatsu Photonics (2005).....	73
Figure 41.	Plant test enclosure with front and sideview showing PMT.....	75
Figure 42.	Spathiphyllum single filter dark adaptation decay spectral analysis. Source: Oros and Alves (2018), S1 Figure. ....	76
Figure 43.	Pre-wound filter wheel spectrum measurements (#2–#5) recorded every 15 minutes (900 s). Source: Oros and Alves (2018), S2 Figure. ....	77
Figure 44.	Pre-wound filter wheel spectrum measurements (#6–# 8) recorded every 15 minutes (900 s). Source: Oros and Alves (2018), S3 Figure. ....	78
Figure 45.	Box plots of filter wheel spectral data. Source: Oros and Alves (2018), S4 Figure. ....	79
Figure 46.	Spathiphyllum single filter aerobic wounding spectral analysis. Source: Oros and Alves (2018), S5 Figure. ....	80
Figure 47.	Post-wound filter wheel spectrum measurements #2–#5. Source: Oros and Alves (2018), S6 Figure. ....	81

THIS PAGE INTENTIONALLY LEFT BLANK

## LIST OF TABLES

Table 1.	Edgepass filters used for spectral analysis. Source: Oros and Alves (2018).....	35
Table 2.	Filter wheel spectral analysis data. Source: Oros and Alves (2018), S1 Table. ....	82



THIS PAGE INTENTIONALLY LEFT BLANK

## LIST OF ACRONYMS AND ABBREVIATIONS

Ar	Argon
AR	Anti-Reflective Coating
BGF	Blue Green Fluorescence
BE	Biophoton Emission
CCD	Charge Coupled Device
CL	Chemiluminescence
Chl	Chlorophyll
CO <sub>2</sub>	Carbon Dioxide
CPS	Counts Per Second
DL	Delayed Luminescence
EM	Electromagnetic
GaAsP	Gallium Arsenide Phosphide
GLV	Green Leaf Volatiles
IPE	Induced Photon Emission
IR	Infrared
LED	Light Emitting Diode
LOX	Lipoxygenase
N <sub>2</sub>	Nitrogen
NM	Nanometers
O <sub>2</sub>	Oxygen
PACU	Pure Air Cleaning Unit
PCS	Photon Counting Statistics
PMT	Photomultiplier Tube
PTR-MS	Proton-Transfer-Reaction Mass Spectrometry
PUFA	Polyunsaturated Fatty Acids
SBE	Self-bioluminescent Emission
UPE	Ultraweak Photon Emission
UV	Ultraviolet
VAR	Variance
VOC	Volatile Organic Compound

THIS PAGE INTENTIONALLY LEFT BLANK

## ACKNOWLEDGMENTS

This research would not have been possible if it were not for my advisors and all of the unique, talented, patient, dedicated, and academically diverse faculty of both the Information Science (IS) and Physics Departments. Rather than creating an IS “disciplinary silo,” you fostered a transdisciplinary educational environment where students and faculty could explore and expand the boundaries of information science. This dissertation would not have been possible without your support in so many ways.

I also am grateful for all of my NPS professors, colleagues and fellow doctoral students who have supported me in and out of the classroom, during research in the field, or sharing a round of cheer at the bar. You have made this a memorable journey indeed.

Lastly, and most importantly, I would like to thank my beloved wife and children who have endured much in support of my academic and professional endeavors. Without them my life’s path would have never led to Monterey and this dissertation would have never been conceived. I am blessed.

THIS PAGE INTENTIONALLY LEFT BLANK

# I. INTRODUCTION

## A. MOTIVATIONS

The field of biophotonics is an emerging, multidisciplinary research field that explores the interaction of light with biological material. It is now well known that all life forms radiate an endogenous, ultraweak, self-induced luminescence. While the source and theoretical foundations of this light emission still remain a topic for focused research and debate, the potential information bearing properties of biological light have intrigued many researchers, including this one.

Biophotonics comes from the Greek words *bios* (life) and *phôs* (light). Biophotonics-related research over the last half century has progressed to a stage prompting many researchers to conceive of biological photons as carriers of intra and intercellular communication. In 1923, long before the advent of photomultiplier tube (PMT) technology, Ukrainian biologist Alexander Gurwitsch discovered that weak ultraviolet (UV) light emitted from onion root cells could induce mitotic activity in neighboring tissue cells. He coined the term “mitogenetic radiation” to explain this phenomenon (Gurwitch, 1925; Gurwitsch, 1988; Popp, Gu, & Li, 1994; Van Wijk, 2001; Voeikov & Belousov, 2007). This was the first case where light (an electromagnetic field) was envisioned to be a medium for the transfer of biological information. Gurwitsch “claimed a ‘morphogenetic field’ [was] responsible for the regulation of cell growth” (Popp, 2003a, p. 387). Nearly a century later, Tufts University researchers discovered that a bioelectric field (ion flux)—in advance of cellular mitosis--pre-imprinted a developing tadpole’s cellular membrane to pattern groups of cells that would eventually map to the gene expression of the eyes, face, gills, etc. (Knight & Collins, 2011; Vandenberg, Morrie, & Adams, 2011). Though not photons per say, this discovery elucidated the role of a field—a bioelectric field in this case—in the “non-molecular” transfer or transformation of biological (i.e., genetic) information. Their pioneering work showed that “all cells, not just nerve and muscle cells, store and transfer information with electrical signals” (“Unlocking the Bioelectric Code,” 2013).

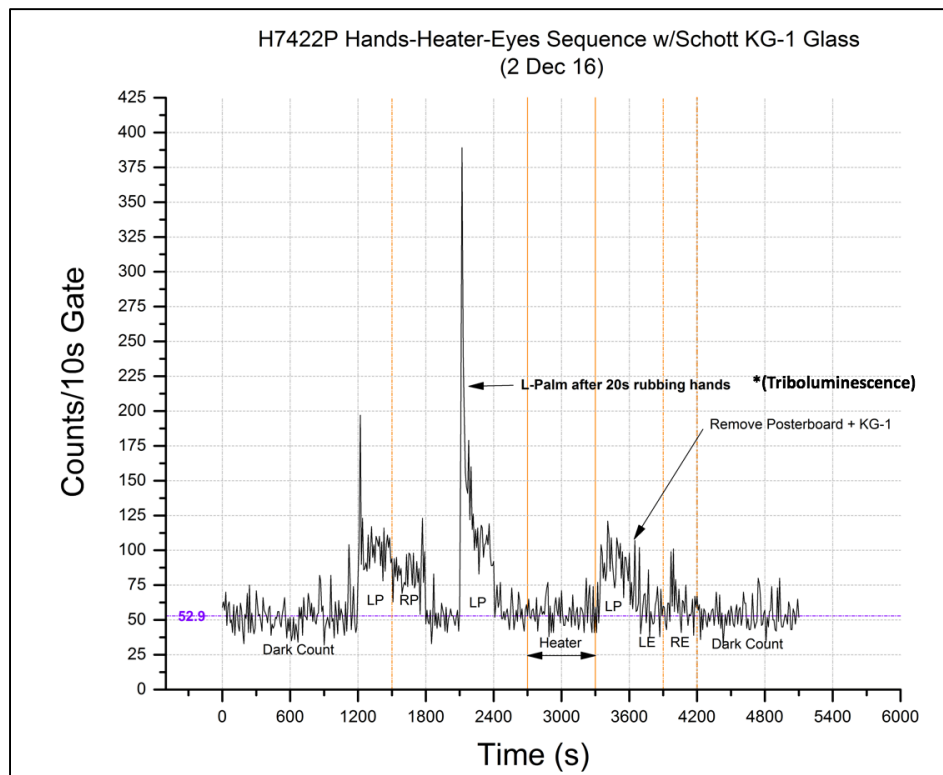
In the 1950s, instruments designed for the detection of ultraweak photon emission (UPE) signals (photomultipliers) improved sufficiently enough for Russian biophysicists to detect noticeable photon emission from living organisms that could not be explained as a product of mere heat radiation. In 1976 Physicist Fritz-Albert Popp coined the term “biophoton,” short for biological photon. “Bio-photons refer to the biological system as a whole [where] the emission of single photons is assumed to point more to a biological quantum phenomenon [*a coherent field*] than to ordinary luminescence” (Van Wijk, 2001, p. 189). Extensive research with plants, animals, and humans over the last 40 years has shown that DNA, RNA, mitochondria, and nerve cells also emit light. Further, injured and diseased cells tend to emit more light than healthy ones. This has prompted the medical biophotonics field to look to biological photoemission as a non-invasive health assessment tool capable of conveying information related to the biological state of the organism under study (Ives et al., 2014).

This dissertation was inspired by the *bio-informational* aspects of biological photoemission. In lieu of previous research to date, it seems the time is appropriate to consider a more prominent role of *photonic* bio-information. From this expansive perspective, biological information is more *photo-electro-chemical* in nature. This has led this information scientist to the question: “*Can light be a potential communication channel for biological information?*” If so, “*what are the potential exogenous stimulants of biophoton emission? What are the resultant “carriers” (emitters, transmitters) of biological photoemission in plants and humans?*” “*Are there novel experimental techniques capable of shedding new ‘light’ in this exciting research domain?*”

The original intent of this dissertation research was to study human subjects biophotonic response to various non-invasive stimuli. However, preliminary exploratory research, setting up of the experimental system with required sensitivity, and locating a suitable laboratory space during the first three years presented some challenges.

Early exploratory experiments by the author investigated UPE of humans and plants as reported in the literature. This assisted in developing the experimental methodology and design essential to accurately detect such low-level photon emissions. These early confirmatory experiments honed the experimental approach and simultaneously provided

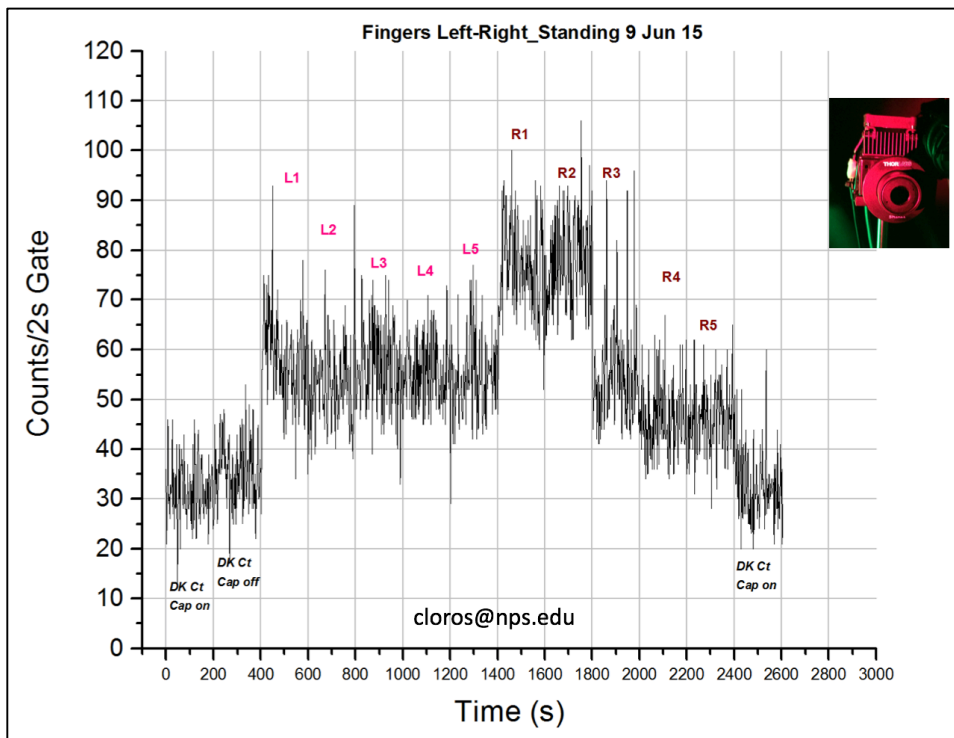
confidence that the data collected was in alignment with previously published research. Early experiments involving passive photon detection of human hands and finger tips clearly revealed photon counts above the noise floor. Collecting eye data proved more sensitive to experiment conditions and early data was inconclusive. Care was also given in these earlier experiments to mitigate potential heat sources of photoemission. Heat absorbent glass and a heater with similar emissivity of human skin were used as controls (see Figure 1 and Figure 2).



UPE of dark adapted (20 min.) left palm (LP), right palm (RP), left eye (LE), right eye (RE). A Thorlabs HT10K flexible Kapton (polyimide) foil heater covered with black electrical tape was used as a control and heated with a TC200 heater controller (Thorlabs). A Schott 4" x 4" KG-1 glass panel was used between the palms and PMT to filter out long wave IR (heat). Arrow indicates LP triboluminescence effects observed after rubbing both palms for 20 sec.

Figure 1. UPE of palms and eyes

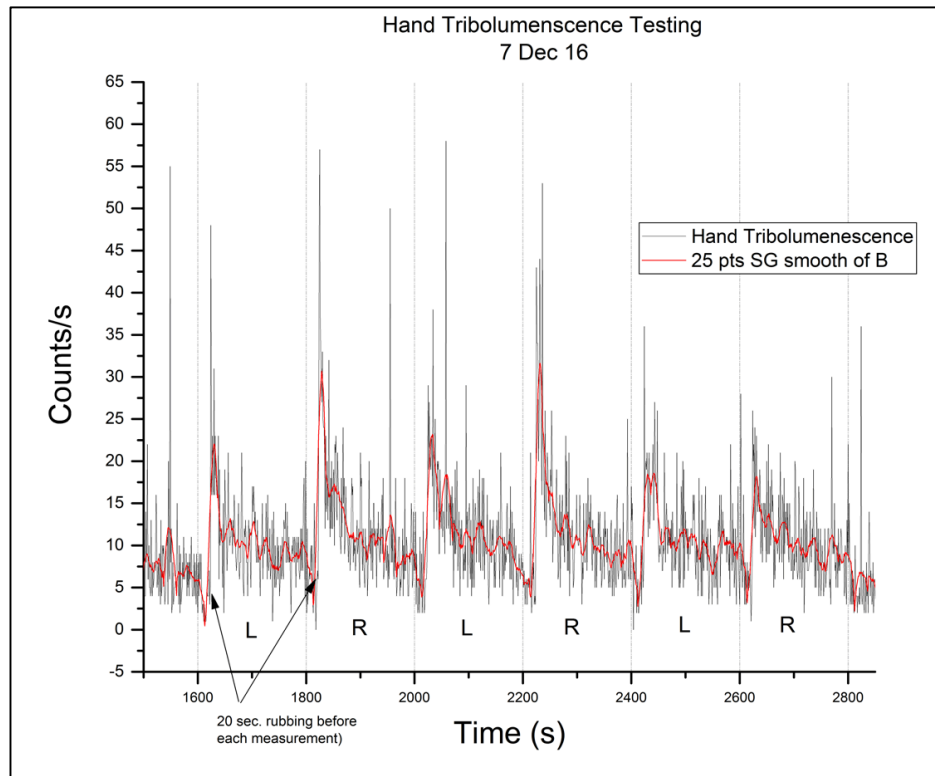




L = left, hand, R = right hand. (1) pinky finger, (2) ring finger, (3) middle finger, (4) index finger & (5) thumb. Data collected with researcher standing. Inset shows 0.5" diam. lens tube opening.

Figure 2. UPE of fingertips

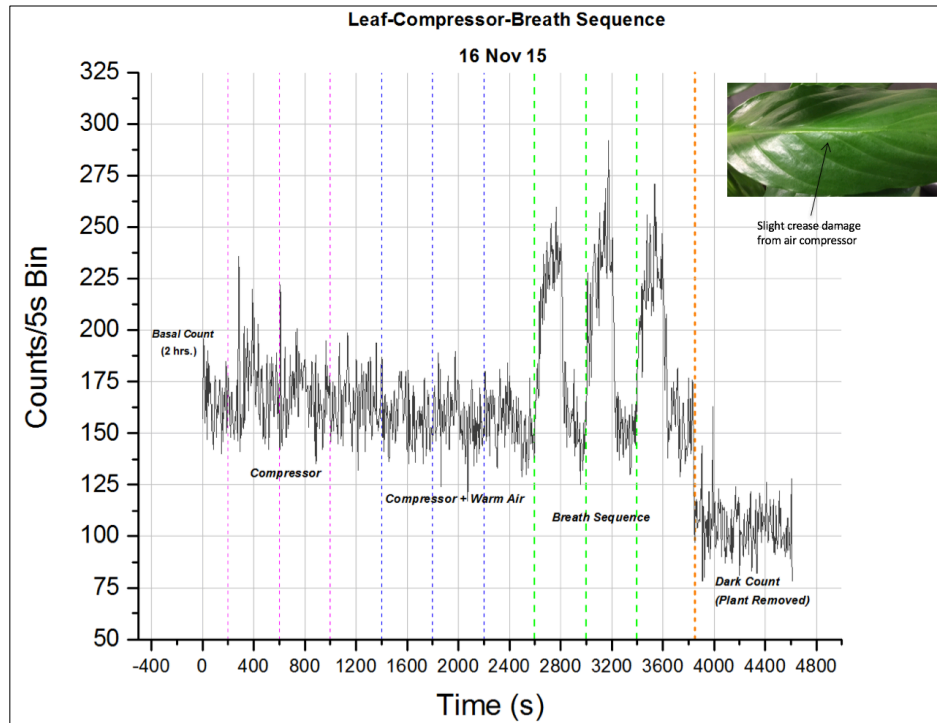
Initial trials also explored the UPE produced by physical rubbing (i.e., mechanical luminescence, or triboluminescence) of palms to better understand other potential sources of light. Figure 3 shows the UPE and resultant decay produced by hand rubbing for 20 seconds. Similar results were reported by Sauermann, Mei, Hoppe, and Stab (1999, p. 425).



Hands were washed (purified water) and then dark adapted for 20 min. Hands were then rubbed palm on palm for 20 seconds and photoemission was immediately recorded for 200 s. Palms were alternated for each measurement (L = left, R = right). Red curve is 25-point smoothing of data for visualization.

Figure 3. In vivo triboluminescence induced by rubbing of both palms

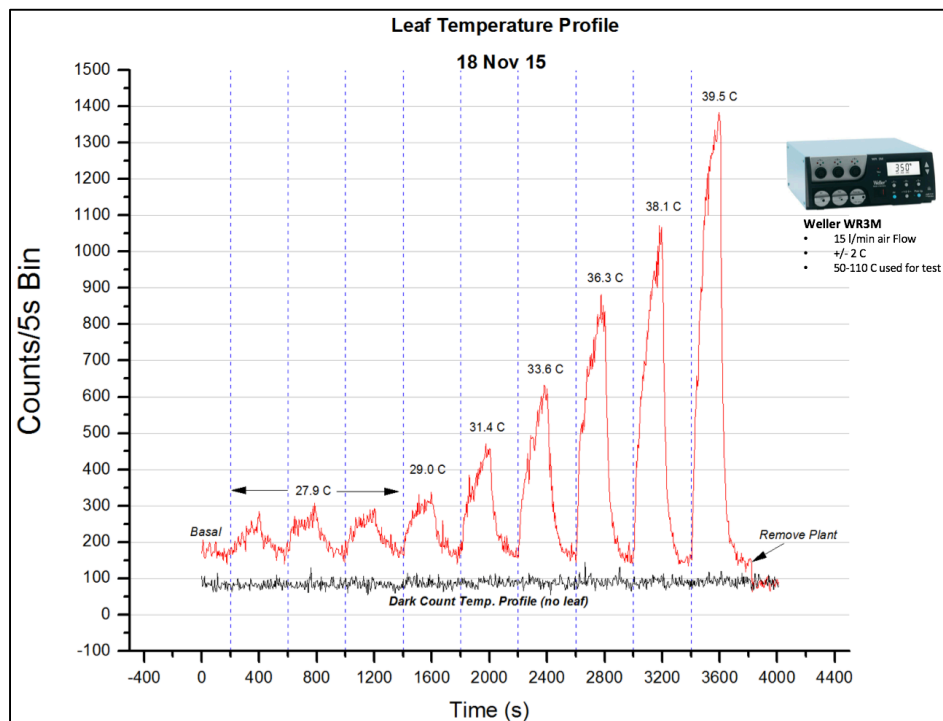
Plant response to heating (*in vivo*) was also explored. Figure 4 shows the plant UPE response to an air compressor (warm air) and a human breath sequence. Moist human breath rapidly induced a significant photon response.



Room temperature air was blown on a leaf using a small compressor. UPE dramatically increased when warmer air (breath sequence directed via a tube) was introduced.

Figure 4. Leaf heat-induced photon emission

To rule out potential for chemical induced photoemission caused by organic compounds in exhaled human breath, a more careful experiment was conducted with variable, controlled heated air from a professional soldering station. Care was taken not to injure the leaves with extreme heat. Figure 5 shows the leaf's response to varying degrees of heat within the plants normal, tropical temperature range.



A Weller WR3M soldering station was configured to blow warm air on a *Spathiphyllum* leaf in preset intervals. Temperatures as indicated in Celsius. Dark count shown for reference. Note UPE returned to initial state after each warm air sequence. Care was taken to avoid heat-induced injury so temperature did not exceed 39.5 C (103.1 F).

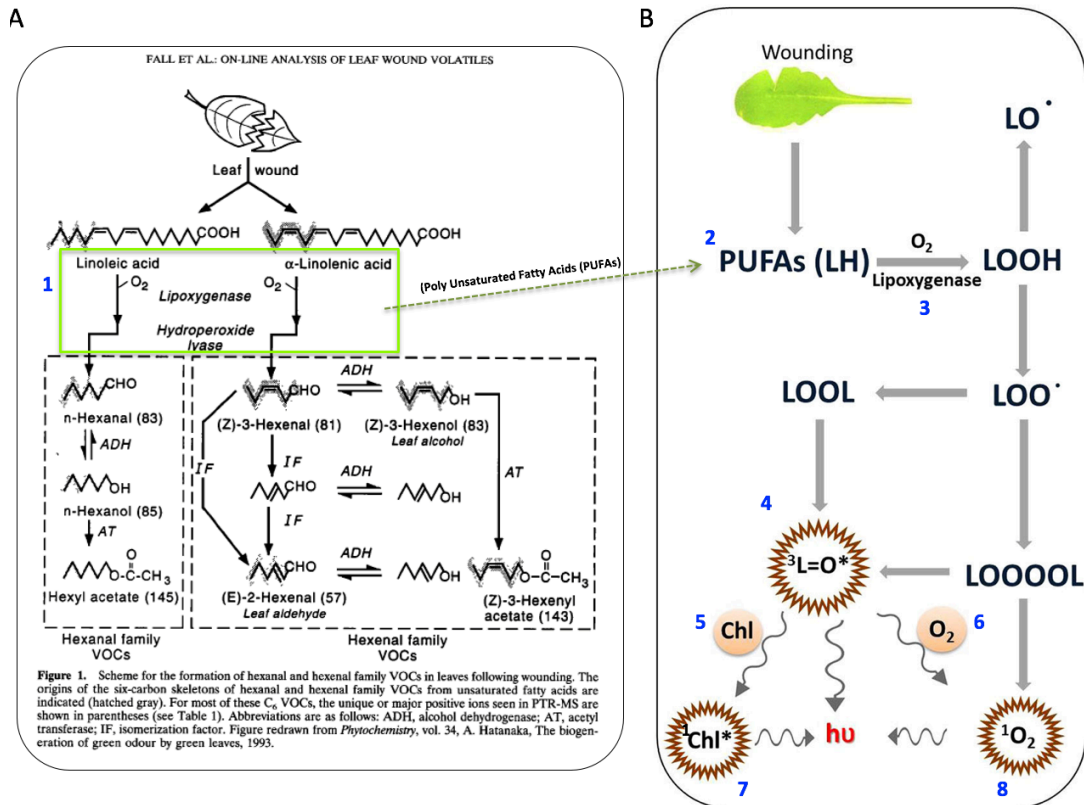
Figure 5. Leaf UPE induced as a function of increasing air temperature

These early experiments with plants assisted in perfecting the optical design, data acquisition procedures, and statistical analysis techniques. The plant literature review revealed a whole body of research focused on plant chemical as well as photonic responses to injury (i.e., disease, mechanical wounding, bacteria, herbivory) and stress (i.e., temperature, anoxia). There is also a body of plant research devoted to “plant signaling” and “plant neurobiology” that focuses on “how plants process the information they obtain

from the environment to develop, prosper and reproduce optimally” (Brenner et al., 2006). Plant cells are also similar to animal/human cells in that they contain mitochondria, DNA, and various pigment molecules capable of light absorption and emission. Further, chlorophyll and hemoglobin share similar molecular structures (hemoglobin with an iron atom and chlorophyll containing magnesium). It was during this early investigatory phase that I discovered a research “gap.” No one had ever investigated the induced photoemission of a whole, mechanically wounded plant (*in vivo*) in an anoxic (non-oxygen containing) environment. This novel approach was significant in that it provided another data point to support related research findings that had shown the dependence of an enzyme (lipoxygenase) and oxygen in the production of wound-induced biochemical reactions that ultimately lead to the photoemission of singlet chlorophyll and singlet oxygen molecules. Over the course of ten months, which included experiment design, testing, data analysis, led to a submission of a journal paper which was published after successfully addressing the reviewer’s comments. This dissertation documents this scientific contribution and lays the foundation for future research that builds on the methods and experimental apparatus that resulted from this endeavor.

## **B. RESEARCH QUESTIONS AND OVERVIEW OF RESEARCH PERFORMED**

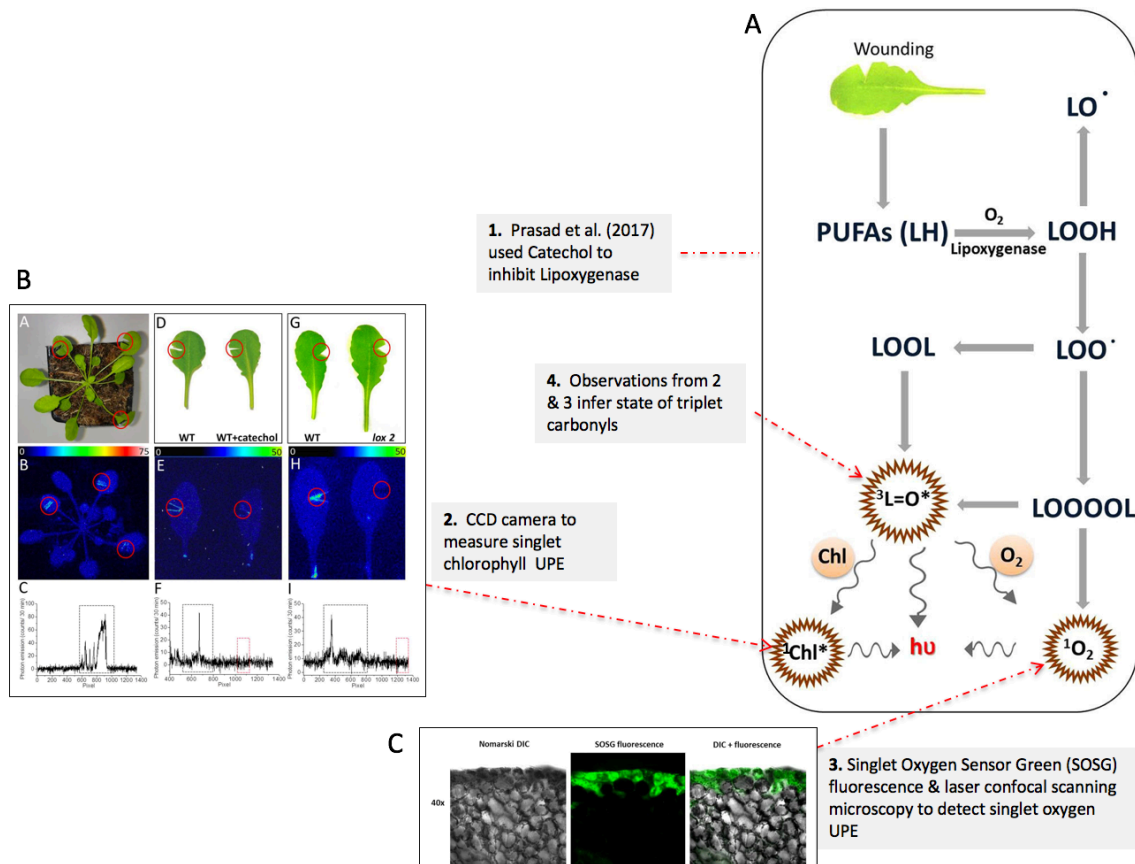
Upon conducting my literature review involving plant wounding and UPE, it became apparent that no one had recorded the photon emission of mechanically wounded plants (*in vivo*) while in an anoxic environment. Fall, Hansel, Jordan, & Lindinger, (1999) (Figure 6 A) wounded a leaf with scissors in a bag of nitrogen gas and showed that the formation of certain volatile organic compounds was dependent upon oxygen-- which is required for the lipoxygenase reaction that triggers the formation of fatty acid hydroperoxides.



(A) Adapted from: Fall et al. (1999, Figure 1.); (B) Adapted from: Prasad et al. (2017, Figure. 1, [singlet chlorophyll diagram “7” corrected by the author]), (1, 2) generation of polyunsaturated fatty acids in response to mechanical wounding, (3) Lipoxygenase catalyzes molecular oxygen to produce lipid hydroperoxide (LOOH) and other high energy intermediates, (4) high energy reaction intermediates decompose to form triplet carbonyls ( $^3L=O^*$ ), excitation energy is also transferred to chlorophylls (5) and to molecular oxygen (6), forming (7) singlet chlorophyll ( $^1Chl^*$ ) and (8) singlet oxygen ( $^1O_2$ ) respectively.

Figure 6. Biochemical explanations for leaf wound-induced photo-chemical response. Figures and description adapted from Fall et al. (1999) and Prasad et al. (2017).

A more recent paper published by Prasad, Sedlářová, Kale, & Pospíšil, (2017) demonstrated that chemically inhibiting lipoxygenase in wounded leaves would ultimately prevent the reaction chain from creating triplet excited carbonyls and thus prevent/inhibit singlet chlorophyll and singlet oxygen UPE (Figure 6 B and Figure 7 A-C).

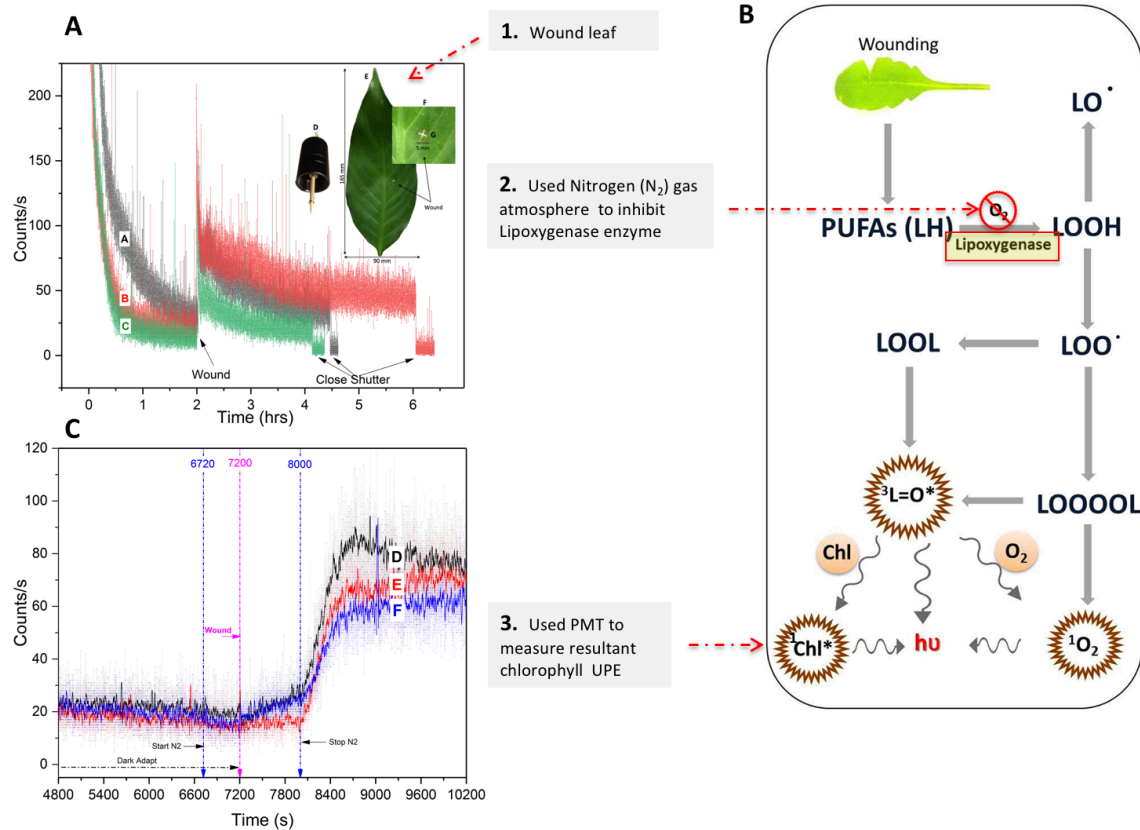


(A-C) Adapted from: Prasad et al. (2017, Figures. 1, 2, and 3 [modified]). (1) Prasad et al. used catechol to inhibit the lipoxygenase reaction, (2, B) a CCD camera was used record UPE from chlorophyll, (3, C) Singlet Oxygen Sensor Green (SOSG) & laser confocal scanning microscopy was used to detect UPE from singlet oxygen, Observations from steps (2) and (3) were used to infer the state of triplet carbonyls.

Figure 7. UPE from singlet oxygen and singlet chlorophyll in response to wounding. Adapted from Prasad et al. (2017).

This prompted our research questions: *Would plant wound-induced photoemission (in vivo) be inhibited in an oxygen deprived (anoxic) environment? Further, would an anoxic environment affect leaf self-induced (or endogenous) UPE?* Our experimental approach is depicted in Figure 8. Nitrogen gas was used in a closed chamber with dark adapted whole plants. Plant photon counts were collected during pre and post wounding phases. Our results corroborated the findings of Prasad et al. (2017) and revealed that wound-induced photon counts were inhibited when under anoxic stress and that the preponderance of UPE was 650 nm or above, which indicated chlorophyll

(most likely singlet chlorophyll) as the likely emitter. The results also showed that the anoxic environment had minimal effect on the basal (pre-wound) photoemissions.



(1) Leaf anoxic wounding (in  $N_2$  atmosphere) was used to (2) inhibit the Lipoxygenase reaction chain. (3) A PMT configured with spectral filters was used to record the resultant UPE.

Figure 8. Experimental approach. (A, C) source: Oros and Alves (2018).  
(B) adapted from Prasad et al. (2017).



THIS PAGE INTENTIONALLY LEFT BLANK

## II. BIOPHOTONS AND BIOINFORMATION: MESSAGE, MEDIUM, OR MATTER?

The greatest thing by far is to be a master of metaphor. It is the one thing that cannot be learnt from others; it is also a sign of genius, since a good metaphor implies an intuitive perception of the similarity in dissimilars.

—Aristotle’s *De Poetica* (as quoted in Garfield, 1986, p. 310)

Information is a “polymorphic phenomenon and a polysemantic concept” (Floridi, 2015). Volumes have been composed on this subject. Machlup (1983) provides a thorough overview of some of the “semantic quirks” related to the study of information and knowledge. An in-depth discussion of the semantic origins and numerous uses of information is well beyond the scope of this dissertation. For context, I will, however, provide a brief overview of the salient semantic themes I deem relevant to the topic of information as it relates to biological systems.

### A. MAKING SENSE OF THE MANY “SENSES” OF INFORMATION

In their book *In Athena’s Camp: Preparing for Conflict in the Information Age*, Arquilla and Ronfeldt (1997, pp. 144–149) provide a concise, insightful synopsis of three prevalent views of information: information as *message*, information as *medium* and information as *physical matter*. I provide a brief overview of these semantic themes to assist in conceptualizing the concept of information as it spans the hierarchy of socio-technical-biological contexts.

The word *information* (first cited in 1387) is one of the earliest 9% of 3,800 entries recorded in the Oxford English Dictionary (OED) in the decade 1380–1389 (“Information,” n.d.). The OED lists 63 different meanings, or “senses” for information. Of these 63 total senses and subentry senses recorded, two main themes stand out as relevant to this discussion: (1) *the imparting of knowledge in general*, and much rarer, (2) *the giving of form*. Neither of these senses are mutually exclusive of each other. However, each possesses tacit ontological assumptions.

In the mainstream sense, imparting knowledge concerns the communication of a particular fact, subject, event as in “reports, instructions, and programs” (Wright 1989, cited in Arquilla & Ronfeldt, 1997, p. 145). Here information is viewed as an *immaterial message* or signal and hence a flow. This results in what is commonly referred to as the Data-Information-Knowledge-Wisdom (DIKW) pyramid where information “is obtained by the processing of data” (“Information,” n.d.). Knowledge in this main sense is discretized into sub-isolable elements generated from data and information. The linear aggregation of data—information—knowledge is conceived to ultimately culminate in the attainment of wisdom. Though each successive layer rests on the one before it, it cannot be inferred that more data = more information = more knowledge. While the pyramid construct seems intuitive, it is not extensible to the design and architecture of information technology systems (IT), let alone is it applicable to complex biological systems. Further, it has been subject to several critiques (Frické, 2009; Rowley, 2007; Tuomi, 1999). It should also be pointed out that knowledge within this anthropocentric construct is the sole province of a human agent. Thus, void of a cognizing homunculus at the cellular level, the DIKW pyramid construct provides little utility.

Closely related to this sense is the view of *information as medium*. This perspective incorporates the transmitting system as well as the message sent from the sender to the receiver. This sense is derived from Shannon’s communication theory, expressed as a “mathematically defined quantity divorced from any concept of news or meaning; the degree of choice exercised in the selection or formation of one particular symbol, message, etc., out of a number of possible ones...” (“Information,” n.d.). While Shannon’s theory (Shannon, 1948; Shannon & Weaver, 1963) was principally applicable to computing and network communication contexts, it has also been extended to human communication constructs as well as genetics (Akhter, Bailey, Salamon, Aziz, & Edwards, 2013; Battail, 2006; Bi & Rogan, 2004; Schneider, 2006; Schneider & Mastrorarde, 1996). This view of information is more concerned with the effective communication of the message (i.e., accurate transmission of data or gene encoding of proteins in a noisy channel) rather than with semantics or knowledge. To Shannon, the “semantic aspects of communication [were] irrelevant to the engineering problem” (Shannon, 1948, p. 379). The conceptualization of

information as the opposite of entropy (disorder) was later generalized to equate information with organization. Cybernetics emerged out of this view and integrated information control and feedback into a system's context to improve control. This was pivotal to governing and regulating systemic processes. In contrast with an open system that exchanges matter, energy, and information with its environment, cybernetic systems were viewed as closed systems that were open to energy but closed to information (i.e., "information tight").

Even whether the system is closed to energy or open is often irrelevant; what is important is the extent to which the system is subject to determining and controlling factors. So no information or signal or determining factor may pass from part to part without its being recorded as a significant event. Cybernetics might, in fact, be defined as the study of systems that are open to energy but closed to information and control systems that are "information-tight" (Ashby, 1956, pp. 3–4)

The OED's second, much more intriguing sense of the word information—*the giving of form*—lends to a more non-anthropocentric perspective of information. Knowledge in this sense is intrinsic. In this context, information transcends mere building blocks and embodies an "essential character to something; the action of imbuing with a particular quality; animation (esp. of the body by the soul)." This meaning originates from the Latin word *informare*, or the verb "inform." "To put into (material) form or shape; to form, shape, mould, fashion, create; (also) to put into proper form or order" ("Inform," n.d.). To give form or determinant character to, Hence: "to imbue, or impregnate *with* a specific quality or attribute; to impart some pervading quality..." ("Inform," n.d.). Given this perspective, all biological life forms can be viewed as embodying "information" as a direct reflection of their state of systemic complexity. The ontology then shifts from a discrete "sender-receiver" flow model to the system as a whole, where information manifests as "the pattern of organization of matter and energy" (Parker, 1973, p. 1) or as living systems theorist J. G. Miller put it "the patterning of matter-energy in systems" (Miller, 1978, p. 1030). The Austrian biologist and founder of General Systems Theory (GST), Ludwig von Bertalanffy, did not view "the organism [as] a static system closed to the outside and always containing the identical components; [but rather as] an open system in a (quasi-)steady state, maintained constant in its mass relations in a continuous change

of component material and energies, in which material continually enters from, and leaves into, the outside environment” (von Bertalanffy, 1969, p. 121). Further, he never conceived of the open & closed system attributes as being mutually exclusive:

In summary, the feedback model is preeminently applicable to “**secondary**” regulations, i.e., regulations based on structural arrangements in the wide sense of the word. . . . “**primary**” regulations must evolve from the dynamics in an open system. Increasingly, the organism becomes “mechanized” in the course of development; hence later regulations particularly correspond to feedback mechanisms (homeostasis, goal directed behavior, etc.). (p. 150, emphasis added)

Living systems are open systems, that are far from equilibrium, exhibit irreversible thermodynamics, and exist in a “flowing balance” (Bertalanffy). They exchange “energy and information, mainly through electromagnetic interaction with the environment. The stream of matter which is dissipated during the life cycle interacts mainly via electromagnetic fields” (Schwabl & Klima, 2005, pp. 86–87). Arquilla and Ronfeldt present this view as information and Physical Matter where information “is an embedded physical property of all objects that exhibit organizational structure... [applicable] to dirt clods as well as DNA strands” (Arquilla & Ronfeldt, 1997, p. 148). They summarize:

The views of information as message and medium persist, but are embedded in a view that all matter and energy in the universe are not only based on information but are designed to process and convey it. Information is the prime mover. Both order and chaos depend upon it. (p. 149)

Though it would be convenient for researchers to “collapse” the term information into a “dead metaphor” (i.e., scientific fact), the ramifications of such an act would unnaturally bias and limit one’s capacity for inquiry. Information, when invoked as metaphor, however, takes on a more transcendent, luminous quality that invites the inquirer to partake in other potential vistas of thought. After all, “reality” does present us with novel situations and opportunities for investigating nature and phenomena. Is it not important then to not only borrow from the past knowledge structures but also to think anew and generate new perspectives and beliefs as well? Thomas Kuhn, in *Metaphor in Science*, summarized it this way:

Metaphor plays an essential role in establishing a link between scientific language and the world. Those links are not, however, given once and for all. Theory change, in particular, is accompanied by a change in some of the relevant metaphors and in the corresponding parts of the network of similarities through which terms attach to nature. (Kuhn, 1993, p. 539)

Information science then is the study of the form, structure, and patterning of information spanning multiple phenomena (bio-socio-technical). In discussing the “content of form” in the “Invisible substrate of information science” (albeit from a human agency (and library science) perspective), Bates (1999) similarly aligns with this ethos.

In applied information science, we find ourselves primarily concerned with the form and organization of information, its underlying structure, and only secondarily with its content. (p. 1044)

## **B. BIOLOGICAL INFORMATION**

### **1. Philosophical Issues**

Applying informational language to biology is not without its “thorny” philosophical issues (cf. P. Godfrey-Smith & Sterelny, 2016; Peter Godfrey-Smith, 2007). As discussed previously, many of these issues naturally arise out of the polysemantic/metaphoric capacity of the term. The potential for confusion is further exacerbated as the discussion shifts from isolable, observable, causal “information” chains (i.e., cells, genes, hormones, molecules, photo-electrical signals) to less ontologically determinable factors (i.e., epigenetics, the environment, coherence effects related to electromagnetic gradients and fields (Frohlich, 1970; Li, Popp, Nagl, & Klima, 1983; Pokorny, 2009), quantum fields (Hameroff S.R., 1988), and potential quantum state reduction at Planck’s scale in microtubules (Hameroff & Penrose, 2014)).

It is a daunting, if not ill-advised task, to attempt to reconcile these diverse ontological perspectives. The semantics surrounding information are directly related to the context of the discourse and level of analysis. There are no clear lines of delineation. Especially, when one considers that the “structure (i.e., order of parts) and function (order of processes) may be the very same thing: in the physical world matter dissolves into a play of energies, and in the biological world structures are the expression of a flow of processes” (von Bertalanffy, 1969, p. 27).

The perspective of information discussed in this paper is more closely related to photo-chemical signaling and related processes, though I do not associate these photo signals to be “Shannon-like” where their reception and information bearing content would be dependent upon a choice among alternative photons.

## **2. Plant Signaling and Communication**

Plants have evolved a variety of means to sense and adapt to their environment. A relatively new field of “plant neurobiology” views plants as “information processing organisms with complex communication throughout the individual plant” (“International Laboratory of Plant Neurobiology,” n.d.). The goal of this new plant field of study is to elucidate the “information network that exists within plants (Brenner et al., 2006). Though use of the word neuron today strongly implies an anthropocentric bent, the etymology actually traces back to ancient Greek (Plato) where it was used to connote “vegetal fibre or anything fibrous in nature” (Brenner et al., 2006, p. 414). Hence the field is engaged in a systems-biology approach to understand plant cellular and intracellular communication. Very little has been published regarding biophoton aspects of plant communication.

Creath (2008) and Creath & Schwartz (2005) hypothesized that the biophoton emission and subsequent reabsorption by localized plant leaves in effect create a positive feedback loop where energy and bioinformation are able to be transferred. Plants also emit light in response to wounding and stress. This will be covered in more detail in the plant biophoton wounding section.

This research focuses on an aspect of plant signaling and communication. It explores the biological photo emission source and associated wounding biochemical processes under aerobic and anoxic conditions.

### III. BACKGROUND AND LITERATURE REVIEW

#### A. GENERAL CHARACTERISTICS OF BIOLOGICAL PHOTONS

Biological photon (biophoton) emission is a spontaneous, low intensity photon emission from all living systems (Popp, Gurwitsch, Inaba, Slawinski, Cilento, Van Wijk, & Schamhart, 1988; Slawinska & Slawinski, 1983). It is extremely weak, ranging from ~10 to 1,000 photons per  $s^{-1} cm^{-2}$ , corresponding to a flux of  $< 10^{-15}$  W. This weak photoemission is orders of magnitude below the human eye's detectable threshold and is observed typically in the visual to near infrared band (200–800 nm). This low-level photoemission has been referred to as chemiluminescence (CL), biophotons (Popp), biophoton emission, ultraweak photon emission (UPE), ultraweak bioluminescence, autoluminescence, and self-bioluminescent emission (SBE). (We use the terms UPE, biophoton, and photoemission interchangeably throughout this paper). UPE is not to be confused with bioluminescence or chemiluminescence caused by optical markers and is distinctly different from the “firefly” gene type luciferin/luciferase oxidative enzyme reactions. This weak biological chemiluminescence is emitted as part of chemical reactions related to normal metabolic reactions, such as “oxidative metabolism, cell division and death, photosynthesis, carcinogenesis, and possibly growth regulation” (Shen, X., Liu, F., Li, 1993, p. 291). However, this emission can also be induced via light induction, wounding (i.e., mechanical, chemical, heat shock) and disease. UPE has been observed in plants in response to fungal pathogens, nematodes, herbivory, hormones, temperature changes, and herbicide treatments (Kato, Iyozumi, Kageyama, Inagaki, & Yamaguchi, 2014, p. 54). It generally observed that that healthy, unstressed and uninjured plant and animal cells emit less light than unhealthy, stressed, or injured ones (Creath, 2008; Popp et al., 1994; Van Wijk, 2001). These minute quantities of light can only be detected through the use of sensitive photomultiplier tubes (PMT) or charge coupled device (CCD) cameras. PMT technology first became available in the 1950s. Figure 9 shows the comparative photon flux ranging from a traditional incandescent light bulb to the UPE of the palm of one's hand. Even though the term “biophoton” (discussed in the next section) connotes emission stemming from a coherent biofield, for the purposes of this dissertation, we will treat all



biological photons as carriers of bioinformation and use UPE, biophoton, and BE interchangeably.

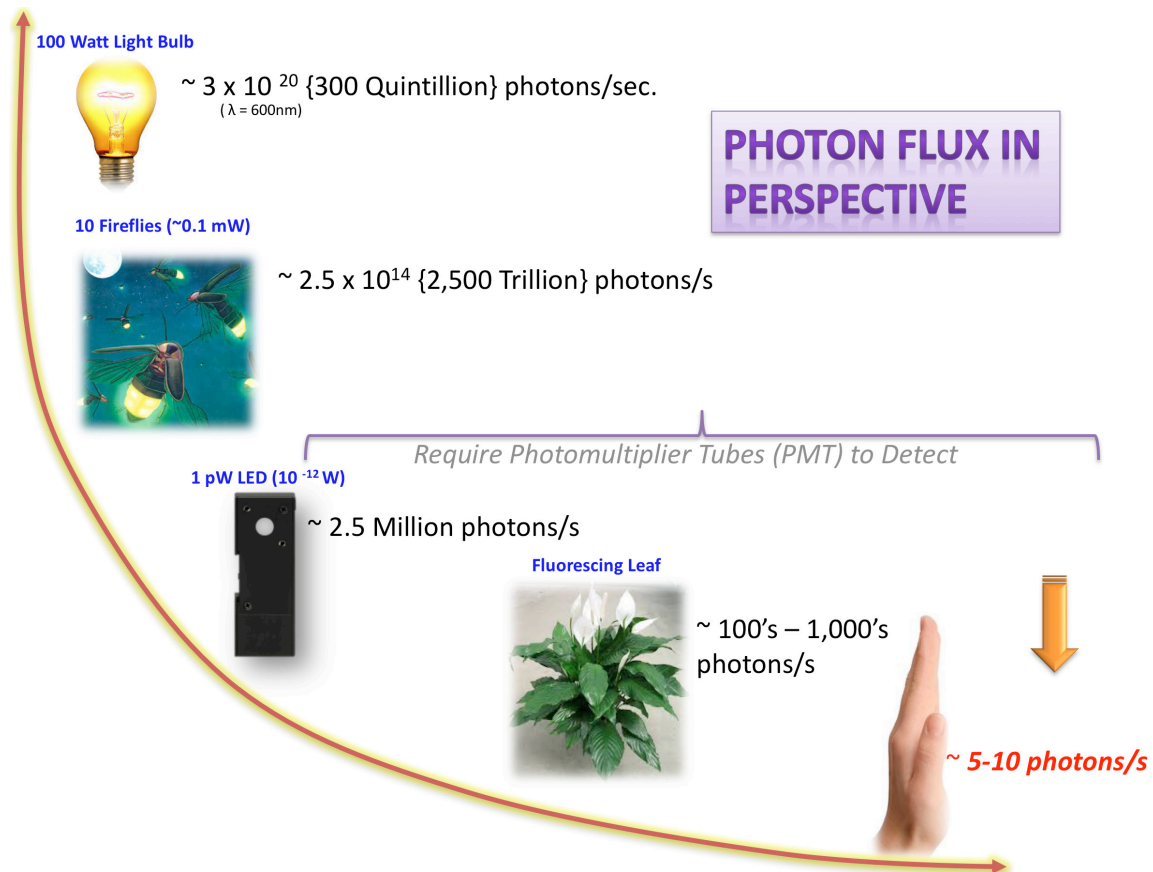


Figure 9. Photon flux in perspective

## B. EXISTING THEORIES

There are two theories that seek to explain biological photoemission. The first considers UPE to be a byproduct of chemical reactions. The second views UPE as generated from a coherent biophotonic field.

### 1. Biochemical Theory: Light as Metabolic Byproduct

Proponents of this perspective view UPE solely as a byproduct of metabolic and thermal activity related to reactive oxygen species (ROS) and excited states of biomolecules. UPE that result from chemically induced means is generally termed

chemical luminescence (CL). Broadly, ROS are formed during enzyme-catalyzing reactions or also during a response to biotic and abiotic stress. “Stress-induced ultra-weak photon emission originates from relaxation of chemically excited species formed under abiotic (physical and chemical) and biotic (virus, bacteria, fungi) stress reaction” (Pospíšil, Prasad, & Rác, 2014, p. 11). These organic biochemical reactions have been studied for some time (c.f. Abeles, 1986; Boveris, Cadenas, & Chance, 1980). This orthodox CL view does not address nor explain the potential bio-informational aspects of photon emission.

## **2. Biophoton Theory: Light Results from a Coherent Biological Field**

The view that biological photons play a role in cellular communication stems from Alexander Gurwitsch’s pioneering work in the early 1900s in which he tried to understand how living tissues transfer information to cells and organs. This theory views biological photoemission as resulting from a “coherent electromagnetic field within and between the cells, from which photons are emitted either by random perturbations or by rather physical processes (Popp et al., 1994, p. 1277). In Gurwitsch’s 1912 paper on morphogenetic field theory, he put forth a theory that the “behaviour of both individual cells and organ rudiments is controlled by a field of forces common to all the elements of an embryo. This field regulates behaviour of individual cells in a developing embryo, routes their movements, controls their divisions and differentiation, and evolves itself with embryo growth” (Voeikov & Belousov, 2007, p. 2). The term “biophoton,” coined by Popp, intentionally refers to this “biophysical” aspect of biological light. Popp too viewed the “photon field as a regulator for the excitation of biological matter” (Popp, 2003a, p. 389). Similarly, Rubik (2002) viewed the “living state [as] a multilevel informed and informing complex dynamic regulatory system” [where] “as part of biologic regulation and maintenance of homeodynamics, cells and tissues may engage in continuous EM [electromagnetic] field sensing and exchange of information” (p. 713). Thus, this theory views the “photon field in living systems as the regulator for the excitation of the biological matter” (Popp, 2003a, p. 389).

Popp contends that the observed hyperbolic relaxation fit as well as the associated Poissonian photon count statistics (PCS) provide evidence that the observed interactions

of light in matter cannot result from random scattering. Other researchers have also extended this coherence view into the quantum nature of light, namely its “squeezed state” thus providing more theoretical support to this perspective (cf. Bajpai, 2004, 2005, 2008; Racine, Rastogi, & Bajpai, 2013).

This dissertation, and the published paper (Oros and Alves 2018) that it draws from, does not argue in support of either theory. Biological systems exhibit properties of both classical biochemical and quantum attributes depending upon the level of analysis and the explanatory description desired. We simply present our results and show alignment with similar published findings in the existing literature.

## **C. WOUND-INDUCED BIOPHOTONS**

The content of this section has been drawn directly from Oros and Alves (2018) with full rights and permissions for usage under the creative commons [CC0 public domain dedication license](https://creativecommons.org/licenses/by/4.0/). The original article can be accessed here: <https://doi.org/10.1371/journal.pone.0198962>

### **1. Plant Photo-Chemical Wounding Responses**

Plants have evolved a variety of means to energetically sense and respond to abiotic and biotic environmental stress. Two typical photochemical signaling responses involve the emission of volatile organic compounds (VOC) and light. Plants are known to release VOCs and green leaf volatiles (GLVs) when tissues are injured (Brilli et al., 2011; Fall et al., 1999; Loreto, Barta, Brilli, & Nogues, 2006; Matsui, Sugimoto, Mano, Ozawa, & Takabayashi, 2012). Both of these emission types are known to occur naturally (i.e., they are self-induced) (Yang, Son, & Kays, 2009) or they can be induced in response to abiotic stress (i.e., temperature, wind, wounding) as well as damage inflicted by herbivores, fungicides, viruses, and bactericides (Matsui et al., 2012). GLVs are derived from the peroxidation of polyunsaturated fatty acids (PUFAs) and are considered the major VOC constituents released by plants. These volatiles are believed to play a role in plant signaling and herbivore plant defense (Matsui et al., 2012; ul Hassan, Zainal, & Ismail, 2015; Wei et al., 2007).

In addition to chemical emissions, all living organisms emit a low intensity luminescence which is spontaneous (or self-induced) as well as induced via injury (Abeles, 1986; Cifra & Pospíšil, 2014; Creath, 2008; Popp, Gurwitsch, Inaba, Slawinski, Cilento, Van Wijk, Schamhart, 1988; Popp, 2003b; Pospíšil et al., 2014; Slawinska & Slawinski, 1983). This phenomenon has been extensively studied in numerous plants, animals, and humans. Further, diseased and injured cells have also been observed to emit more light than healthy ones. Research has revealed that light emitted due to the plant wounding process is related to chlorophyll (Birtic et al., 2011; Flor-Henry, McCabe, de Bruxelles, & Roberts, 2004; Prasad & Pospíšil, 2011), namely singlet chlorophyll ( $^1\text{Chl}^*$ ) within the injured chloroplasts (Pospíšil et al., 2014; Prasad et al., 2017) and that oxygen and lipoxygenase (LOX) are two of the key initiating chemical components essential for wound induced volatiles and biophoton emission.

Lipoxygenase is central to both wound induced volatile chemical and photon emission and requires oxygen for its catalyzing reaction (Abeles, 1986; Boveris et al., 1980). Proton-transfer-reaction mass spectrometry (PTR-MS) analysis of beech and aspen leaf wound induced VOCs in both oxygen ( $\text{O}_2$ ) and nitrogen ( $\text{N}_2$ ) atmospheres revealed that the formation of the hexyl and hexenyl family of compounds was dependent upon oxygen which is essential for the lipoxygenase (LOX) reaction to trigger the formation of fatty acids and hydroperoxides (Fall et al., 1999). Fall et al. also discovered that the emission of the hexenyl family of compounds was not dependent upon light and that there was no pooling of  $\text{C}_6$  aldehydes or alcohols in the unwounded leaves. Similar experiments with *Phragmites australis* reported that the emission of all VOCs, with the exception of acetaldehyde, were oxygen dependent and undetectable in an  $\text{N}_2$  atmosphere (Loreto et al., 2006).

It has been shown that lipid peroxidation is the main source of stress induced photo emission in plants (Birtic et al., 2011; Pospíšil et al., 2014) and that lipoxygenase (LOX2) is responsible for the formation of GLVs in *Arabidopsis* leaves (Mochizuki, Sugimoto, Koeduka, & Matsui, 2016). Lipoxygenases are enzymes that catalyze oxygenation of polyunsaturated fatty acids to form fatty acid hydroperoxides (HPO). Recent studies employing Singlet Oxygen Sensor Green (SOSG) fluorescence imaging (Flors et al., 2006;

Prasad et al., 2017) have shown that singlet oxygen is produced in response to leaf wounding even in the dark. Employment of lipoxygenase inhibitors has also been shown to restrict the formation of triplet carbonyls ( $^3L=O^*$ ) that ultimately inhibit/prevent the formation of singlet chlorophyll ( $^1Chl^*$ ) and singlet oxygen ( $^1O_2$ ) in wounded *Arabidopsis* leaves and bacteria (Morker & Roberts, 2011; Prasad & Pospíšil, 2011; Prasad et al., 2017). These results mutually support the observation that disruption of the lipid peroxidation pathway by inhibiting lipoxygenase—either through elimination of  $O_2$  or through the use of inhibitors (i.e., catechol)—prevents both the hexenyl family VOC emission and singlet chlorophyll and singlet oxygen production. Current research suggests that singlet oxygen and singlet chlorophyll within damaged chloroplasts are mutually implicated in the wound induced photo luminescence process, leading to singlet chlorophyll as the final photon emitters (Pospíšil et al., 2014; Prasad et al., 2017).

We contribute to this body of research by showing that wound-induced leaf photon emission of whole *Spathiphyllum* leaves (*in vivo*) is inhibited when under anoxic stress. Spectral analysis using optical edgepass filters reveal the preponderance of photoemission is  $> 650$  nm. This supports published research identifying chlorophyll molecules as the main emitters of wound induced UPE. These findings support experimental data provided in (Prasad et al., 2017) that inhibition of lipoxygenase production directly effects singlet oxygen production; ultimately inhibiting singlet chlorophyll luminescence.

## **2. Plant Anaerobic Stress**

Plants depend on a continuous supply of environmental oxygen to support life-sustaining biological processes. The effects of plant tissue hypoxia, or anoxia, and its effect on UPE (or chemiluminescence, as it was termed) has been known and studied for some time (Abeles, 1986; Radotic, Radenovic, & Jeremic, 1998; Vartapetian, 2015; Vartapetian, Agapova, Averianov, & Veselovsky, 1974; Vartapetian & Jackson, 1997). Italian and Russian researchers were the initial groups to report on UPE dependence on oxygen in whole plants and extracts of non-chlorophyll containing (etiolated) seedlings of wheat, beans, lentils, and corn (Colli, Facchini, & Guidotti, 1955) and wheat roots (Veselovskii, Sekamova, & Tarusov, 1963). Research involving a variety of plant types: barley seedlings

(Gasanov, Mamedov, & Tarusov, 1963), spinach, hibiscus (Roschger, Devaraj, Scott, & Inaba, 1992), peas, beans, corn seedlings and roots (F. Abeles, Leather, & Forrence, 1978) and pumpkin roots and seedlings (Vartapetian, 2005) in different types of anoxic gasses (N<sub>2</sub>, CO<sub>2</sub>, Ar) have shown that luminescence decreases significantly when plants are placed under anaerobic stress (~90% in N<sub>2</sub> [Abeles et al., 1978]). Further, UPE due to peroxidation of membrane lipids was previously found to be detectable only when oxygen was present in the medium (Vartapetian, 2005). Many of these early studies were performed with first generation photomultiplier tubes (PMTs) and liquid scintillation spectrophotometers (Abeles et al., 1978) with detached / destroyed leaves or leaf and biochemical extracts. Not many UPE experiments, including more recent ones, have examined whole plants in vivo. Our results extend previous research and show that that short periods of anaerobic stress do not completely extinguish UPE and wound induced UPE is significantly inhibited under anoxic conditions. We additionally provide a novel methodology to examine wound induced UPE in aerobic and anaerobic environments.

THIS PAGE INTENTIONALLY LEFT BLANK

## IV. EXPERIMENTAL DESIGN: MATERIALS AND METHODS

The majority of content of this chapter has been drawn directly from Oros and Alves (2018) with full rights and permissions for usage under the creative commons [CC0 public domain dedication license](https://creativecommons.org/licenses/by/4.0/). The original article can be accessed here: <https://doi.org/10.1371/journal.pone.0198962>

### A. SPATHIPHYLLUM TEST CONDITIONS

Plants consisted of two identical Spathiphyllum cultivars also referred to as leaf spathe or Peace Lily, purchased from different local floral merchants. The actual cultivar type (Chen, McConnell, Henny, Everitt, & Anthurium, 2003) was unknown but it was not of the petite variety. Spathiphyllum is an indoor, low-light foliage plant with amphistomatic leaves (Akoumianaki-Ioannidou, Georgakopoulos, Fasseas, & Argyroudi-Akoyunoglou, 2004). The “Spaths” were selected for their small size and large leaves. This enabled measurements to be performed in vivo and allowed the leaf to completely cover the lens aperture. One spath was used for both the aerobic testing (leaves A-C) and the anoxic tests (leaves D-F). The second spath was used for the spectral analysis tests. The plants were not blooming at the time the anoxic and single filter tests were performed. However, the second spath was beginning to bloom during the filter wheel spectrum measurements. The plants were typically kept under indirect sunlight and brought to the lab only on the morning of testing. Once in the lab, plants were exposed to routine laboratory overhead white LED lighting before being placed in the dark enclosure. Non-actinic indirect light (3 W green LED bulb) was used in the dark tent to provide the researcher enough ambient lighting to safely place the plant in the dark enclosure while minimizing light stimulation of the leaf. The leaf was secured to the lens aperture with the upper epidermis facing the photocathode (Figure 10).





*Spathiphyllum* in plant enclosure (S). Shown with single filter lens assembly and front panel removed.

Figure 10. Plant test enclosure. Source: Oros and Alves (2018).

The total enclosure process preparation time averaged approximately 10–15 min. Wounded leaves were only measured once. A new, unwounded leaf was selected for each test (except for the filter wheel spectrum measurement which could not be avoided). The

enclosure was then closed and sealed with 2” AT205 black aluminum foil tape (Thorlabs, Newton, NJ, USA) and the wounding assembly was emplaced.

## **B. PLANT AND DARK TENT TEST ENCLOSURES**

The plant enclosure (vol. 0.019 m<sup>3</sup>) was constructed with 5 mm thick, black plastic-coated TB4 foam hardboard (Thorlabs, Newton, NJ, USA) [Figure 10].

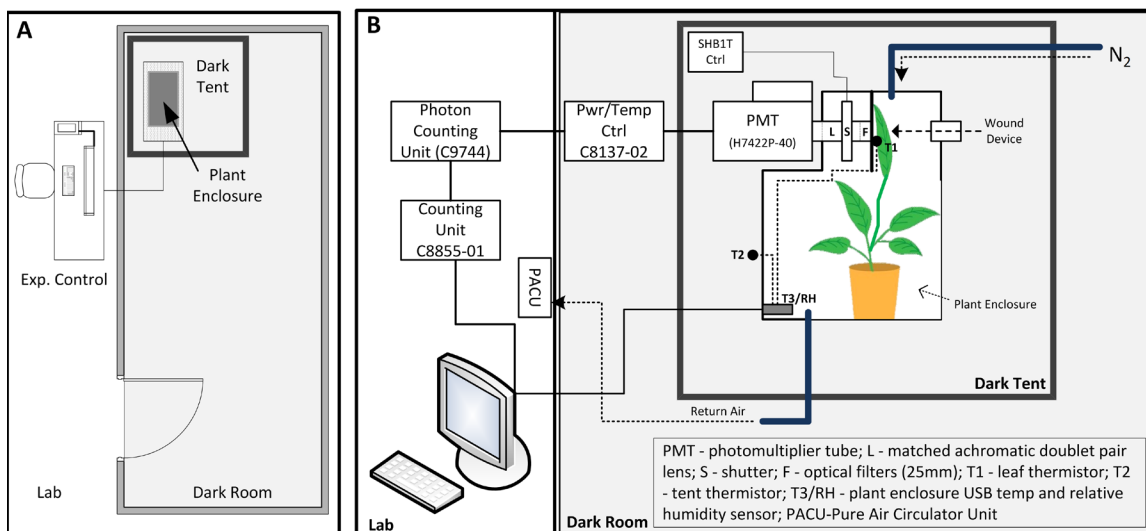
Continuous temperature and relative humidity data were collected during each measurement. A USB temperature and relative humidity (RH) data logger TSP01 (Thorlabs, Newton, NJ, USA), with the status indicator LED removed, was placed inside the plant dark enclosure. The TSP01 monitored the plant enclosure temperature and relative humidity (%). Two thermistors were connected to the TSP01 to additionally measure (1) leaf temperature at the lens tube aperture and (2) dark tent room temperature (connected outside the dark box enclosure).

A small square piece of foam poster board with a 25 mm hole was affixed to the lens tube assembly and used to hold the leaf in place parallel to the focal plane of the lens. A 25 mm hole was cut in the front panel of the plant enclosure and rigged with a lens tube wounding apparatus.

The wounding apparatus was constructed with 25 mm lens tubes, a spring, and a 3 mm bamboo skewer. A 3 mm hole was drilled through the lens caps on each side of the lens tube assembly to guide the skewer to puncture the leaf near the center of the focal plane. The spring allowed the skewer (1) remain retracted while the leaf was positioned to avoid premature plant wounding and (2) to allow it to return to the pre-wounding position. The wound apparatus was operated manually by hand.

The plant enclosure was located inside a dark tent, GGT 5x5 (Gorilla Grow Tent, Inc., Santa Rosa, CA, USA) measuring 1.5 m x 1.5 m x 2.1 m. The inside of the dark tent was lined (4 sides and ceiling) with blackout curtains (Textron) to cover the tent’s internal silver reflective coating. The supplied reflective floor mat was inverted so that the flat black side faced upward. The entrance to the tent was not zippered shut but remained completely covered by overlapping blackout curtains. This allowed easy access. The tent was housed

inside the lab's dark room (6.5 m x 2.8 m x 3.6 m), which was painted black, and the door to the room was covered with an additional blackout curtain to further reduce external light. The overall lab and experiment setup is provided in Figure 11.



(A) Overview of lab and dark room. (B) Photon counting experiment setup.

Figure 11. Experiment layout and test equipment. Source: Oros and Alves (2018).

### C. TESTS INVOLVING NITROGEN (N<sub>2</sub>) GAS

A cylinder of nitrogen gas was placed just outside of the dark tent and ¼” fluoropolymer tubing was run into the tent via a side access vent. When signaled by the synchronization trigger, the researcher entered the dark room and manually turned on/off the N<sub>2</sub> gas. Gas flow was estimated to be ~ 10 liters/s. The air return line of a Pure Air Circulator Unit (PACU) (Thorlabs, Newton, NJ, USA) was connected to the plant enclosure to assist in evacuating room air (4 liters/s) as N<sub>2</sub> gas filled the box. The PACU was not used in closed loop mode. The wounded leaves were exposed to N<sub>2</sub> for 21.3 minutes (t = 6,720–8,000 sec). N<sub>2</sub> and the PACU were then secured and the plant box was allowed to return to normal atmospheric concentrations.

It was anticipated that the PACU would be able to provide clean, dry, VOC-free air in a closed loop mode to the plant enclosure. Aerobic experiment data revealed the combined ambient humidity and large volume of the plant enclosure quickly saturated the

PACU desiccant filter. Subsequent spectral analysis tests did not employ the PACU in closed loop mode. The PACU was only used to assist in air removal of the plant enclosure during the anoxic experiments.

#### **D. ULTRAWEAK PHOTON EMISSION MEASUREMENT**

##### **1. Highly Sensitive PMT**

One-dimensional photon counting was performed using a low noise H7422P-40 (Hamamatsu Photonics, K.K., Iwata City, Japan) photo sensor module (or photomultiplier tube (PMT)). The PMT has a 5 mm gallium arsenide phosphide (GaAsP) photocathode with a spectral response in the visible range of 300–720 nm and a 40% quantum efficiency (QE) at 580 nm. The PMT was configured with a stock heat sink, fan, and Peltier thermoelectric cooling element cable of maintaining the photocathode at a temperature of 0° C. The H7422P-40 was powered with a C8137-02 power and temperature controller (Hamamatsu Photonics, K.K., Iwata City, Japan). Consistently measured dark counts with the lens cap off in the dark room were 5 counts per second (cps) ( $N = 10$ ,  $n = 1,000$ ,  $\langle n \rangle = 4.54$ ,  $\sigma = 3.58$ ). The PMT was connected to a C9744 amplifier and pulse shaping unit (Hamamatsu Photonics, K.K., Iwata City, Japan) and then to a C8855-01 photon counting unit (Hamamatsu Photonics, K.K., Iwata City, Japan) and connected via USB to either an Apple iMAC or Macbook Pro (running VMware, Win7E) or via PC (Win7E). The photon counting hardware is shown in Figure 12. The discrimination level of the C9744 was manually set to 80 mV. The C8855-01 employs dual counters and is capable of measuring input signals with no dead time.

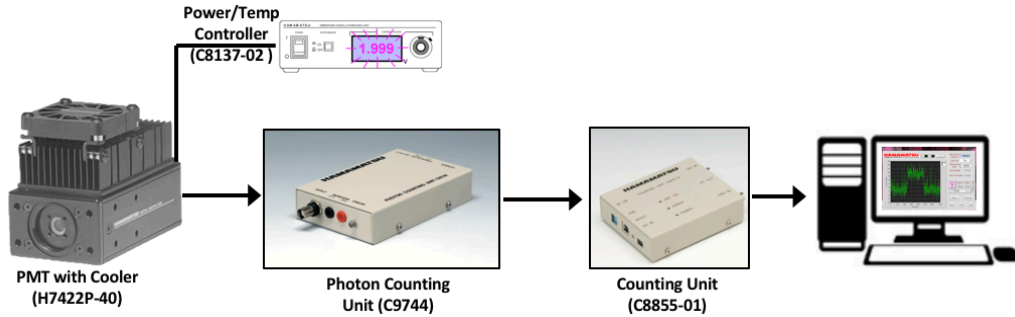
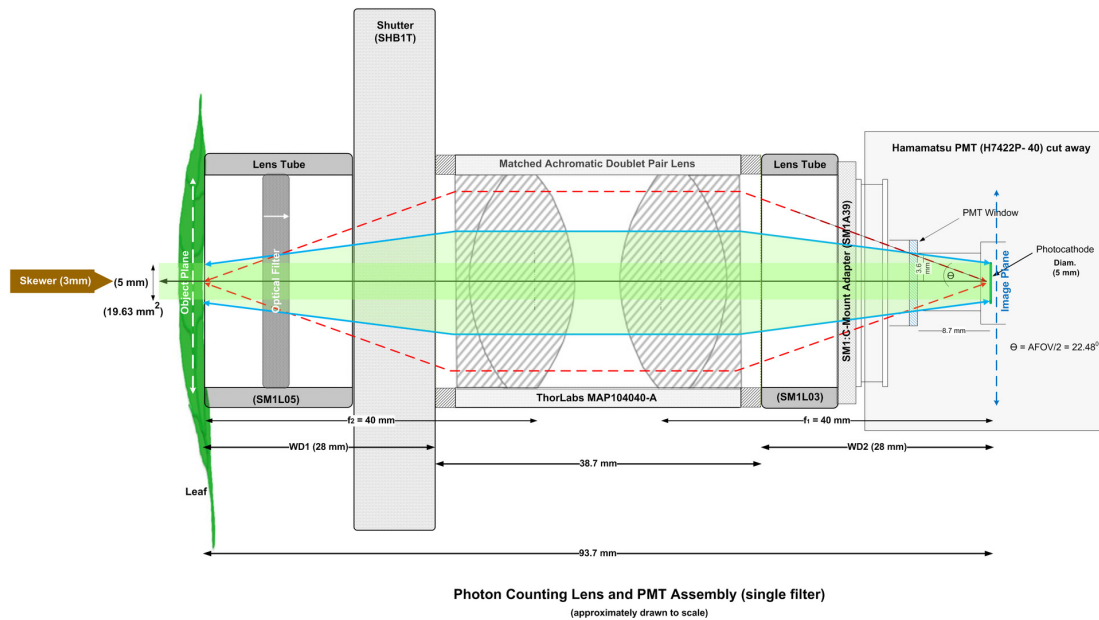


Figure 12. Photon counting hardware Source: Hamamatsu Photonics (2018a, 2018b, 2005).

The PMT was equipped with an anti-reflective (AR) coated, matched achromatic doublet pair lens. A matched achromatic doublet pair lens consists of two identical achromatic doublet pairs housed (in this case) in an SM1 (1.035"-40) lens tube. When combined they create a finite conjugate configuration where the object and image are a finite distance from the lens pair. This creates an image relay system as opposed to an image magnifier. Two such lenses were used: (1) MAP104040-A for the four individual leaf measurements and (2) MAP105050-A (both from Thorlabs, Newton, NJ, USA) for the filter wheel spectroscopy experiments. The lens system magnification was 1:1 with focal lengths ( $f_1$  &  $f_2$ ) of 40 mm and 50 mm respectively. Similarly, the working distances (where  $WD_1 = WD_2$ ) of the MAP104040-A and MAP105050-A were 28 mm and 38 mm respectively. The object and image planes were located at the lens WD. In this arrangement, the object image height is equal to the photocathode diameter of 5 mm, equating to an object image area of  $19.63 \text{ mm}^2$ . The angular field of view (AFOV), ( $44.96^\circ$  for the MAP-104040 and  $32.8^\circ$  for the MAP-105050 lens assemblies), was constrained by both the PMT housing and the photocathode size, which was recessed  $\sim 16.3$  mm from the front face of the PMT module. (See Figure 13 and Figure 31 for a complete description of the lens assemblies).



Primary PMT lens configuration with matched achromatic doublet pair lens ( $f=40$  mm) and mechanical shutter (SHB1T). Single edgepass filters were manually inserted as indicated when used for spectroscopy measurements.

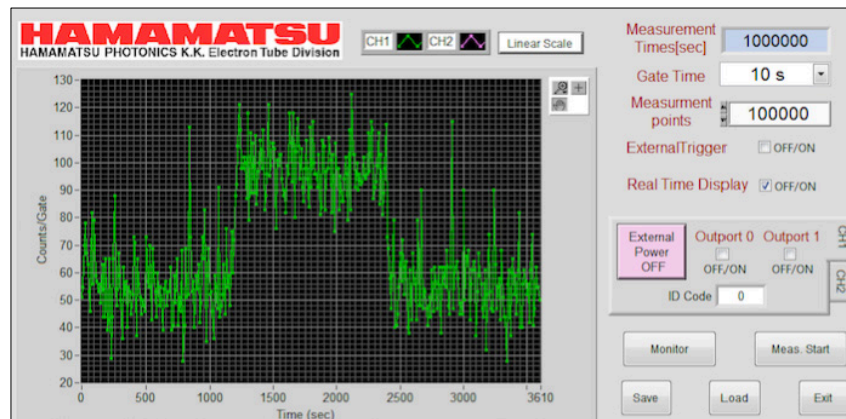
Figure 13. Primary photon counting lens and PMT assembly. Source: Oros and Alves (2018).

An electronic shutter SHB1T (Thorlabs, Newton, NJ, USA) was inserted between the lens tube and the matched achromatic doublet pair. The shutter controller was inside the dark tent and was controlled manually. The SHB1T's LEDs were blacked out with a combination of black liquid tape and black aluminum tape to prevent any light leakage. The shutter was removed for the filter wheel spectroscopy measurements and a black aluminum 25 mm disk (filter wheel position #2) was used instead.

## 2. Software

The C8855-01 supplied software (Figure 14) was used to control the PMT and record the photocount data. Photon counting data (.csv) and temperature log files (.txt) were saved and uploaded into Origin Pro 2017 and Microsoft Excel (2011) for post-experiment data analysis as required. MS Excel was used to further analyze Origin Pro photon counting statistic data to calculate bin frequencies and predicted Poisson distribution data. The spreadsheet formula "POISSON.DIST(x, mean, FALSE)" was used

to calculate the predicted Poisson distribution where in our case  $x = \text{Bin}$  (or “expected count”),  $\text{mean} = \text{mean}$ , and  $\text{FALSE} = \text{the cumulative value to return the probability mass function that the number of events occurring will be exactly } x$ . Calculated values were then imported back into Origin Pro for graphing and further analysis.



A one-second gate time was used for all experiments.

Figure 14. Screen shot of Hamamatsu-supplied photon counting software

The open source sound editing software Audacity (v 2.1.2) was used to provide the experimenter warning tones to synchronize the controlled timing of manual wound inducement and filter wheel positioning.

## E. SPECTROSCOPY MEASUREMENTS

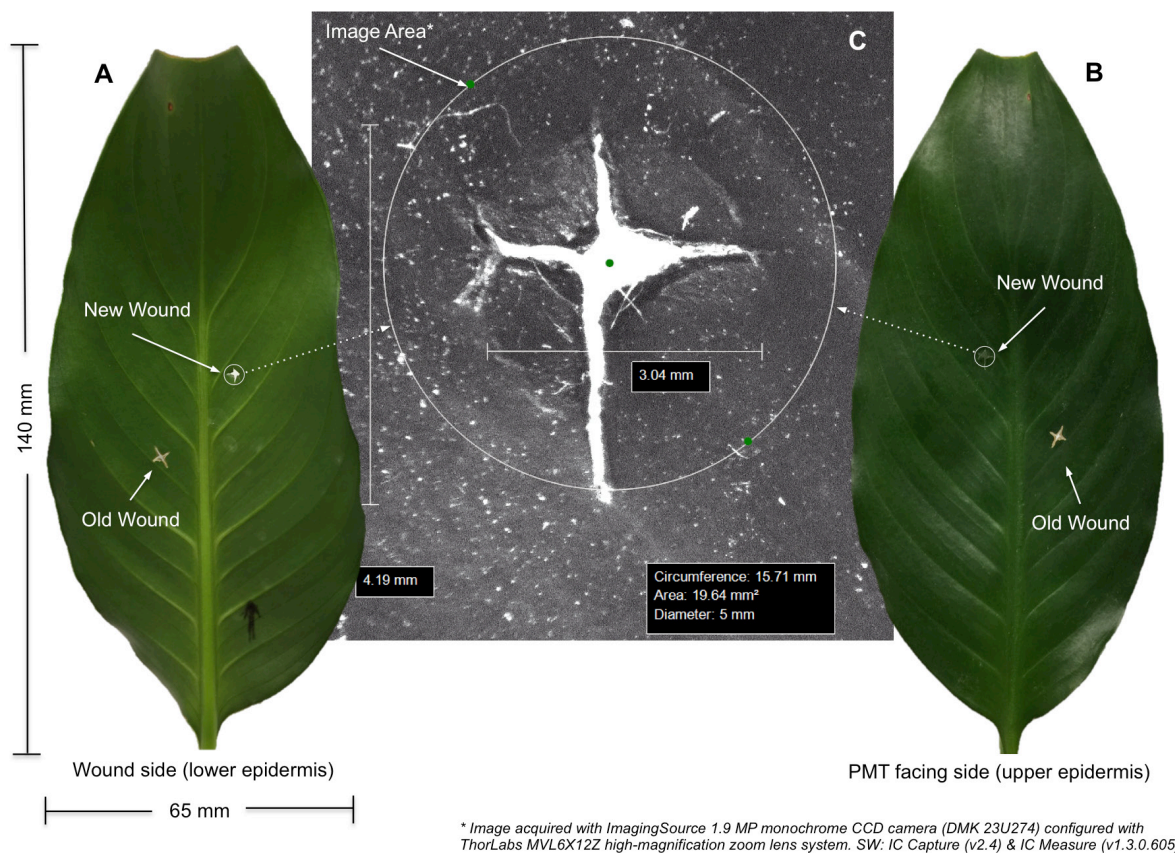
One of the two Spaths was dedicated to the spectral analysis experiments. Two types of spectral analysis tests were performed. The first set of tests consisted of four separate, long duration (~3.5–5 hr) measurements using a single edgepass filter with the primary lens assembly (Figure 13). The optical filters (Thorlabs, Newton, NJ, USA) are listed in Table 1. A new, healthy, unwounded leaf was used for each of these tests. Leaf spectral response was measured continuously throughout the dark adaptation and wounding phases using filters 1, 2, 5, and 6 (see Table 1).

Table 1. Edgepass filters used for spectral analysis. Source: Oros and Alves (2018).

Filter	Filter Type/ (Model #)	Cutoff (λ)	Overall Band (λ)	Avg. Transmittance
1	Short Pass (SP500) (FESH0500)	500 nm	388 – 501 nm	93.72%
2	Long Pass (LP550) (FELH0550)	550 nm	546 – 720 nm	94.70%
3	Short Pass (SP600) (FESH0600)	600 nm	393 - 600 nm	95.73%
4	Long Pass (LP600) (FELH0600)	600 nm	596 – 720 nm	95.37%
5	Long Pass (LP650) (FELH0650)	650 nm	647 – 720 nm	94.43%
6	Long Pass (LP700) (FELH0700)	700 nm	700 – 720 nm	85.04%

The second spectral test employed a USB controlled, 25 mm, 8-position High Speed filter wheel (HSFW), Model 84–889 (Edmund Optics, Barrington, NJ, USA) and the MAP105050-A achromatic doublet pair lens (Figure 31). A single previously wounded leaf was used for this measurement though the new wound site was targeted on a healthy portion of the leaf opposite the midrib of the original wound that was over 60 days old (Figure 15).





(A) Leaf lower epidermis (wound side) showing previous healed wound, and new wound site. (B) Leaf upper epidermis (PMT facing side) showing old and new wounds. (C) High magnification CCD image capture of wound site. Circle is approximate image area (19.64 mm<sup>2</sup>).

Figure 15. Images of leaf used for filter wheel wound spectrum measurements.  
Source: Oros and Alves (2018).

Thirteen measurement sequences were recorded over 4.5 hrs using filters 3, 4, 5, and 6 (see Table 1). Spectrum was measured with each filter for ~ 20 sec. The open (O)-no filter and (B) black – black aluminum disk positions were used to visually identify filter positions in the data (duration 5 sec). The filter wheel measurement sequence (total 130 s): | (O) | (B) | SP600 | (O) | (B) | LP600 | (O) | (B) | LP650 | (O) | (B) | LP700 | (O) | (B) | was repeated every 15 minutes (from t = 60 s to t = 6,300 s; N = 8) until wounding. The filter sequence was then repeated four times continuously beginning 60 s after wounding (N = 4). The last measurement was recorded at ~4.375 hrs (N = 1). Dark counts during these tests were obtained with the “black” filter position. No shutter was used with this lens

configuration. The leaf and enclosure temperatures (23.7° C / 21.0° C) respectively, were stable within 1° C from wounding through the end of the experiment with relative humidity (RH) increasing only 3% over the same time period from 60.9–63.9%.

Filter data was normalized by dividing the measured photon counts by each filter's average transmission (%) value (manufacturer provided) for the respective wavelength band (see Table 1). Filter movement was controlled manually from in the lab via supplied software (OPTEC, Inc., v2.0.9) using an audio timing sequence created in Audacity (see Software).

THIS PAGE INTENTIONALLY LEFT BLANK

## V. EXPERIMENTAL RESULTS AND DISCUSSION

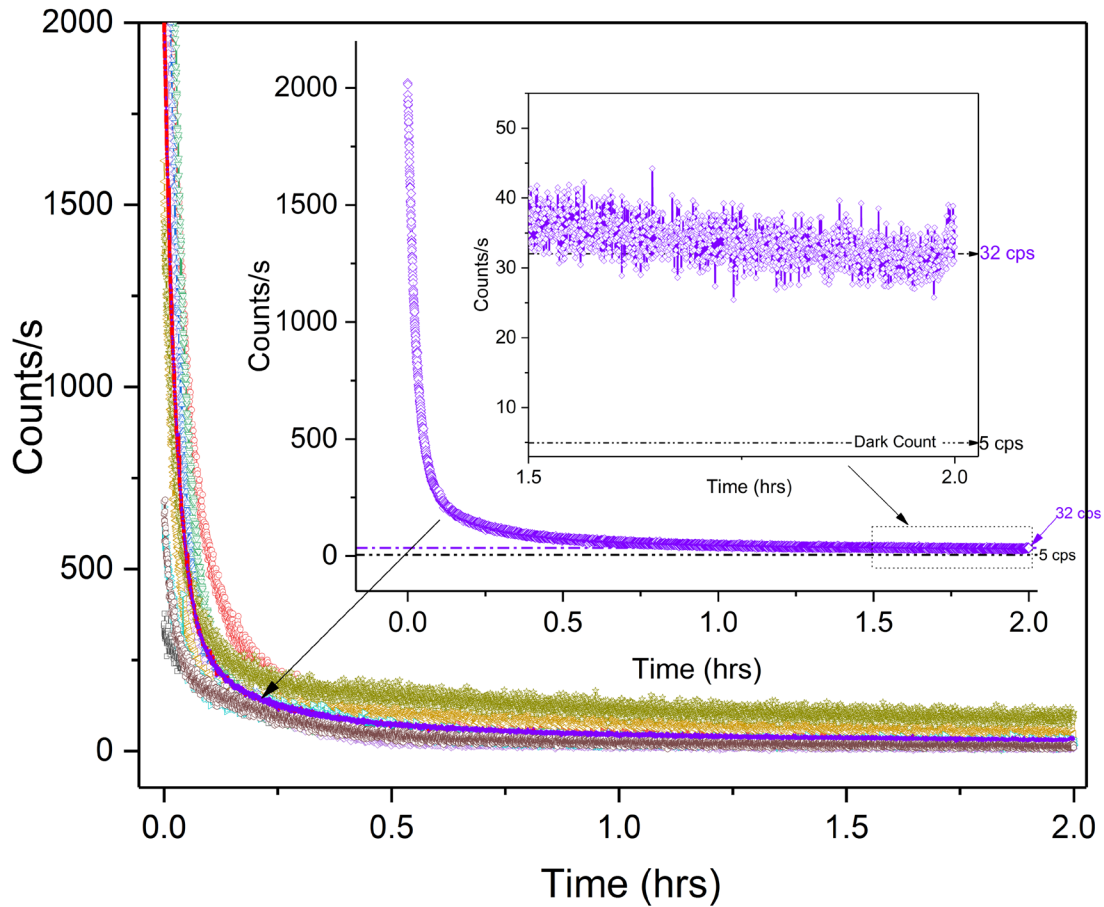
The majority of content of this chapter has been drawn directly from Oros and Alves (2018) with full rights and permissions for usage under the creative commons [CC0 public domain dedication license](https://creativecommons.org/licenses/by/4.0/). The original article can be accessed here: <https://doi.org/10.1371/journal.pone.0198962>

### A. SPONTANEOUS ULTRAWEAK PHOTON EMISSION FROM SPATHIPHYLLUM LEAVES

Spontaneous ultraweak photon emission from *Spathiphyllum* leaves was measured *in vivo* with a low noise, high quantum efficiency (QE; 580 nm) electronically cooled PMT model H7422P-40 (Hamamatsu Photonics, K.K., Iwata City, Japan) fitted with a matched achromatic doublet pair lens (Figure 13). This matched lens pair forms an image relay system where the image height is equal to the photocathode diameter. (See material and methods section for more details). The spectral response of the PMT is in the visible wavelength band (300–720 nm). All experiments were carried out in a controlled, nested dark room lab environment (Figure 11). Whole plants were placed in a dark box enclosure while under non-actinic green LED light. The selected upper leaf epidermis was placed facing the photocathode in the object plane. Care was taken to ensure leaves were not unintentionally wounded during emplacement. Once secured in place, the plants were allowed to dark-adapt for two hours prior to mechanical wounding. Plants were wounded by manually piercing the lamina between the midrib and veins with a 3 mm diameter bamboo skewer approximately centered in the object plane. Continuous photon counting was performed from fluorescent decay throughout the wounding-decay sequence. Dark count measurements were crosschecked against historical data by closing the lens shutter at the completion of each experiment. Dark counts never exceeded 5 cps. Two non-blooming *Spaths* (of non-petite variety) were used for the wounding and single filter spectroscopy measurements. Only healthy, unwounded leaves were used for these tests. The spectral filter wheel test was performed with an early blooming *spath* on a previously wounded leaf.

## B. BIOPHOTON PRE-WOUND DARK ADAPTATION ANALYSIS

Figure 16 shows the two-hour fluorescent decay plots recorded in the visual wavelength band (300–720 nm) for nine different dark-adapting *Spathiphyllum* leaves previously exposed to routine, overhead laboratory white LED lighting.



Nine sample decay plots of dark-adapting *Spathiphyllum*. Purple curve (and inset) depicts the sample average. Enlarged scale of basal count (1.5–2.0 hrs.) reveals 32 cps after two hours. Average dark count is 5 cps.

Figure 16. *Spathiphyllum* dark-adaptation decay plots. Source: Oros and Alves (2018).

We chose a two hour pre-wounding dark adaptation time to be consistent with similar studies (Birtic et al., 2011; Flor-Henry et al., 2004). The nine individual decay plots were averaged (purple plot). Only extreme outliers ( $> 2.7 \sigma$ ) attributable to PMT shot noise

or other electrical disturbances were masked and removed from data calculations. It should be noted that the overall fluorescent decay required ~2 hours for the decay rate to minimize. However, the photoemission never reached zero and yielding an average basal photocount of 32 cps (27 cps greater than the typical dark count of the PMT). Our data clearly shows a significant basal photo luminescence well after what is considered normal chlorophyll fluorescent decay.

The average decay data was then fit to both double exponential and hyperbolic decay functions. The double exponential decay curve was fit to the equation:

$$y = A_1 e^{(-x/t_1)} + A_2 e^{(-x/t_2)} + y_0, \quad (1)$$

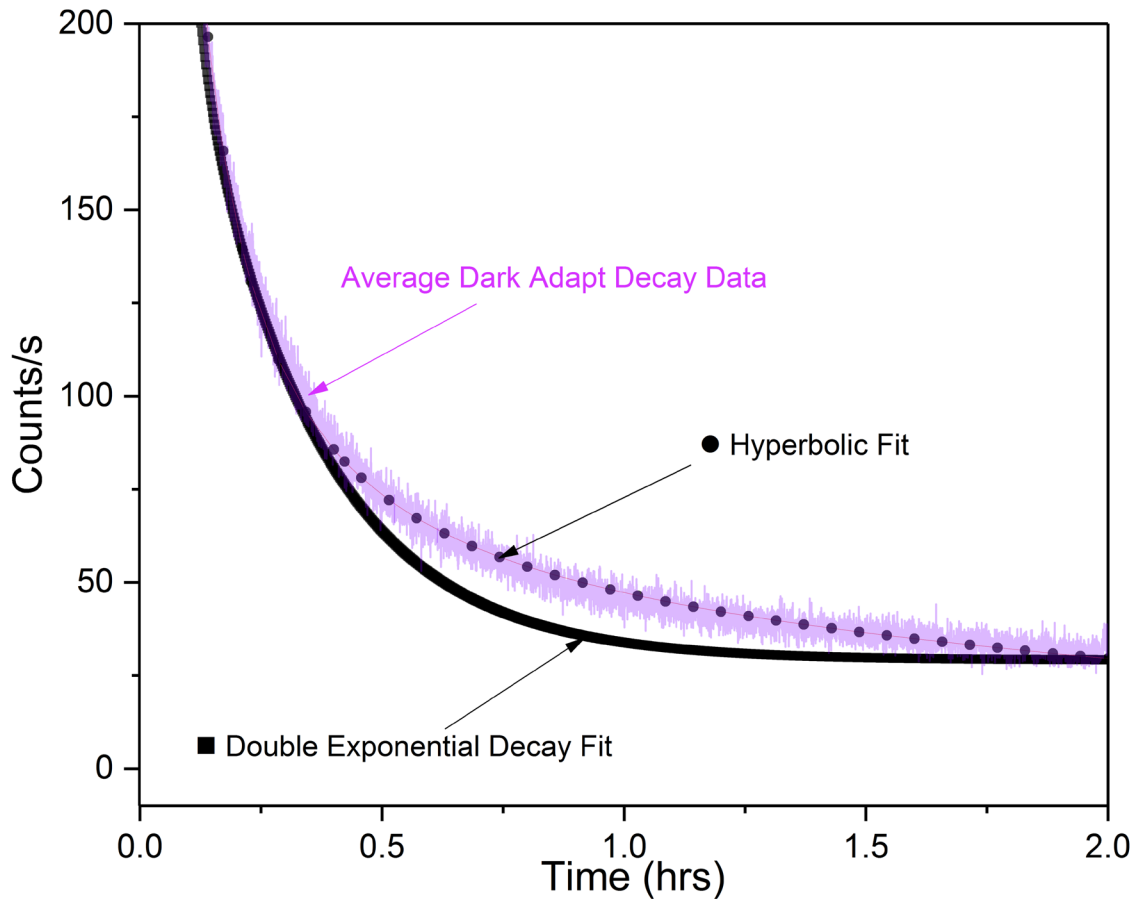
where ( $y_0 = 36.5$ ;  $A_1=1721$ ;  $t_1=99$ ;  $A_2=245$ ; and  $t_2=955$ ).

The hyperbolic decay curve was fit to the function:

$$f = ax^2 + bxy + cy^2 + dx + e(y-1) \quad (2)$$

where ( $a = 2.1 \times 10^{-8}$ ,  $b = 1.2 \times 10^{-5}$ ,  $c = 3.4 \times 10^{-7}$ ,  $d = -3.8 \times 10^{-4}$ ,  $e = -2.7 \times 10^{-4}$ ).

The hyperbolic function best fit the data (Figure 17). These results correspond with previously reported research that observed the hyperbolic relaxation nature of stimulated biophoton emission both from actinic light (Popp, 2003a; Popp et al., 1994; Shen, 2003) and through total destruction of a plant (Winkler, Guttenberger, & Klima, 2009). Research involving UPE of anti-cancer herbs stressed through water deprivation, however, reported a double exponential fit though experimental details were limited (Wu & He, 2009).



Comparison of *Spathiphyllum* dark-adaptation decay data with double exponential and hyperbolic curve equations. Magenta line is 9 sample average decay data. Figure shows hyperbolic curve most closely approximates the data.

Figure 17. Dark-adaptation decay curve fitting. Source: Oros and Alves (2018).

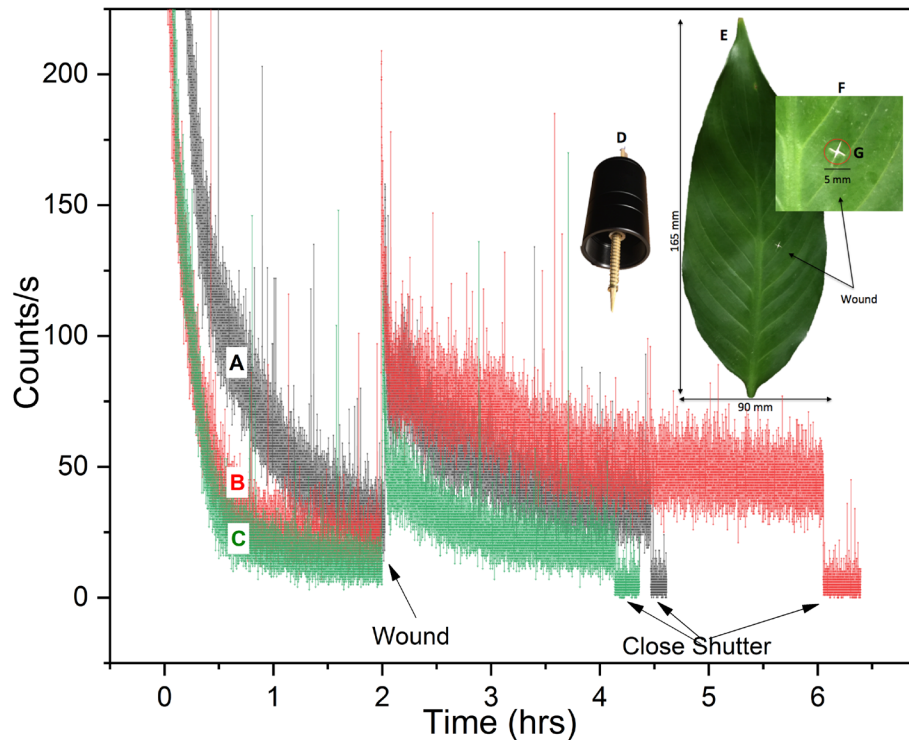
### C. BIOPHOTON WOUND ANALYSES

To investigate the dependency of wound induced UPE on oxygen; we first characterized leaf luminescence in air at room temperature. Two dark enclosures were eventually constructed. The initial, large enclosure (L) measured 25'' x 17'' x 21'' (~ 5.2 ft<sup>3</sup>) and was placed on the optical table in the dark tent. This large enclosure housed both the PMT and the plant. To mitigate possible effects caused from the PMT cooling fan's air circulation, a smaller enclosure (S) was constructed that allowed only the PMT lens assembly to protrude into the plant box. Plant (#1) was used for aerobic (leaves A-C) and anoxic (leaves D-F) wounding experiments. Plant (#2) was used for the spectral analysis

tests. Only leaf (A) was tested in enclosure (L). All subsequent tests were performed in enclosure (S). No more than one test/day was performed and the plant was returned to indirect natural lighting at the end of each day's testing.

### 1. Wound-Induced Biophoton Emission (Aerobic)

Wounding of dark-adapted *Spathiphyllum* leaves under aerobic conditions induced significant biophoton emission. Photon counts increased from about 79–126 cps above the pre-wound basal rate and did not decay back to the pre-wound level even after 4 hours of continuous observation (leaf B). Figure 18 depicts the aerobic wound data recorded for each leaf. The photo inset shows the wounding apparatus and a typical leaf wound site. Observed wounding profiles were similar to those of cucumber and wheat seedlings treated with a toxic agents (Popp et al., 1994, 1981).

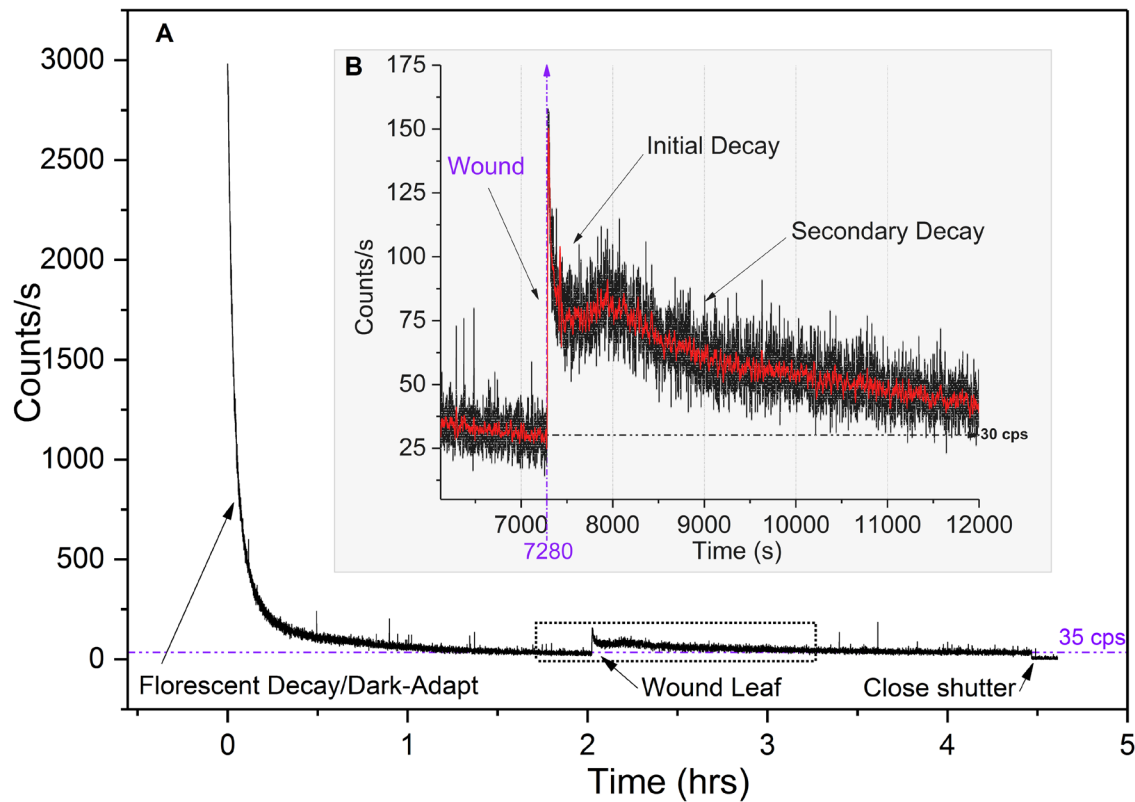


UPE (300–720 nm) of three *Spathiphyllum* leaves (A-C) during aerobic dark-adaptation and wounding at room temperature. (A) Plant in original (large) enclosure. (B-C) Plant placed in smaller enclosure. Photo inset shows wounding apparatus (D) with 3.0 mm bamboo skewer a typical leaf with wound site highlighted (E) and enlargement of the wound (F) showing approximate image area.

Figure 18. Aerobic wounding UPE. Source: Oros and Alves (2018).



Detailed analysis of the aerobic wound induced photon count data revealed two distinct post-wound exponential decays. As expected, the initial decay was observed immediately upon wounding. Secondary decays were observed about 200–300 s after the initial wound decay following a brief plateau in 6 out of 7 measurements. Figure 19 shows the photon count results from one aerobic decay-wound sequence. The enlarged inset highlights the primary and secondary decays.



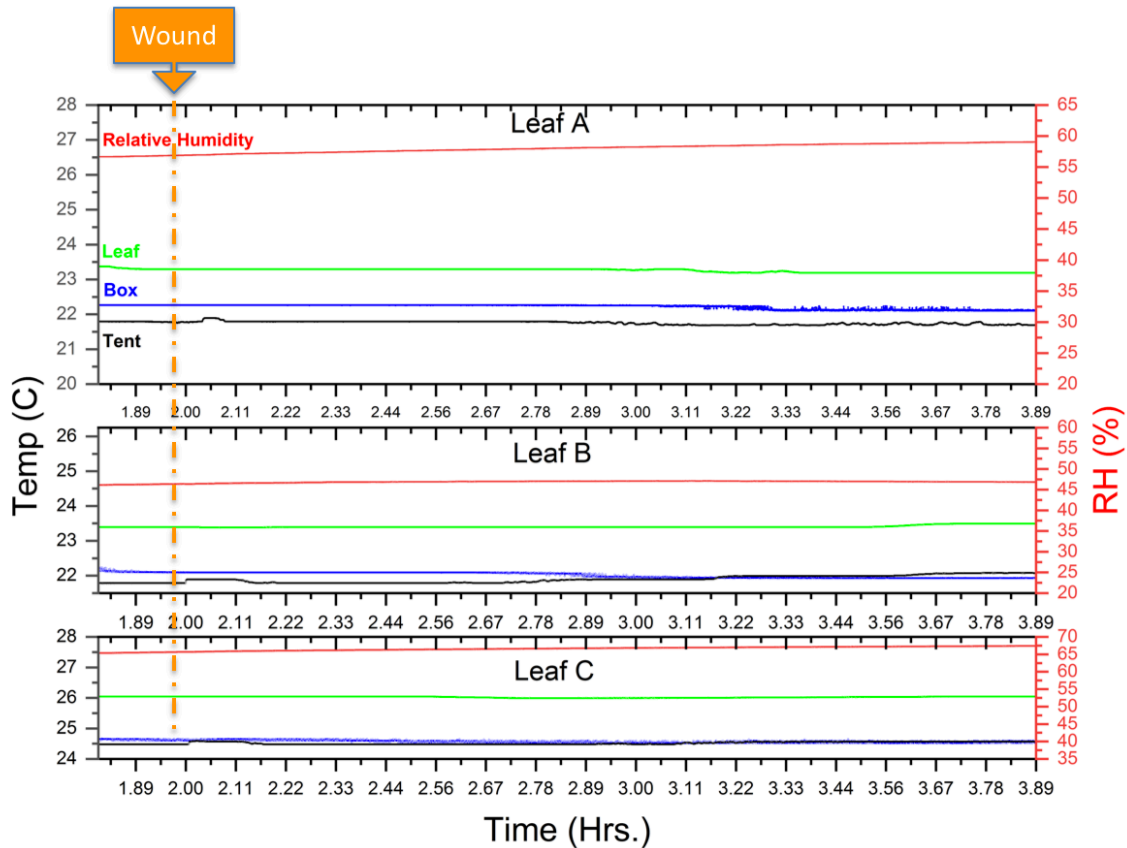
Typical hyperbolic and dual post wound exponential decays (in air). (A) Complete fluorescent decay/dark-adapt—wounding profile. (B) Enlarged view of wounding data. Note primary and secondary post wound decays. Red curve is 25-point data smoothing for trend visibility.

Figure 19. Aerobic wound decay trends. Source: Oros and Alves (2018).

Both initial and secondary decay curves were fit to a double exponential decay function (see photon counting statistics (PCS) section). The mechanical wounding decay plots differ from typical white or monochromatic light induced excitation decays in that they exhibited no hyperbolic relaxation even after 3.8 hours. We analyzed both pre-wound

(post hyperbolic decay) and post wound (secondary exponential decay) photocount data and found both pre- and post-wound photon count distributions closely approximate a Poisson distribution (See PCS section).

It is unclear what biological processes underlay the dual decay phenomena observed. Leaf temperature and humidity did not appear to be significant factors, varying only by 0.2°C and 2–4% respectively during the wounding phase (Figure 20).



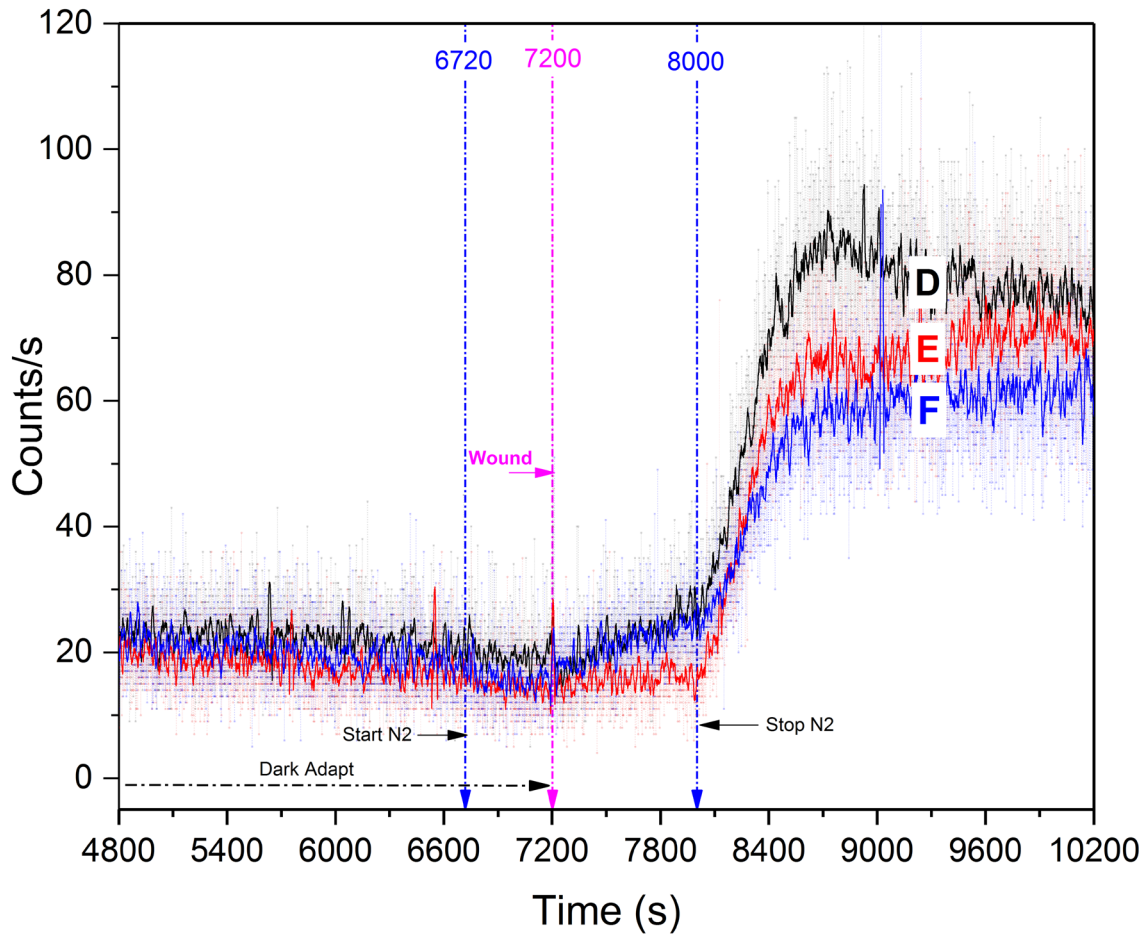
Temperature (C) and relative humidity (RH) data collected during aerobic wounding experiments for each leaf (A-C). Box = plant enclosure; Tent = dark tent. Leaf temperature did not vary during wounding phase. Slight increase in tent temperature reflects temperature change when researcher temporarily entered the tent to induce wounding.

Figure 20. Aerobic wounding temperature and humidity data

We suspect that extreme photon counts occasionally observed during the initial tissue wound is attributable to a combination of physical rubbing and destruction of the cell membranes (triboluminescence) coupled with immediate, localized wound induced biochemical processes (oxidative reactions (Prasad et al., 2017)) that have been extensively studied and reported. In addition, chlorophyll molecules are able to reabsorb fluorescence emitted at 680–690 nm within a leaf (Cordón & Lagorio, 2006; Evans, von Caemmerer, 2018; Lagorio, Cordon, & Iriel, 2015; Misra, Misra, & Singh, 2012; Pedrós, Moya, Goulas, & Jacquemoud, 2008). Therefore, wound site UPE are continually re-absorbed/re-emitted and possibly contribute to the brief secondary rise in luminescence (leading to the plateau) coinciding with the buildup and longer duration lipid peroxidation processes and singlet oxygen/singlet chlorophyll generation cycle. These induced metabolic processes eventually reach a quasi-steady state that is then evidenced in the Poissonian photocount distributions.

## **2. Wound-Induced Biophoton Emission (Anaerobic Conditions)**

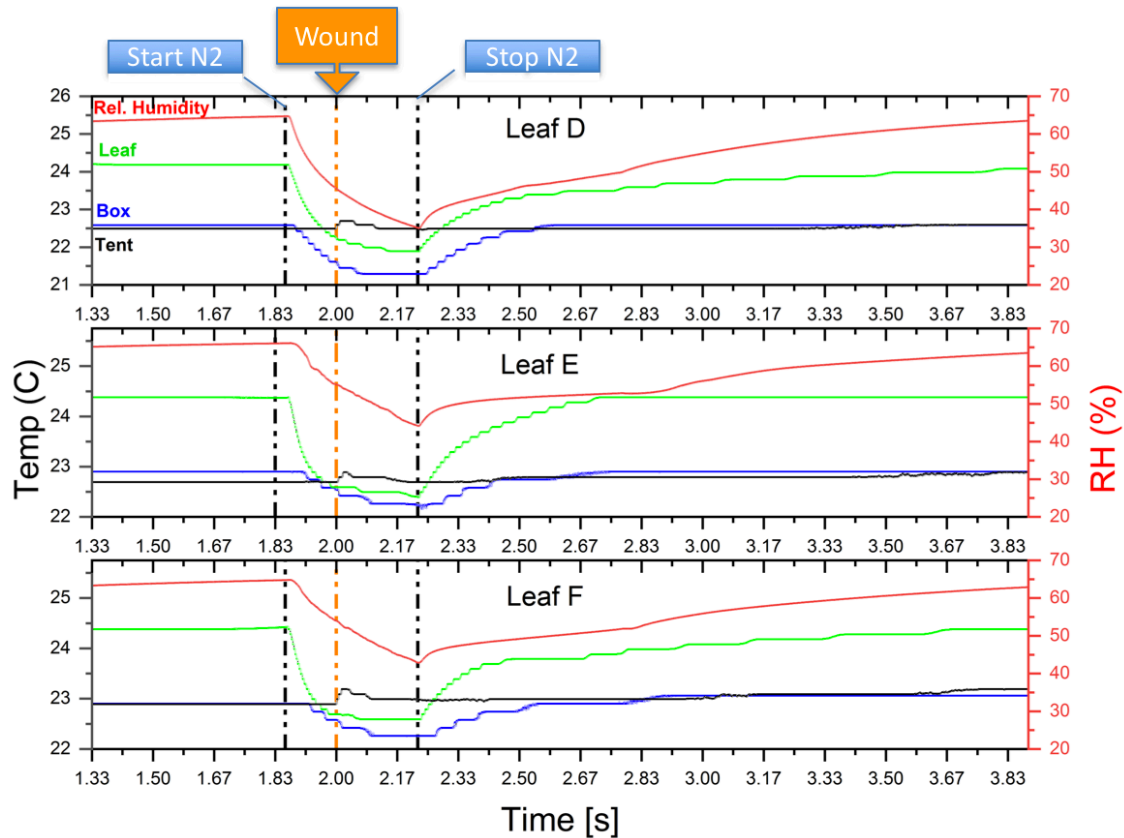
Nitrogen gas was flowed into the plant chamber at  $t = 6,700$  s and was secured at  $t = 8,000$  s for a total incubation time of 1,300 s (21.67 min.). Three leaves were tested, each on separate days. Nitrogen had no noticeable effect on dark adaptation decay photocounts. Photon counts decreased only by 2–3 cps below the basal rate when nitrogen was introduced 500 s prior to wounding but UPE remained well above the noise floor. At no time did UPE decrease to zero and no transient increase in photocounts was observed when  $N_2$  was introduced, showing a good agreement to what was as previously reported by other researchers (Roschger et al., 1992; Vartapetian et al., 1974). While others have reported significant red light induced UPE from leaves under  $N_2$  incubation (Buttler, 1962), We observed that wound-induced photon emission intensity was greatly inhibited by the anoxic environment, increasing only  $\sim 8$  cps in 2/3 trials. Once nitrogen flow was ceased, biophoton emission increased significantly (peaking  $\sim 90$  cps (Leaf D)) as the chamber was allowed to slowly return to normal aerobic atmospheric conditions (Figure 21). Pre and post anoxic stress linear regression of average wound data was analyzed and is discussed in the PCS section.



Moderate increase in photocounts was observed upon anoxic wounding in leaves (D, F). No increase in counts was observed with leaf (E). 25-point smoothing of curve data was used for data visualization.

Figure 21. *Spathiphyllum* wounding UPE while under anoxic stress (nitrogen gas). Source: Oros and Alves (2018).

Anoxic wounding temperature data (Figure 22) revealed a slight temperature decrease of  $\sim 2^{\circ}\text{C}$  (leaf and plant enclosure) upon introduction of nitrogen into the enclosure. This was expected since the nitrogen gas released from the cylinder was much colder than the ambient temperature. Displacement of ambient atmosphere with pure nitrogen gas also depleted the atmospheric water vapor resulting in a decrease in relative humidity of  $\sim 30\%$ . These minor atmospheric affects were negligible and could not account for the suppression of anoxic photoemission.



Temperature (C) and relative humidity (RH) data collected during anoxic wounding experiments for each leaf (D-F). A decrease in both leaf and plant enclosure (box) temperatures ( $\sim 2^{\circ}$  C) and relative humidity ( $\sim 30\%$ ) were observed during nitrogen incubation. Dark tent temperature remained constant (slight increase indicates when researcher temporarily entered the tent to inflict wound). Temperature and humidity eventually returned to initial conditions upon cessation of nitrogen flow.

Figure 22. Anoxic wounding temperature and humidity data

The purpose of these anoxic tests was to complement recent research that has shown that chemical inhibition of lipoxygenase directly effects wound induced UPE. We believe we have shown that wounding of leaves *in vivo* in an anaerobic environment restricts the amount of oxygen available for the lipoxygenase catalyzed wounding reactions and ultimately inhibits biophoton emission.

#### D. PHOTON COUNTING STATISTICS (PCS) OF PRE- AND POST-WOUND DATA

We measured photon count statistics of wounded leaves in air and nitrogen in order to compare the observed frequencies with a Poissonian probability distribution as performed in previous studies (Popp, Li, Mei, Galle, & Neurohr, 1988; Popp, 2003a; Shen, Liu, Li, 1993; Shen, 2003). The frequencies of which  $k_n$  photon counts were registered within a bin ( $n$ ) were obtained using: □

$$F(k_n) = \frac{k_n}{k_t}, \quad (3)$$

where the total photon bin counts is given by

$$k_t = \sum_{i=0}^{imax} k_i. \quad (4)$$

Extreme outliers were excluded from the total counts. The Poisson predicted probability distributions of registering ( $n$ ) photons in a preset time interval ( $\Delta t$ ) was then calculated by:

$$p(n, \Delta t) = \frac{\langle n \rangle^n}{n!} e^{-\langle n \rangle}, \quad (5)$$

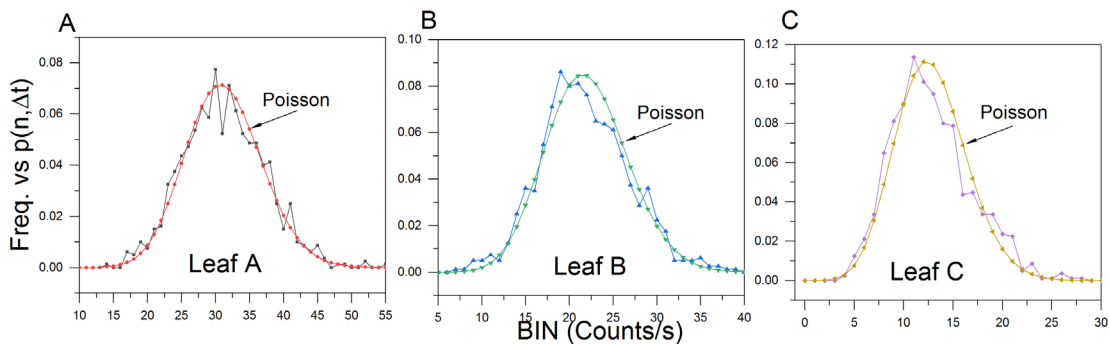
where  $n$  = Bin photon count ( $n = 0, 1, 2, 3 \dots \max$ ),  $\langle n \rangle$  = mean of all counts within preset time  $\Delta t$ , and Variance =  $\sigma^2 = \langle n \rangle$ .

Pre-wound (air & N<sub>2</sub>), wound (air & N<sub>2</sub>), and post wound (air) frequency and Poisson calculations were performed.

## 1. Aerobic PCS

### a. *Pre-wounding Hyperbolic Fluorescence/Dark-Adaptation Decay*

Hyperbolic relaxation decay of normal (photosynthetic) and stimulated (actinic) biophoton emission data has been used to support theoretic claims that a non-local coherent electromagnetic field regulates photon emission (Bajpai, 1999; Popp, Li, Mei, Galle, Neurohr, 1988; Popp, 2003a; Popp et al., 1994; Shen, Liu, Li, 1993; Shen, 2003). Research has also shown that upon hyperbolic relaxation to a “quasi-stationary state,” the probability  $p(n, \Delta t)$  of registering  $n$  photons ( $n = 0, 1, 2, \dots$ ) within the preset time interval ( $\Delta t$ ) follows a Poissonian distribution (Popp et al., 1994). PCS analysis of the last 800s of aerobic hyperbolic relaxation decay curve data closely follows a Poisson distribution (Figure 23).

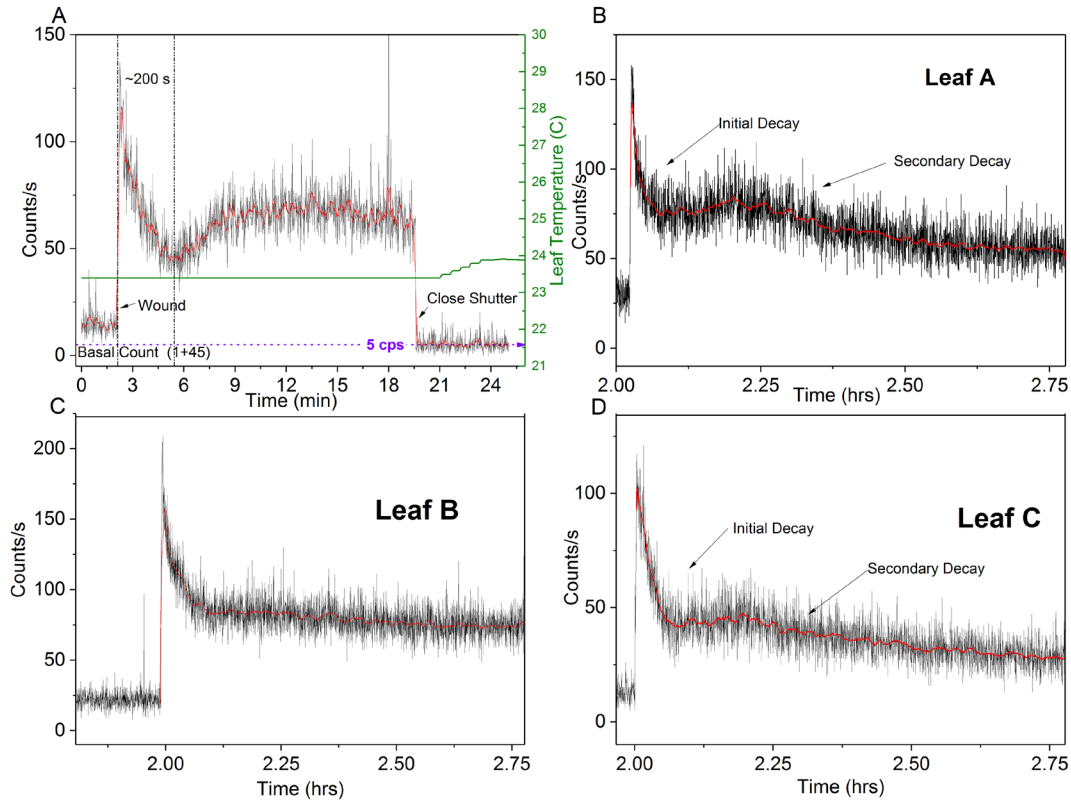


Aerobic photocount observed frequencies vs. Poisson predicted distributions (leaves A-C) of the hyperbolic decay data (last 800 s). Observed photon count frequencies closely approximate a Poisson predicted distribution ( $\mu_A = 31.25$ ;  $\mu_B = 22.03$  and  $\mu_C = 12.82$ ).

Figure 23. Aerobic pre-wound photocount distributions. Source: Oros and Alves (2018).

### b. *Wound-Induced Exponential Decay*

In contrast to the coherent excited field (hyperbolic), it has also been suggested that an excited chaotic field decays in accordance with an exponential function (Popp et al., 1994). Two distinct wound-induced exponential decays were observed in 6/7 aerobic tests (Figure 24). Each decay was fitted to both single and double exponential decay functions.

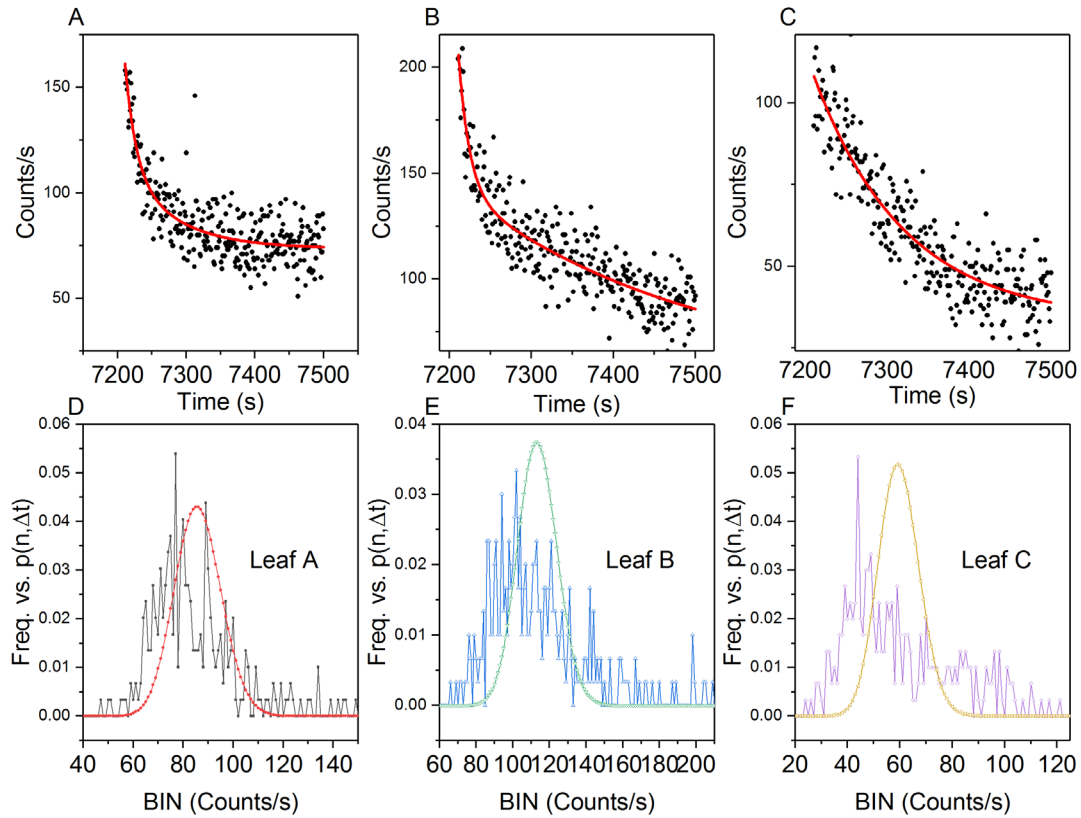


Spathiphyllum wounding in air showing distinct peak, secondary rise & subsequent exponential decays (A, B, D). No secondary exponential decay was observed in leaf B (C). Red curve is 10-point smoothing for trend visualization.

Figure 24. Leaf aerobic wounding photocount comparison. Source: Oros and Alves (2018).

The Origin Pro software was unable to converge on a hyperbolic curve fitting function for the data. Comparison models were used to quantitatively assess the curve fitness: Akaike’s Information Criterion (AIC), Bayesian Information Criterion (BIC), and F-tests ( $p = 0.05$ ). All three models preferred the double exponential decay for the initial decay data (Figure 25, A–C).

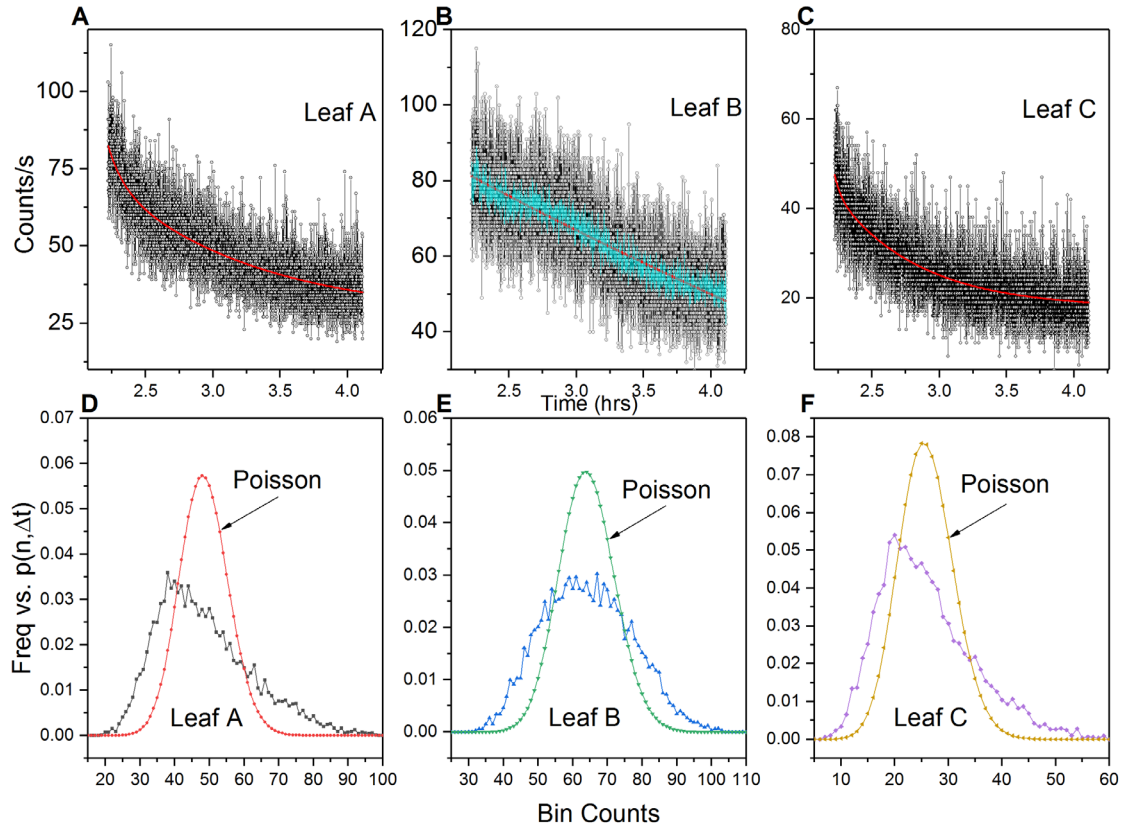




Leaves A, B, & C photocounts (A-C) with double exponential decay fit line (red). (D-F) Observed photon count frequency vs. Poisson predicted distribution corresponding to each leaf ( $\mu_A = 85.97$ ;  $\mu_B = 113.53$  and  $\mu_C = 59.66$ ).

Figure 25. Aerobic post-wound initial decay analysis (300s). Source: Oros and Alves (2018).

Two of the three models (AIC: 965 times more likely; F-test:  $F(3, 6792) = 6.58$ ,  $p = 0.05$ ) preferred the double exponential decay fit for the secondary decay data (Figure 26, A–C).



Leaves A, B, & C photocounts with double exponential decay fit line (red) (A-C). Leaf B (B) did not display a secondary decay peak. Cyan curve in (B) is 10 pt smoothed to highlight the decay profile. Red lines (A, C) reflect double exponential curve fit. (D-F) Observed photon count frequency vs. Poisson predicted distribution for each leaf ( $\mu_A = 48.55$ ;  $\mu_B = 64.19$  and  $\mu_C = 25.90$ ).

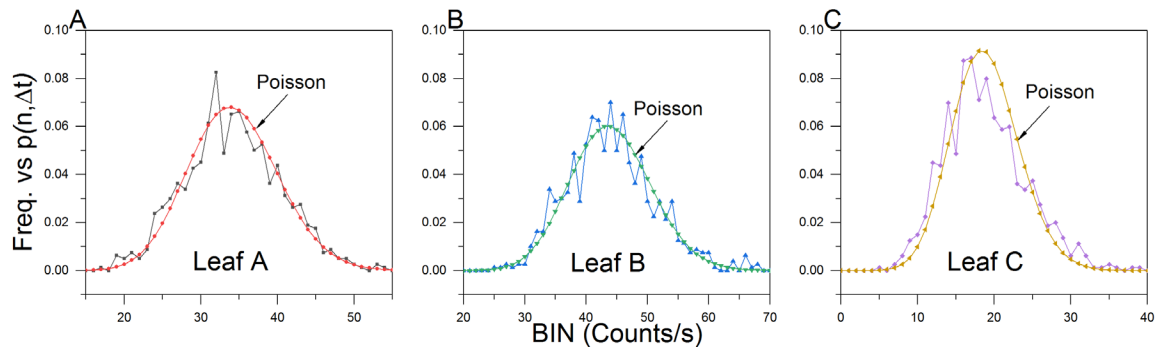
Figure 26. Aerobic post-wound secondary exponential decay. Source: Oros and Alves (2018).

The second order exponential decay equation is given by:

$$y = y_0 + A_1 e^{-(x-x_0)/t_1} + A_2 e^{-(x-x_0)/t_2} \quad (6)$$

PCS analysis of the initial and secondary exponential decays showed no Poissonian distribution agreement (Figure 25, D-F) and Figure 26, D-F).

End analysis of the aerobic post-wound exponential data (800s before closing the shutter) revealed that the exponential UPE decay did in fact exhibit a Poisson distribution once the wound site reached a “quasi-stable” state (Figure 27).



Photon count statistics of leaves (A-C) approach a Poissonian distribution upon exponential decay relaxation (800 s). ( $\mu_A = 34.32$ ;  $\mu_B = 44.06$  and  $\mu_C = 18.90$ ).

Figure 27. Aerobic post-wound secondary decay photocount distributions.  
Source: Oros and Alves (2018).

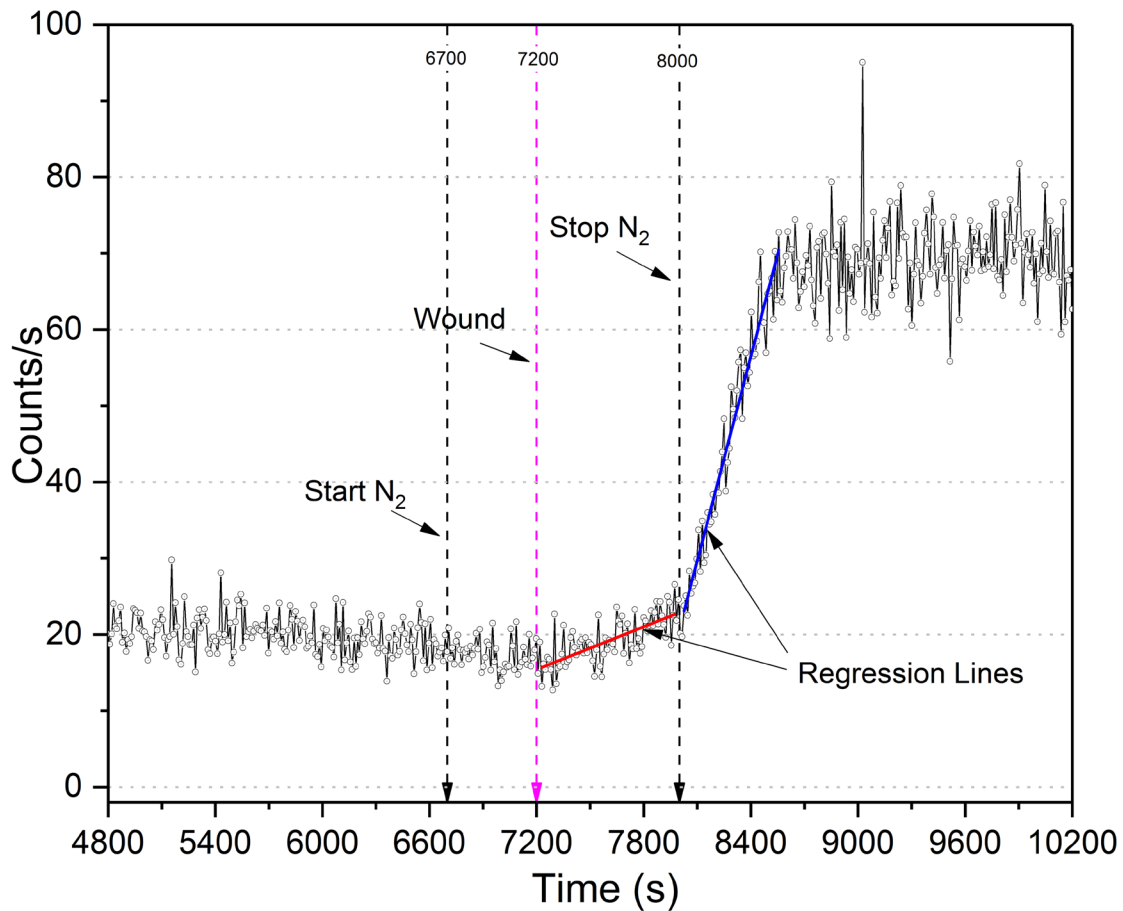
While we cannot assess the degree of coherence of the plant’s nonlocal field (i.e., macro level), we have observed that the photon counts produced at a single leaf’s wounding site (micro level) do exhibit an exponential decay. We are not suggesting that the leaf or plant as a whole becomes an “incoherent” source, but rather the biophoton emission invoked through highly localized, physical destruction of leaf tissue and resultant wounding response, abruptly change the leaf’s energetic “steady state.” This can perhaps be considered a “chaotic” source of UPE at the level of analysis of the wound site. Further measurements would need to be made to determine if the plant’s overall UPE responds to the micro-level wounding event.

As Shen et al. point out, the existence of a Poissonian photocount distribution is a necessary but insufficient condition for coherence (Shen, X., Liu, F., Li, 1993). Distinguishing between coherent and chaotic biological fields is challenged when the measurement time is significantly longer than the coherence time of the system. A 1 s gate time was used for all of our photon counting measurements and the distance from the leaf surface (object plane) to the photocathode was approximately 9.4 cm. We do not offer claims for or against the coherence theory. We simply confirm that the “quasi-stable” basal photon counts that follow both hyperbolic and exponential wound-induced biological decays closely approximate a Poisson distribution.

## 2. Anaerobic PCS

### a. Post-wound Analysis ( $N_2$ )

Linear regression of average post-wound anoxic stress leaf photon count data was performed (Figure 28). Photon counts slightly decreased 2–3 cps once the flow of nitrogen was initiated but did not deviate appreciably from the trending decay curve. However, wound induced UPE emission intensity was greatly inhibited by the anoxic environment, increasing by only 8 cps in 500 s of  $N_2$  incubation. The post-nitrogen phase was statistically significant [ $F(2, 123) = 416, p = 0.05$ ]; increasing from ~23 to 70 cps (avg) in 540 s.

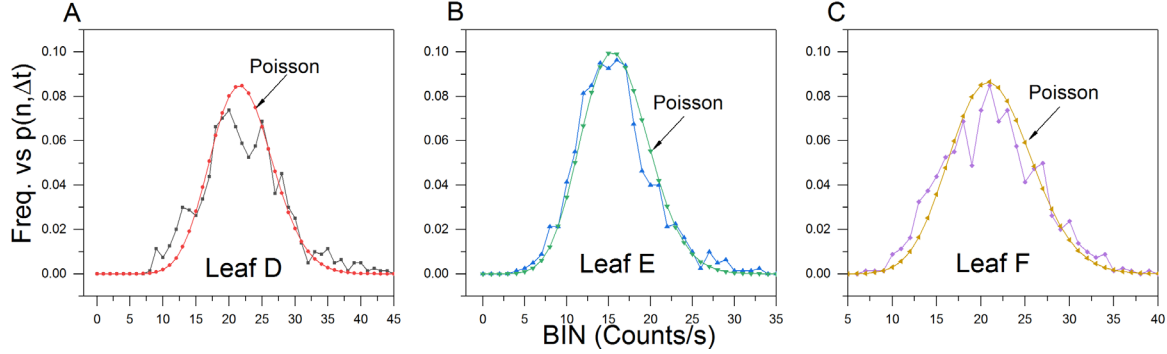


Three sample average of anoxic wounding data.  $N_2$  gas introduced at 6,700 s; plant wounded 7,200 s, and  $N_2$  secured at 8,000 s. The two slopes (red = anoxic, blue = aerobic) differ significantly [ $F(2, 123) = 416, p = 0.05$ ].

Figure 28. Multiple regression comparison of averaged anaerobic wound data.

Source: Oros and Alves (2018).

PCS analysis of the anoxic wounding data (800 s) closely approximated a Poissonian photocount distribution (Figure 29).



(A-C) Photocount statistics of leaf anoxic wound data. Observed photon count frequencies closely approximate a Poisson predicted distribution ( $\mu_D = 22.10$ ;  $\mu_E = 15.96$  and  $\mu_F = 21.34$ ).

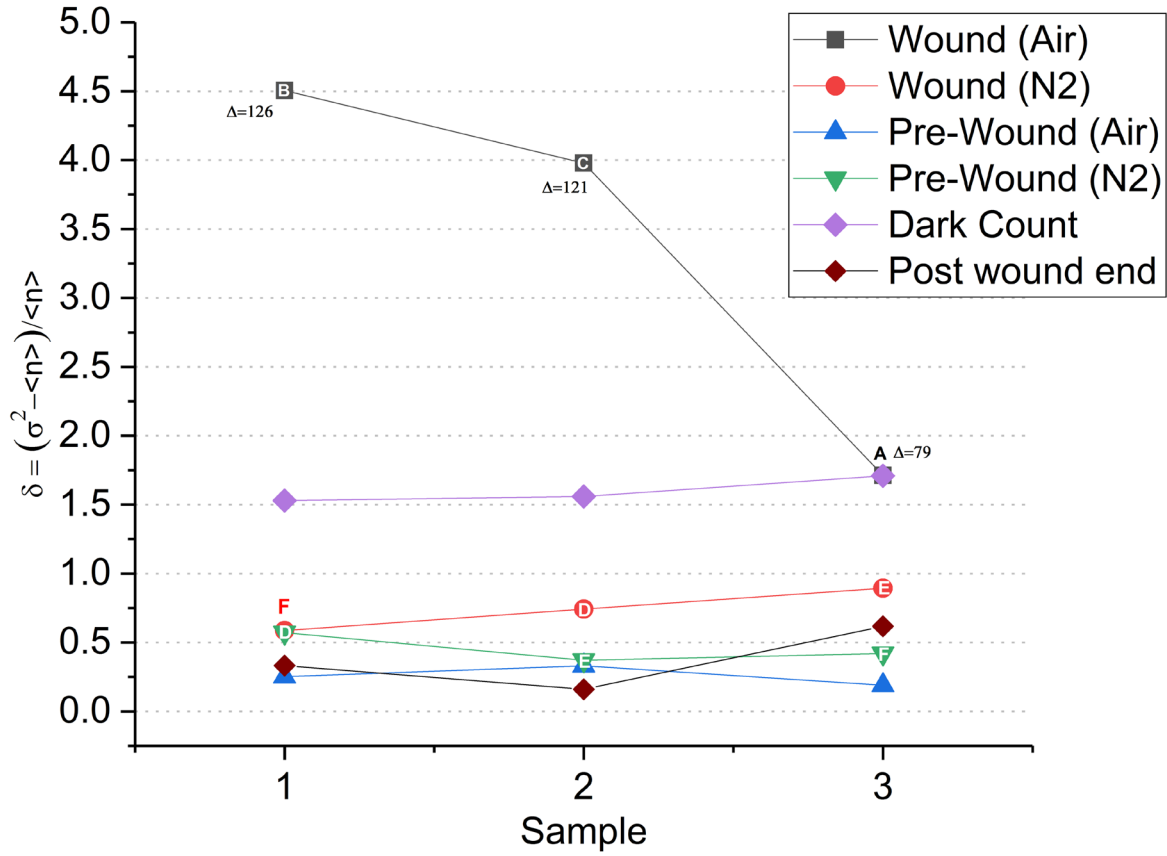
Figure 29. Anoxic wounding photocount distributions. Source: Oros and Alves (2018).

## E. POISSON FITNESS

The degree of fitness with a predicted Poisson distribution, represented by ( $\delta$ ), was calculated using Popp and Shen et al.'s formulation (Popp, 2003a; Shen, Liu, Li, 1993; Shen, 2003), where ( $\delta$ ) is given by

$$\delta = \frac{\sigma^2 - \langle n \rangle}{\langle n \rangle}, \quad (7)$$

where  $\sigma^2$  is the variance and  $\langle n \rangle$  is the mean. The greater the value of ( $\delta$ ) from zero, the less Poissonian the distribution. The ( $\delta$ ) was calculated from pre-wound, wound and dark count data (Figure 30).



Aerobic wound data surpassed PMT dark counts (2/3 samples). ( $\Delta$ ) Indicates the difference in photocounts from basal—wounding peak and correlates with the degree of divergence from Poisson. Aerobic pre-wound, post-wound end, and anoxic ( $\delta$ ) values show close agreement with a Poisson distribution. (Letters = leaves where indicated).

Figure 30. Poisson distribution fitness ( $\delta$ ) of leaf wounding and dark count data. Source: Oros and Alves (2018).

Aerobic wounding produced the greatest deviation from a Poisson fit. The deviation was proportional to the difference between the basal count and initial wound peak. PMT dark count was next highest. All other values fell well below aerobic wounding and random PMT noise data.

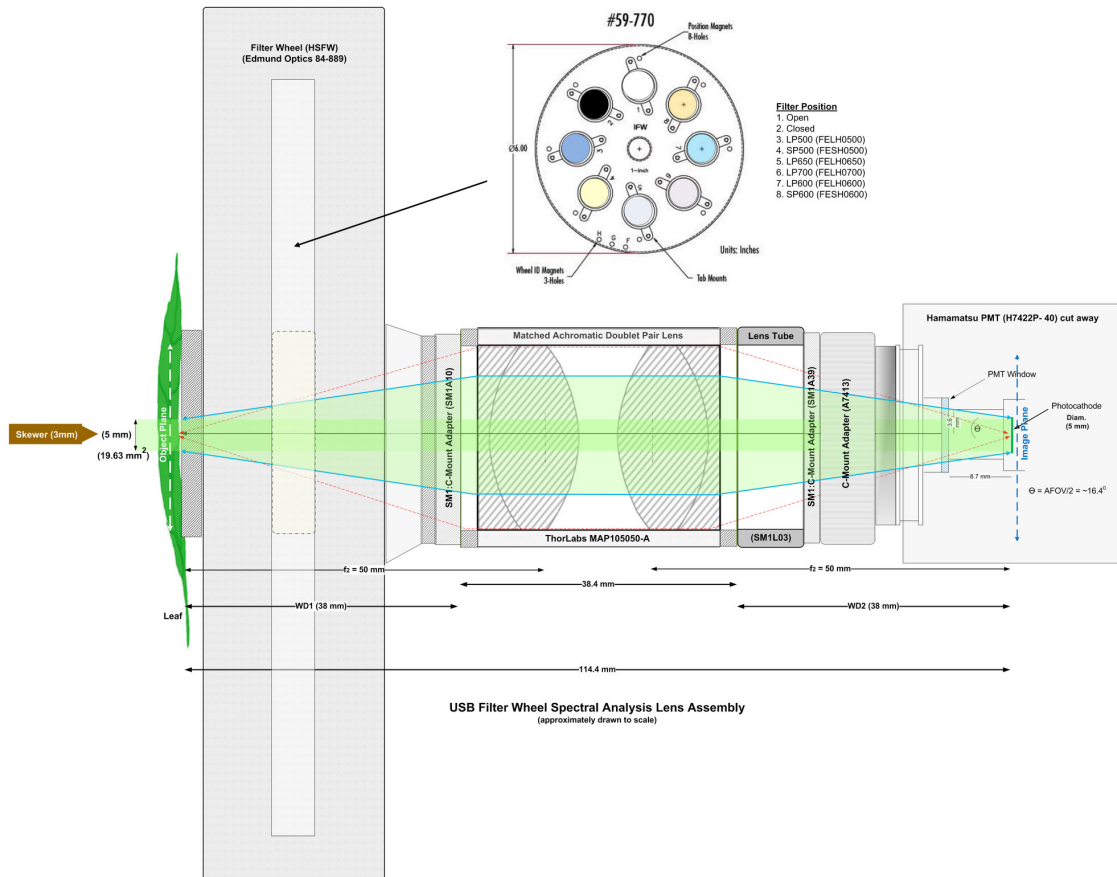
## F. SPECTRAL ANALYSIS

### 1. Pre-wounding Dark Adaptation Spectral Analysis

Room temperature chlorophyll fluorescence results from a combination of related effects (i.e., heat dissipation, dark reduction of plastoquinone, deactivation of Rubisco, and generation of reactive oxygen species (ROS)) (Misra et al., 2012). Typically, two chlorophyll emission maxima are observed at room temperature: (i) a red peak around 680–690 nm (attributable to photo system II (PS II)) and (ii) a far-red region around 720–740 nm (emitted by Photo System I (PS I)) (Misra et al., 2012). While there is a distinct peak maxima at 680 nm at steady state room temperature conditions, the relative emission decreases by ~15% to a 700 nm shoulder before rising to 740–750 nm (Cordón & Lagorio, 2006; Evans, von Caemmerer, 2018; Lagorio et al., 2015; Mukerji & Sauer, 1993). Additionally, the reabsorption of chlorophyll fluorescence within whole, intact leaves by PS II is known to result in a strong emission at 685 nm (Cordón & Lagorio, 2006; Evans & von Caemmerer, 2018; Lagorio et al., 2015; Misra et al., 2012) and 730 nm in isolated spinach chloroplasts (Hideg, Scott, & Inaba, 1989). UV-induced blue-green fluorescence (BGF) (Blue: 430–450; Green: 520–530 nm) is also known to be emitted by green leaf plant pigments (Hideg, Juhász, Bornman, & Asada, 2002; Lichtenthaler, Langsdorf, Lenk, & Buschmann, 2005; Lichtenthaler & Miede, 1997). Chlorophyll-free epidermal cells and major leaf veins are the primary source of green leaf BGF, though the cell walls of green mesophyll cell also contribute to the emission (Lichtenthaler & Miede, 1997).

A second *Spathiphyllum* was used to conduct long duration spectral analysis of the dark-adaptation (2hr.) and wounding phases. Filter spectroscopy measurement details are further discussed in the methods section. Initial filter tests, using the single filter lens configuration revealed a slight UPE decay (~10 cps peak) between 388 – 501 nm (Appendix Figure 42). This decay was only observed during the first 30 minutes of dark adaptation. We suspect this emission may be attributed to UV-induced BGF since the plant was exposed to sunlight and UV radiation from the overhead white LED lighting prior to dark adaptation. Post fluorescent decay basal photon emission was well above the dark count, and in all cases observed to date, the basal UPE never reached the noise floor even after 8 hours of observation.

To more accurately assess the leaf UPE spectra, we performed an additional test on a single leaf using a rotating filter wheel lens assembly (Figure 31) configured with filters 3–6.



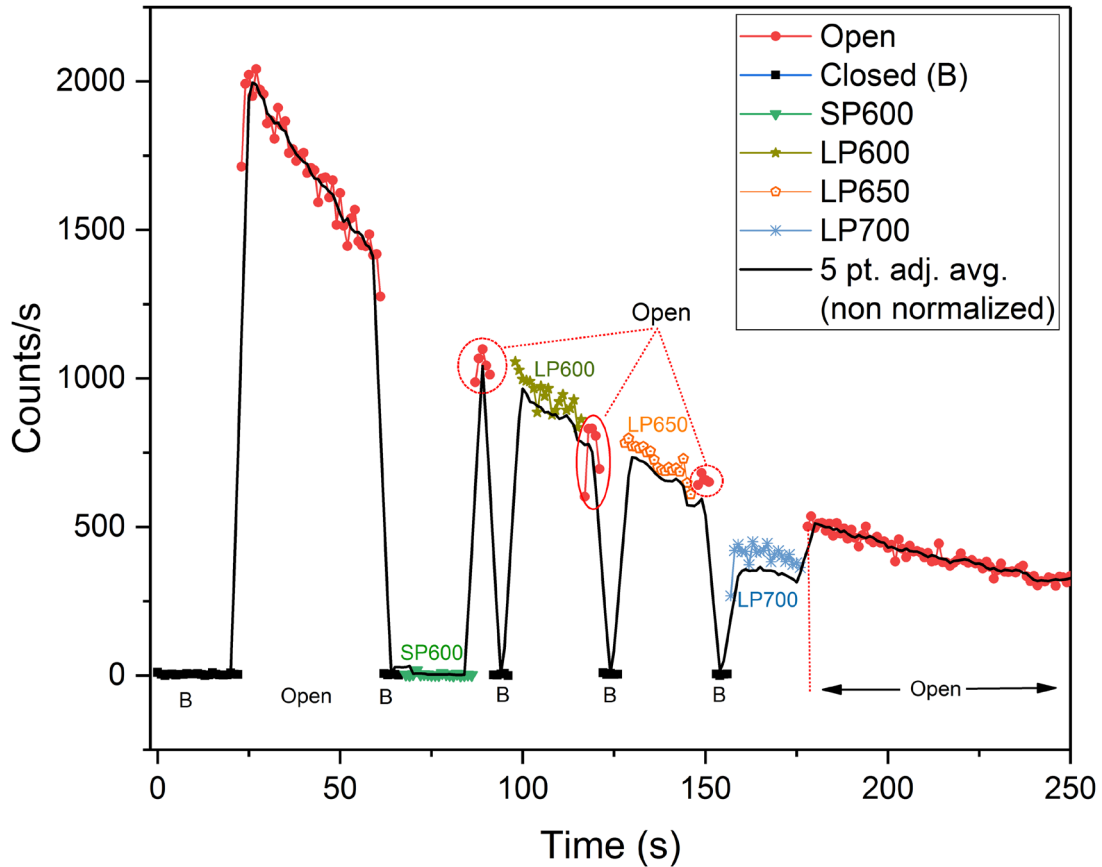
Secondary lens configuration showing matched achromatic doublet pair lens ( $f = 50$  mm) and motorized high speed USB filter wheel (HSFW) used in spectroscopy measurements. Filter wheel inset shows filter type for each position. Only positions 1, 2, 5, 6, 7 and 8 were used for the HSFW spectroscopy measurements.

Figure 31. Secondary photon counting lens and PMT assembly. Source: Oros and Alves (2018).

Eight pre-wound filter measurements were performed approximately every 15 minutes starting from  $T = 60$  (Figure 32) — 6,300 s (Appendix Figure 43 and Figure 44). The first 250 s of dark adaption decay data (Figure 32) showed no significant UPE from 393–600 nm. This differs from previously observed data (10 cps, Figure 42) and may



possibly be due to the slightly different optics and greater optical path length of the filter wheel lens assembly. The equivalent LP600 (N = 237, M = 35, SD = 18, VAR = 328) and LP650 (N = 235, M = 35, SD = 18, VAR = 318) filter data reveals that all of the UPE detected was > 650 nm. Based on these observations it is assumed that this emission is consistent with chlorophyll (PS II), and would be expected during the fluorescent decay process. This does not rule out potential contributing emissions from other excited pigments (550–750 nm) and 1O<sub>2</sub> (634–703 nm) produced through normal metabolic processes that have been reported in this wavelength band (Cifra & Pospíšil, 2014; Pospíšil et al., 2014). The LP700 data, however, is inconclusive as the PMT's cathode radiant sensitivity declines sharply at 700 nm. This precluded any accurate comparison to the other filter data and limited analysis to spectra below 700 nm. Pre-wound box plot data is provided in Appendix, Figure 45.

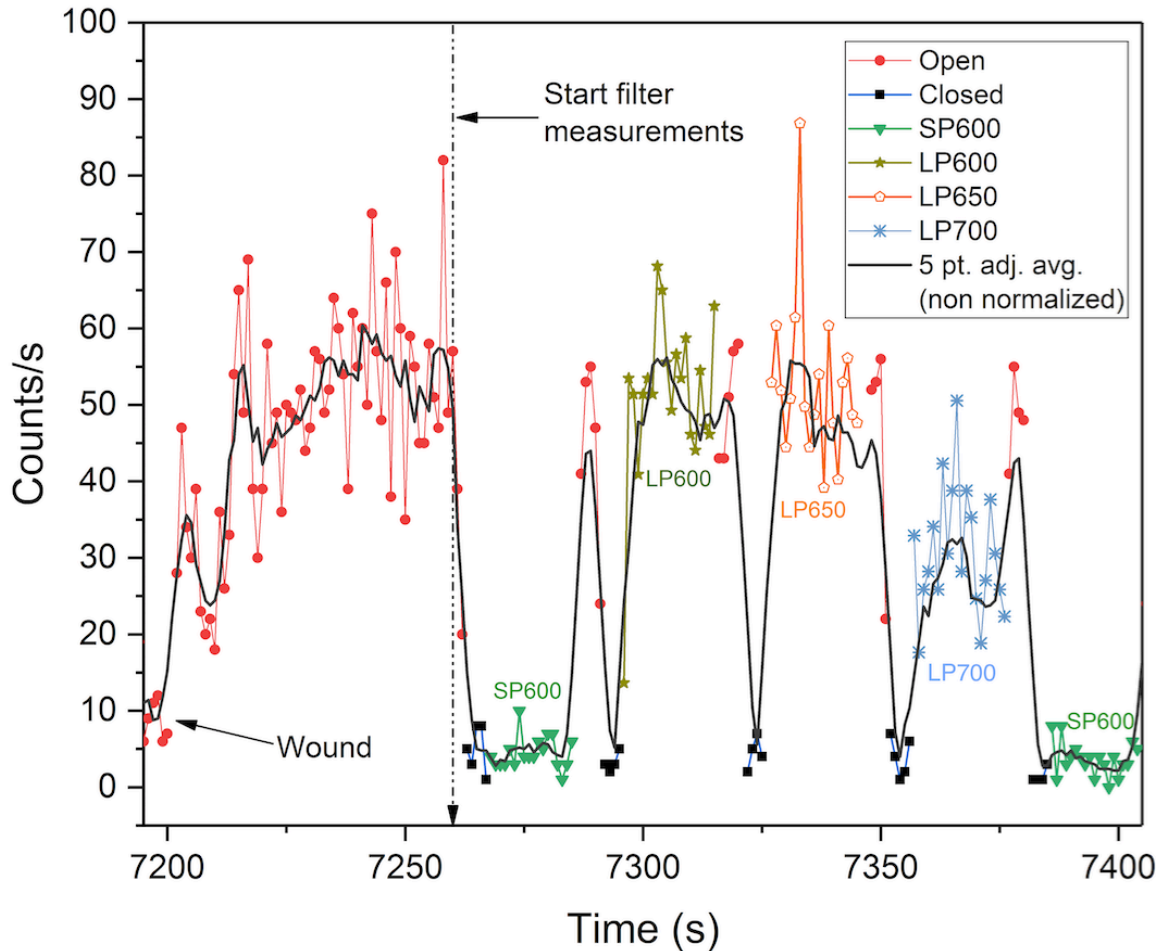


Leaf UPE during the first 250 s of dark adaptation in air using various optical filters. Solid black line is the non-normalized, 5-point smoothed adjacent average photocoount data. Normalized filter data is overlaid for comparison. The decay trend plot is intentionally interrupted by the filter wheel rotation. The filter rotation sequence included a 5 s open (O) and closed (B) phase before each optical edgepass filter measurement (20 s) to better visualize and account for the filter transitions. Data shows no significant UPE above the noise floor from 393–600 nm. Comparison of the LP600 and LP650 plot data reveals that all of the UPE is > 650 nm as the counts are equivalent. The decreased LP700 count data is attributable to the sharp decline of the cathode's radiant sensitivity at 700 nm vice the filter's slightly reduced transmittance and thus is inconclusive.

Figure 32. *Spathiphyllum* dark adaptation filter wheel spectral analysis. Source: Oros and Alves (2018).

## 2. Wound Spectral Analysis

Spectral measurements revealed a sharp increase in UPE (+ 50 cps) immediately upon wounding (Figure 33).



Leaf UPE during the first 200 s of aerobic wounding using various optical filters. Solid black line is the non-normalized, 5-point smoothed adjacent average photocount data. Normalized filter data is overlaid for comparison. Leaf was wounded at 2 hrs (7,200 s). The filter wheel measurement sequence was initiated 60 s after wounding. No UPE was detectable below 600 nm. LP600 and LP650 photocounts are equivalent indicating 100% of observed UPE was > 650nm. The reduced LP700 counts are confounded by the PMT cathode's reduced sensitivity > 700nm.

Figure 33. *Spathiphyllum* aerobic wounding filter wheel spectral analysis.

Source: Oros and Alves (2018).

This agreed with the findings obtained from the single filter tests previously conducted (Appendix Figure 46). Continuous filter wheel measurements ( $N = 4$ ) commenced 60 s after wounding with a final measurement taken at the experiment's end (~4.4 hrs) (Appendix Figure 47).

These results showed that all of the detectable UPE was  $> 650$  nm. Statistical comparison of the LP600 ( $N = 99$ ,  $M = 41$ ,  $SD = 11$ ,  $VAR = 117$ ) and LP650 ( $N = 97$ ,  $M = 42$ ,  $SD = 10$ ,  $VAR = 109$ ) filter data shows the data are nearly equivalent (similar to the pre-wounding results). Though UPE was observed from 700–720 nm, the reduced photon counts of LP700 filter, were most likely to be an effect of the reduced cathode radiant sensitivity  $> 700$ nm. This prevented any comparative quantitative assessment. Filter wheel statistical data are summarized in Appendix Table 2 and in Appendix Figure 45 box plots.

Our optical system was unable to detect any significant wound-induced UPE ( $< 600$  nm) above the noise floor even though UPE spectra has been reported in: lipoxygenase-catalyzed linoleate oxidation reaction emissions (450 nm and 550 nm; shoulder at 630 nm) in a cuvette solution (Boveris et al., 1980), triplet excited carbonyls (350–550 nm) (Cifra & Pospíšil, 2014; Pospíšil et al., 2014); (450–550 nm) (Prasad & Pospíšil, 2011); dimol emission of singlet oxygen (460 nm and 510 nm) (Abeles, 1986); and in oxidized proteins (490–580 nm) (Birtic et al., 2011).

These wound-induced UPE spectral observations contribute to reported research findings in *Arabidopsis* (100% UPE  $> 695$  nm) (Birtic et al., 2011; Prasad et al., 2017); 700–750 nm (Flor-Henry et al., 2004) and in Geraniums (89% UPE 600 – 1000 nm) (Creath & Schwartz, 2005). In addition to singlet excited chlorophyll emissions (670–740 nm) (Cifra & Pospíšil, 2014; Pospíšil et al., 2014), other potential emission sources include singlet excited pigments (550 nm–750 nm) and dimol emission of singlet oxygen (634 nm and 703 nm) (Abeles, 1986; Pospíšil et al., 2014), and oxidation of linolenic acid (640–695 nm) (Birtic et al., 2011).

THIS PAGE INTENTIONALLY LEFT BLANK

## VI. CONTRIBUTIONS

We used a unique *in vivo* plant testing chamber, in combination with a highly sensitive PMT and a simple lens system, to record long duration photon counts spanning dark adaptation through mechanical wounding. We were able to demonstrate that plant wound induced biophoton emission is suppressed in an anoxic environment. Through use of a motorized spectral wheel, we were further able to obtain a variety of long duration spectral measurements which identified chlorophyll as the predominant plant wound signaling emitter.

We believe we are first to report on the successive wound-induced photoemission decay curves as to our knowledge it has not been observed in the literature.

Lastly, photon count statistical analysis was observed to closely approximate a Poissonian distribution when both normal hyperbolic (dark adaptation) and perturbed double exponential decays (wounding) relaxed to a quasi-stationary state. Anoxic incubation significantly inhibited wound-induced biophoton emission and this was further reflected in the close Poissonian photocount distribution.

This novel research contributes to the body of plant wound-induced luminescence research and provides a novel methodology to measure this signaling phenomenon *in vivo* under both aerobic and anoxic/hypoxic conditions.

THIS PAGE INTENTIONALLY LEFT BLANK

## VII. SUMMARY

The content of this chapter has been modified from Oros and Alves (2018) conclusions section with full rights and permissions for usage under the creative commons [CC0 public domain dedication license](https://creativecommons.org/licenses/by/4.0/). The original article can be accessed here: <https://doi.org/10.1371/journal.pone.0198962>

### A. FINDINGS

Long duration ultraweak photon emission of dark-adapting whole *Spathiphyllum* leaves (*in vivo*) was continuously measured, at room temperature, using a low noise PMT in a light trap environment. Leaves were mechanically wounded after two hours of dark adaptation in aerobic and anaerobic conditions.

Under aerobic conditions, the dark adaptation photoemission exhibited a hyperbolic decay. Subsequent mechanical wounding of the leaves induced significant biophoton emission. Photon counts increased from about 79–126 cps above the pre-wound basal count rate and did not decay back to the pre-wound level even after several hours of continuous observation.

Post-wound aerobic photon counts displayed two successive double exponential decays (Figure 34). The primary UPE decay resulting from the leaf's puncture might be attributable to a combination of previously reported oxidative (chlorophyll luminescence) effects as well as triboluminescent contributions resulting from the violent rupture of the leaf's cellular structures, rubbing of the wounding device on the aluminum lens tube, or a combination thereof. The secondary rise, exhibiting much lower intensity and subsequent photoemission decay is more likely to be the result of a combination of reabsorption re-emission of wound-induced UPE as well as the buildup and propagation of longer duration oxidative processes associated with the plant's healing processes. We believe this is the first time such results were reported in the literature.



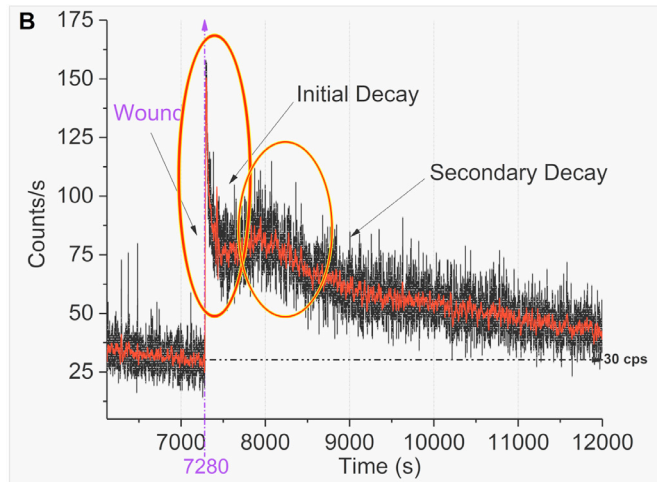


Figure 34. Primary and secondary aerobic wound UPE decay. Adapted from Oros and Alves (2018).

In contrast, leaf wound-induced UPE was significantly suppressed when placed under anoxic stress ( $N_2$  gas) suggesting that wound-induced lipoxygenase reactions are inhibited under anoxic atmospheric conditions. The reduced UPE observed seems to corroborate recent experimental data (Prasad & Pospíšil, 2011; Prasad et al., 2017) that has shown that inhibition of lipoxygenase production through use of chemical agents directly effects singlet chlorophyll and singlet oxygen luminescence (Figure 35).

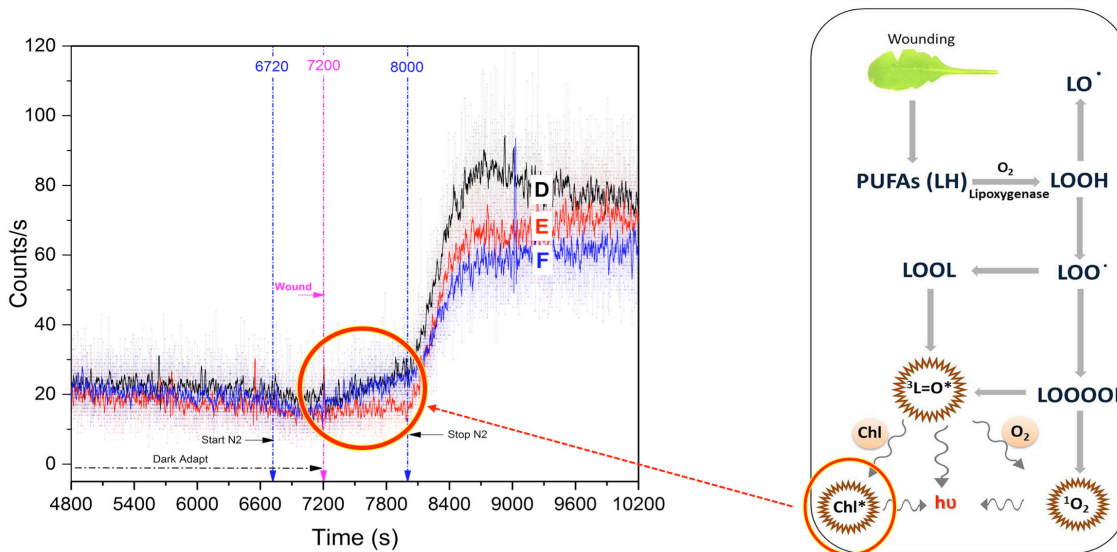


Figure 35. Anoxic wounding photocounts in resulting from singlet chlorophyll as an indicator of the state of triplet carbonyls. Adapted from Oros and Alves (2018) and Prasad et al. (2017).

It was also observed that N<sub>2</sub> incubation (~ 8 min.) did not significantly reduce the dark adaptation fluorescence nor pre-wounding steady state basal photon counts.

Photon counting statistics of pre-wound (aerobic & anoxic) photon counts (Figure 36) were found to closely approximate a Poisson distribution. The pre and post wounding PCS results are consistent with Popp's biophoton theory showing a Poisson distribution as the injured part of the leaf reaches a "quasistationary state" (Popp et al., 1994, p. 1272).

Anoxic wounding PCS revealed that suppression of the lipoxygenase reaction chain also closely fit a Poisson photocount distribution (Figure 36). We assume this is due to suppression of the lipoxygenase catalyzed reaction chain.

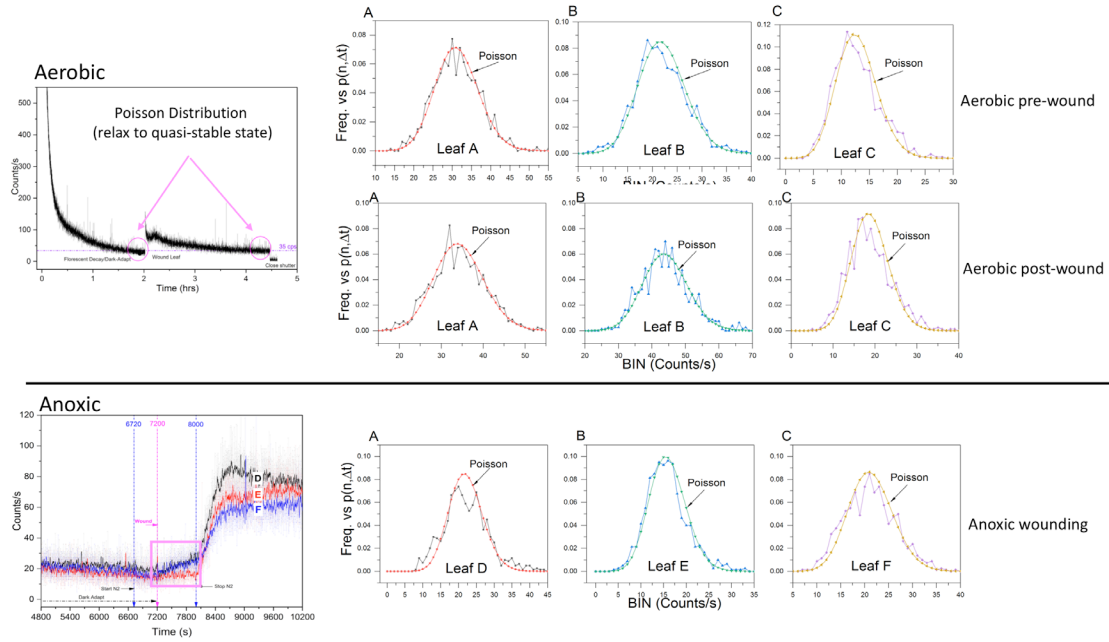


Figure 36. Comparison of aerobic and anoxic Poisson PCS. Adapted from Oros and Alves (2018).

PCS of aerobic wound data were found not to be Poisson distributed. Upon inspection this should seem obvious as the leaf is perturbed into an unstable state immediately upon wounding and this is reflected in the photocount distribution. Analysis of the initial wound decay (Figure 37) is far from Poissonian and not geometrically uniform. As the decay progressed, the secondary rise was observed to be closer to a normal Gaussian distribution (Figure 38).

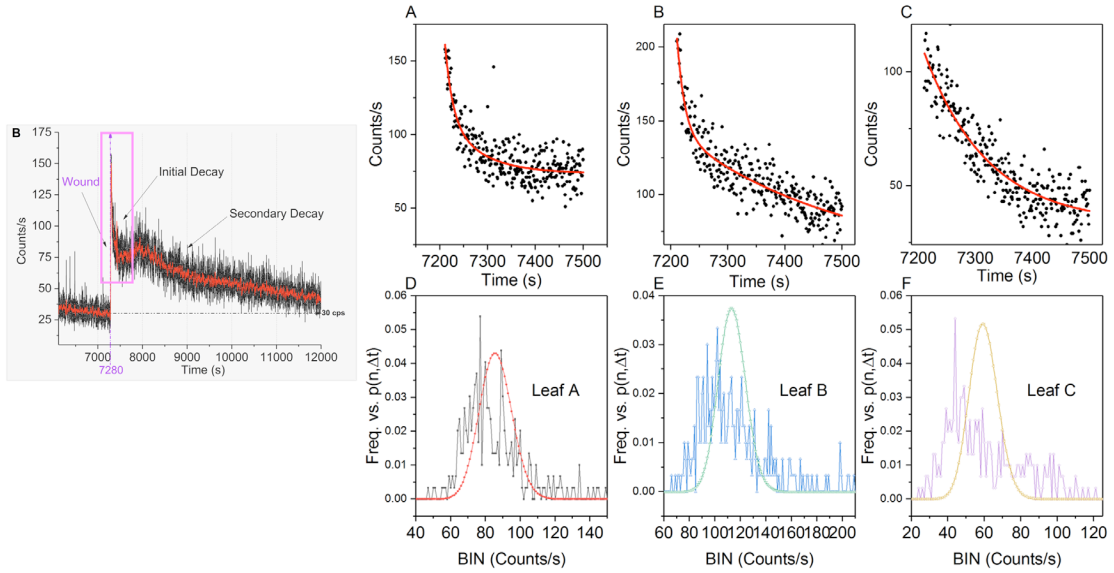


Figure 37. Summary of aerobic wounding initial decay PCS. Adapted from Oros and Alves (2018).

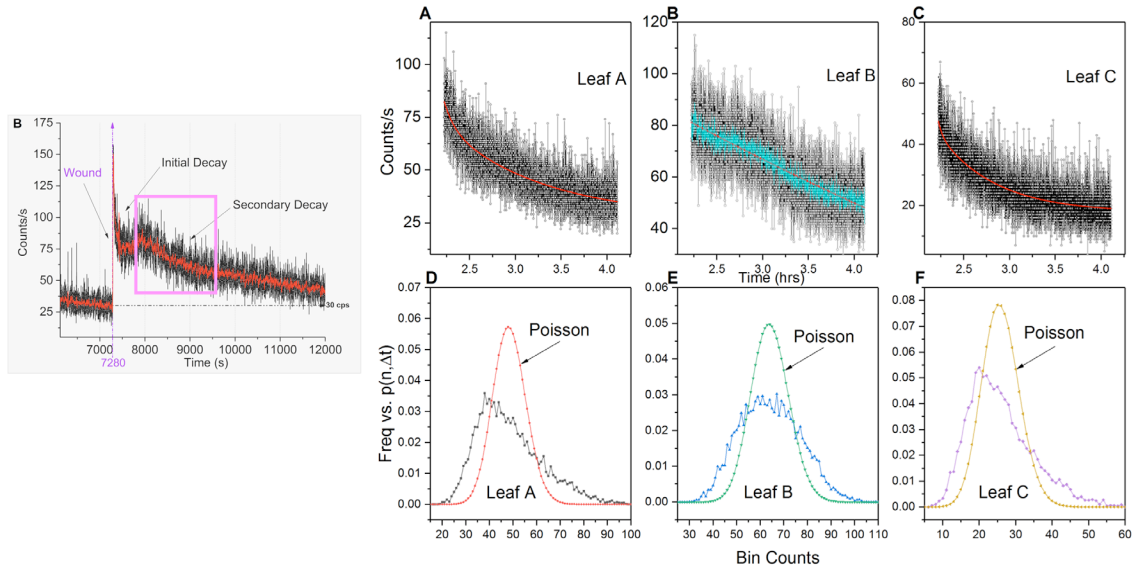


Figure 38. Summary of aerobic wounding secondary decay PCS. Adapted from Oros and Alves (2018).

Spectral analysis of both the aerobic pre-wound and wounded leaves revealed ultraweak photon emission predominates at wavelengths longer than 650 nm, indicating chlorophyll as the most likely emitter. Some UPE (10 cps) was also detected at wavelengths shorter than 500 nm but only during the first 30 minutes of dark adaptation (Appendix Figure 42).

Figure 39 shows a comparison of filter wheel spectral data of the same wounded leaf. The dark adaptation fluorescent decay (highlighted in left graph) shows that the long pass 600 nm and long pass 650 nm filter response are identical. This data confirms most of the light is  $> 650$  nm which is expected for chlorophyll fluorescence. Wounding spectral data (right graph) similarly revealed the same response. Thus, chlorophyll molecules appear to be the principle emitters of biophotons in both healthy and wounded states.

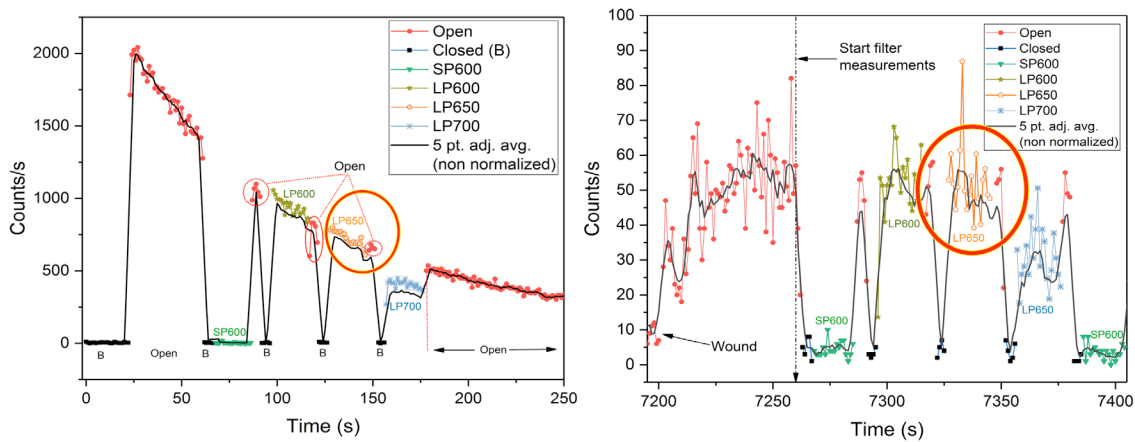


Figure 39. Spectral comparison of aerobic dark adaptation and wounding.  
Adapted from Oros and Alves (2018).

Limitations of the PMT cathode radiant sensitivity, however, prevented accurate analysis in the range 700–720 nm. The H7422P-40's sensitivity drops dramatically after 700 nm decreasing to zero at 720 nm (Figure 40). This is problematic as chlorophyll is known to have emission peaks at 680 and 740 nm. Thus, we were only able to capture chlorophyll emission accurately from 650–700 nm.

● **Typical Spectral Photocathode Radiant Sensitivity**  
(H7422/H7422P Series)

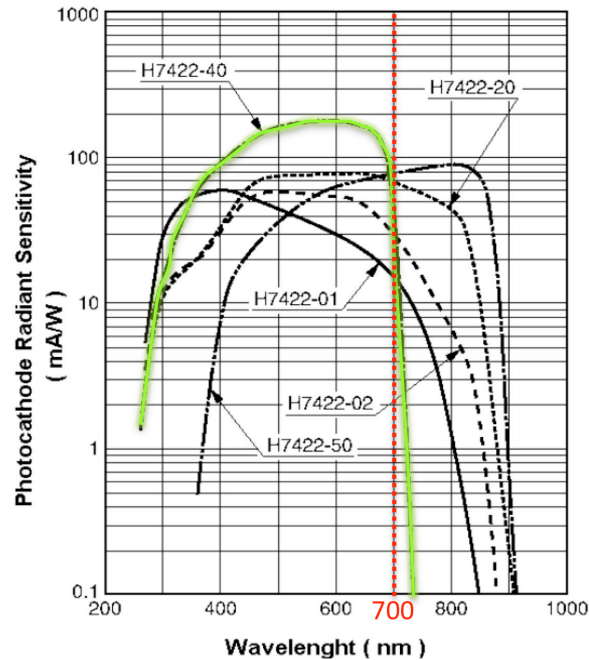


Figure 40. Photocathode radiant sensitivity. Adapted from Hamamatsu Photonics (2005).

**B. RECOMMENDATIONS FOR FOLLOW-ON RESEARCH**

**1. Expand the Wavelength Measurement Sensitivity**

Determination of the exact sources of the UPE detected at wavelengths longer than 650 nm requires greater spectral resolution of the experimental setup. We recommend that future research be conducted using a PMT with a wider spectral range (i.e., the H7422P-50, 380–890 nm) to more accurately observe the full extent of the wound-induced biophoton emission. This would allow for complete measurement of the chlorophyll emission spectra.

**2. Improve Spectral Analysis**

In this research we provided corroborating evidence that chlorophyll molecules are the likely predominant plant signaling emitters. Chlorophyll emission bands are well documented and having precise optical filters (680 nm and 740 nm) would allow for more

accurate measurement of wavelength specific data. It is also known that singlet oxygen (monomol) emits in the far red (1260 nm and 1320 nm) and 634 nm and 703 nm during dimol emission (Abeles, 1986, p. 61). A wider band PMT would be required to capture biophoton emission beyond 890 nm than previously suggested. However, optical band pass filters centered on 634 nm and 703 nm would help differentiate chlorophyll UPE from singlet oxygen.

### **3. Extend Methodology to Human Subjects Research**

The next phase of this research will extend the experimental methodology to explore stimulated biophoton emission from human subjects. Initial funding for this research has been received from the Naval Postgraduate School Foundation and research will commence in early 2019.

## APPENDIX. SUPPORTING FIGURES AND INFORMATION

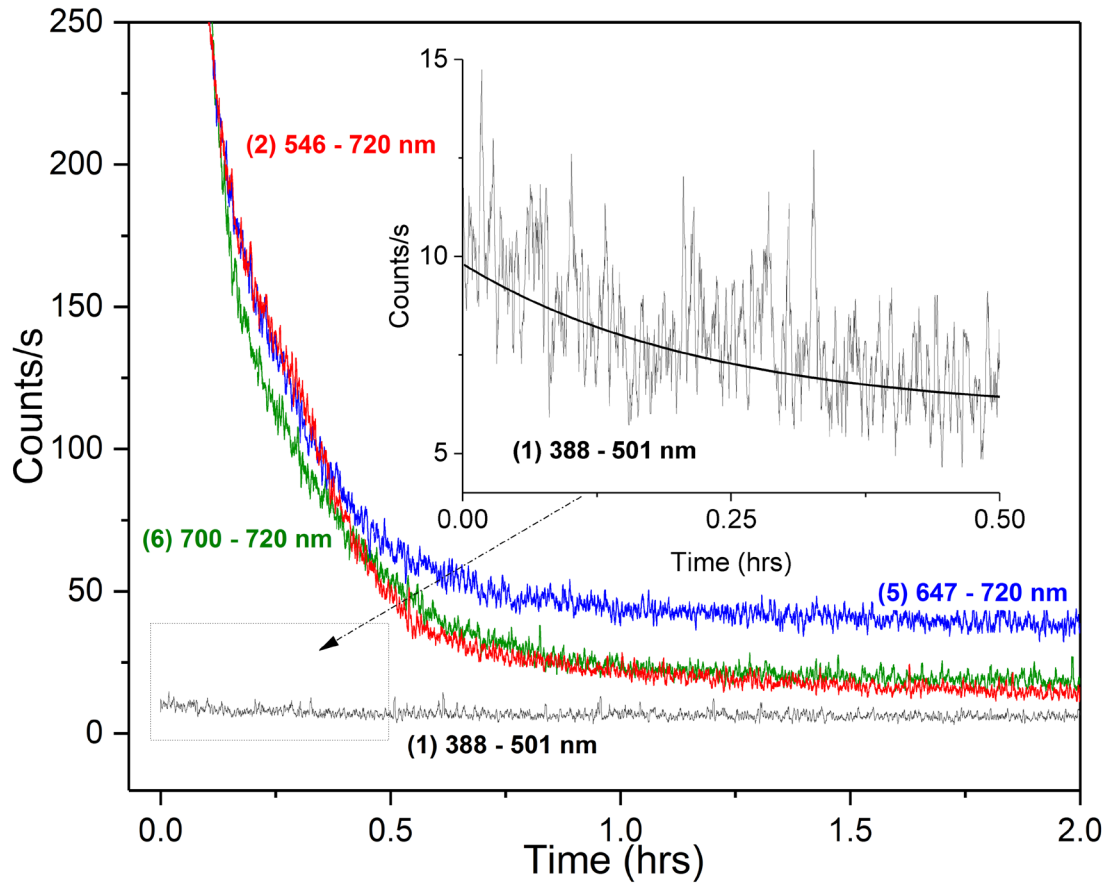
The images in this appendix (where indicated) were sourced from Oros and Alves (2018) with full rights and permissions for usage under the creative commons [CC0 public domain dedication license](https://creativecommons.org/licenses/by/4.0/). The original article can be accessed here: <https://doi.org/10.1371/journal.pone.0198962>

\* Supplementary Information in the form of raw experimental data sets and pictures is also available at <http://doi.org/10.5281/zenodo.1135265>



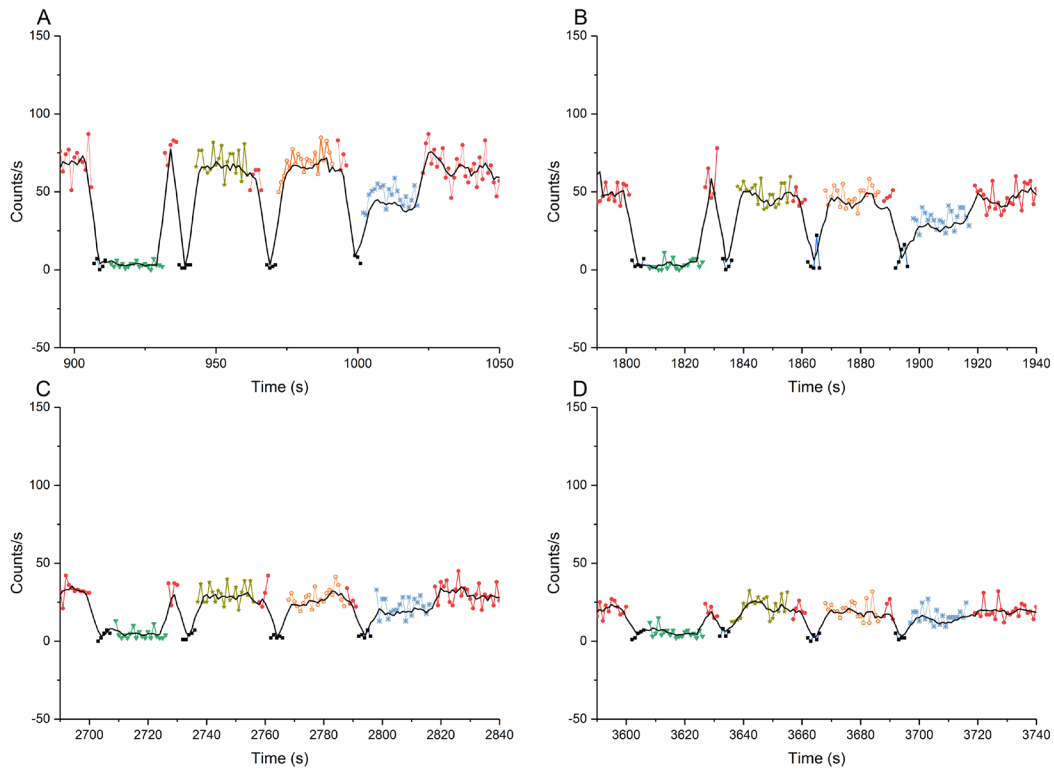
Figure 41. Plant test enclosure with front and sideview showing PMT





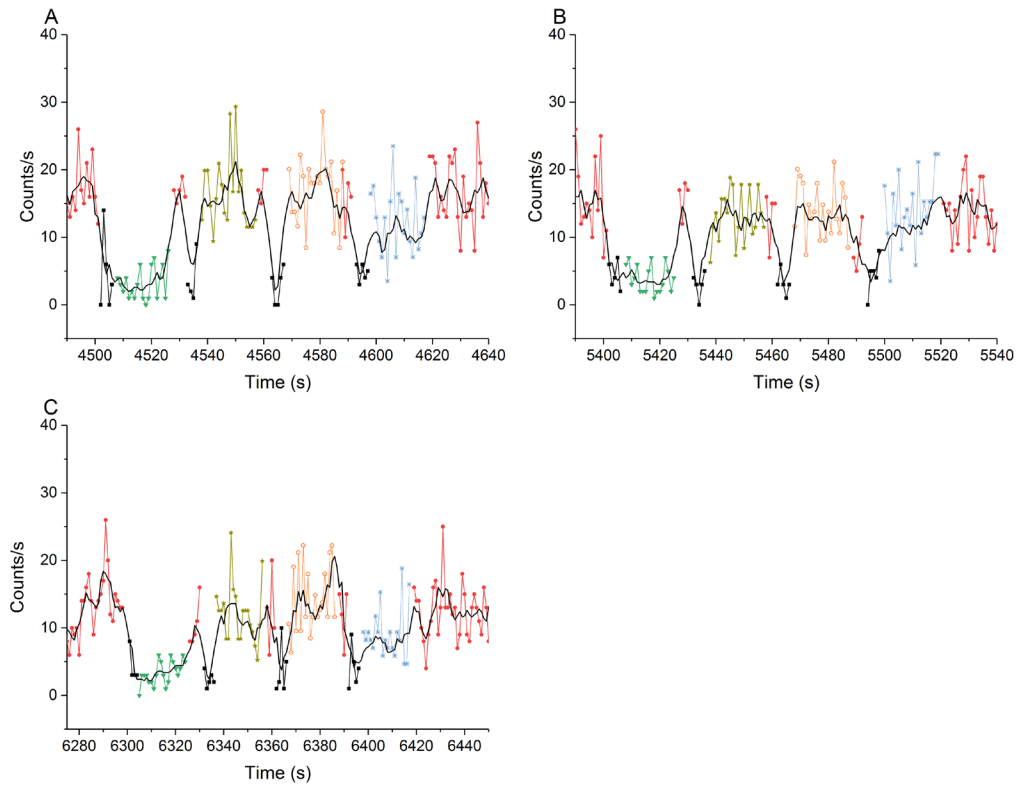
Normalized, 10-point smoothed spectral analysis of dark-adapting *Spathiphyllum* leaves in air using various optical filters (see Table 1). Inset shows subtle decay observed in first 30 min after placing plant in the dark using SP500 filter.

Figure 42. *Spathiphyllum* single filter dark adaptation decay spectral analysis.  
Source: Oros and Alves (2018), S1 Figure.



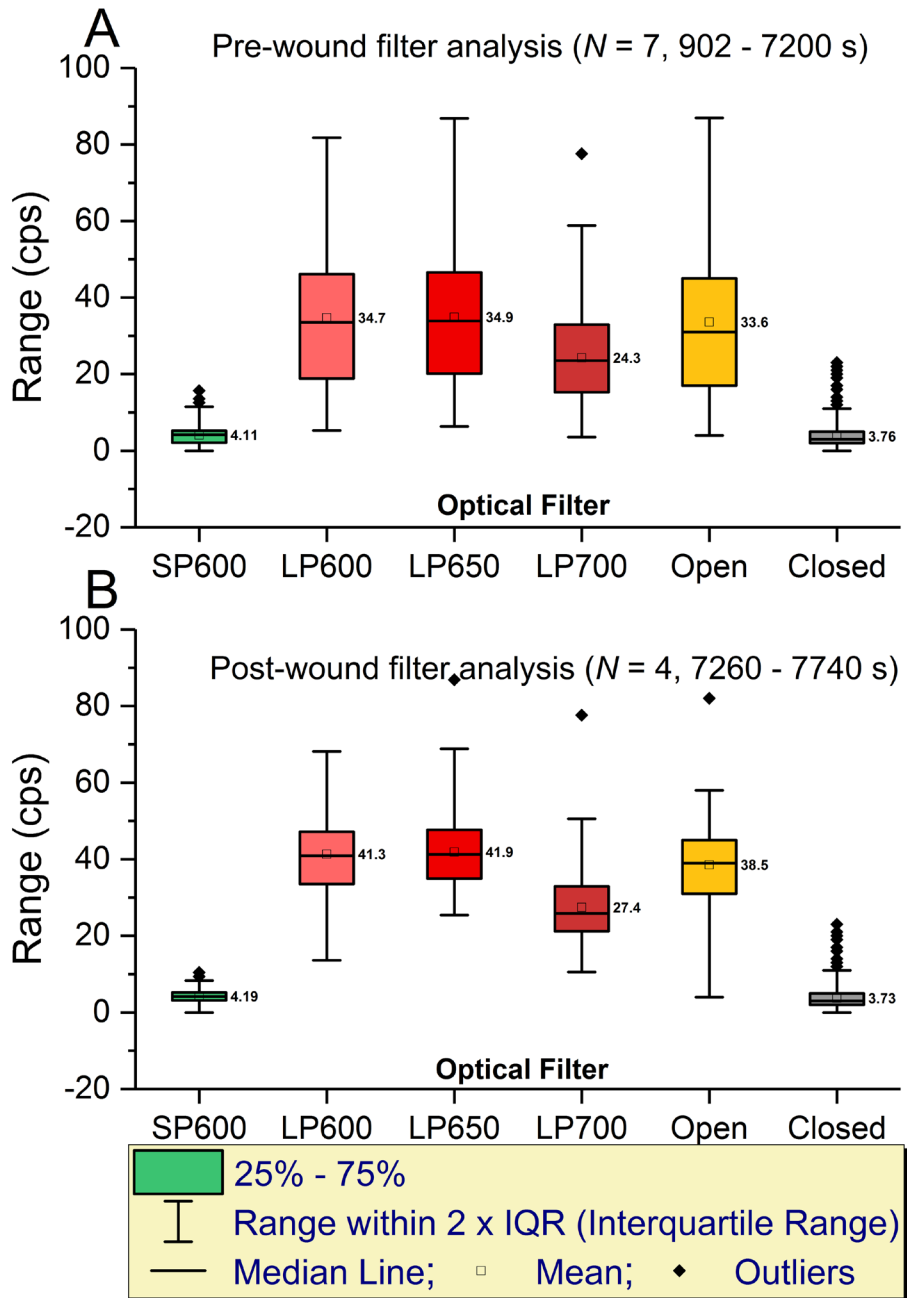
Measurement start times: (A) 900 s, (B) 1800 s, (C) 2700 s and (D) 3600 s.

Figure 43. Pre-wound filter wheel spectrum measurements (#2–#5) recorded every 15 minutes (900 s). Source: Oros and Alves (2018), S2 Figure.



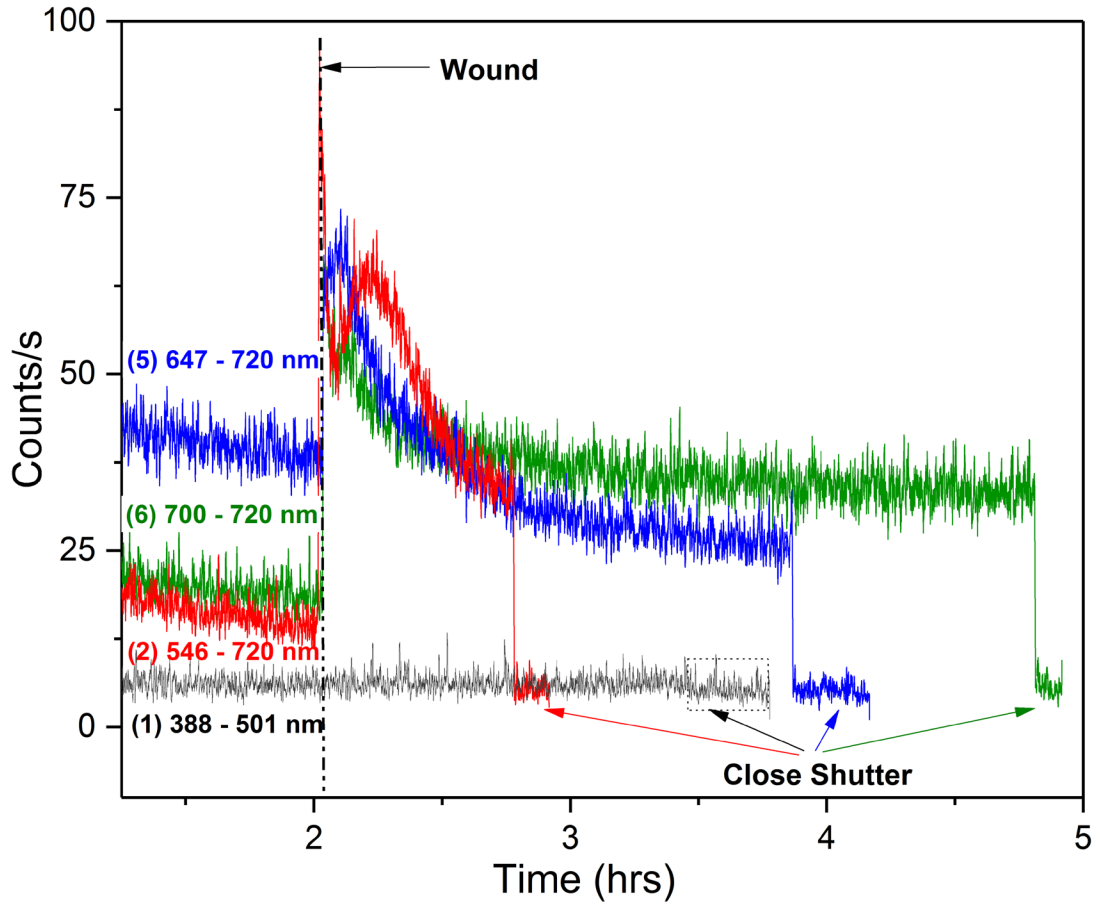
Measurement start times: (A)  $t = 4,500$  s, (B)  $t = 5,400$  s, and (C)  $t = 6,300$  s.

Figure 44. Pre-wound filter wheel spectrum measurements (#6–# 8) recorded every 15 minutes (900 s). Source: Oros and Alves (2018), S3 Figure.



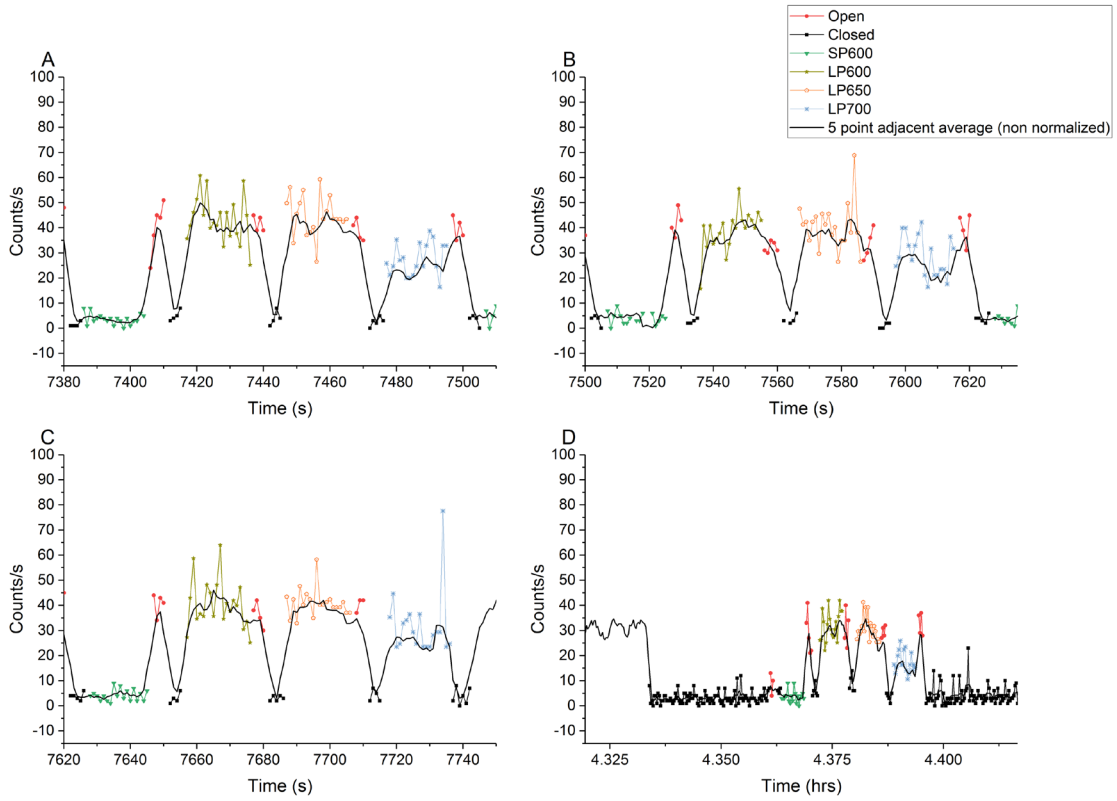
A. Pre wound spectral data. B. Post wound spectral data.

Figure 45. Box plots of filter wheel spectral data. Source: Oros and Alves (2018), S4 Figure.



Normalized, 10-point smoothed spectral analysis of *Spathiphyllum* aerobic wounding. Optical filters and associated wavelength as indicated and listed in Table 1.

Figure 46. *Spathiphyllum* single filter aerobic wounding spectral analysis.  
Source: Oros and Alves (2018), S5 Figure.



Measurements taken at: (A)  $\approx 7,385$  s, (B)  $t \approx 7,505$  s, and (C)  $t \approx 7,625$  s, and (D) final measurement at the end of testing ( $t = 4.375$  hrs).

Figure 47. Post-wound filter wheel spectrum measurements #2–#5. Source: Oros and Alves (2018), S6 Figure.

Table 2. Filter wheel spectral analysis data. Source: Oros and Alves (2018), S1 Table.

	<b>Filter Type</b>	<b>N Total</b>	<b>Mean</b>	<b>SD</b>	<b>VAR</b>
<b><i>Pre-Wound</i></b>	SP600	222	4	3	7
	LP600	237	35	18	328
	LP650	235	35	18	318
	LP700	234	24	12	155
	(O) Open	255	34	19	356
	(B) Black	800	4	3	10
<b><i>Wound</i></b>	SP600	90	4	2	5
	LP600	99	41	11	117
	LP650	97	42	10	109
	LP700	95	27	10	93
	(O) Open	90	39	12	134
	(B) Black	668	4	3	9

## LIST OF REFERENCES

- Abeles, F. B. (1986). Plant chemiluminescence. *Annual Review of Plant Physiology*, 37, 49–72.
- Abeles, F., Leather, G., & Forrence, L. (1978). Plant chemiluminescence. *Plant Physiology*, 62, 696–698.
- Akhter, S., Bailey, B. A., Salamon, P., Aziz, R. K., & Edwards, R. A. (2013). Applying Shannon's information theory to bacterial and phage genomes and metagenomes. *Scientific Reports*, 3, 1–7. <https://doi.org/10.1038/srep01033>
- Akoumianaki-Ioannidou, A., Georgakopoulos, J. H., Fasseas, C., & Argyroudi-Akoyunoglou, J. H. (2004). Photoacclimation in *Spathiphyllum*. *Journal of Photochemistry and Photobiology B: Biology*, 73(3), 149–158. <https://doi.org/10.1016/j.jphotobiol.2003.11.007>
- Arquilla, J., & Ronfeldt, D. (1997). Ch. 6. Information, power, and grand strategy: In Athena's camp - Section 1. In *In Athena's camp: Preparing for conflict in the information age* (Vol. 1, pp. 141–171). Santa Monica, CA: RAND Corp. Retrieved from [https://rand.org/pubs/monograph\\_reports/MR880.html](https://rand.org/pubs/monograph_reports/MR880.html)
- Ashby, W. R. (1956). *An introduction to cybernetics*. Chapman & Hall LTD (Second, Vol. 80). London: Chapman & Hall. <https://doi.org/10.2307/3006723>
- Bajpai, R. (1999). Coherent nature of the radiation emitted in delayed luminescence of leaves. *Journal of Theoretical Biology*, 198(3), 287–299. <https://doi.org/10.1006/jtbi.1999.0899>
- Bajpai, R. P. (2004). Biophoton emission in a squeezed state from a sample of *Parmelia tinctorum*, 322, 131–136. <https://doi.org/10.1016/j.physleta.2003.12.050>
- Bajpai, R. P. (2005). Squeezed state description of spectral decompositions of a biophoton signal, 337, 265–273. <https://doi.org/10.1016/j.physleta.2005.01.079>
- Bajpai, R. P. (2008). Quantum nature of photon signal emitted by *Xanthoria parietina* and its implications to biology, 46(May), 420–432.
- Bates, M. J. (1999). The invisible substrate of information science. *Journal of the American Society for Information Science: The 50th Anniversary of The Journal of the American Society for Information Science. Part 2: Paradigms, Models, and Methods of Information Science*, 50(12), 1043–1050. [https://doi.org/10.1002/\(SICI\)1097-4571\(1999\)50:12<1043::AID-ASII>3.0.CO;2-X](https://doi.org/10.1002/(SICI)1097-4571(1999)50:12<1043::AID-ASII>3.0.CO;2-X)



- Battail, G. (2006). Should genetics get an information-theoretic education? *IEEE Engineering in Medicine and Biology Magazine*, (February), 34–45.
- Bi, C., & Rogan, P. K. (2004). Information theory as a model of genomic sequences. In S. Subramaniam (Ed.), *Encyclopedia of genetics, genomics, proteomics and Bioinformatics* (October). John Wiley & Sons, Inc. <https://doi.org/10.1002/047001153X.g402204>
- Birtic, S., Ksas, B., Genty, B., Mueller, M. J., Triantaphylidès, C., & Havaux, M. (2011). Using spontaneous photon emission to image lipid oxidation patterns in plant tissues. *Plant Journal*, 67(6), 1103–1115. <https://doi.org/10.1111/j.1365-313X.2011.04646.x>
- Boveris, A., Cadenas, E., & Chance, B. (1980). Low-level chemiluminescence of the lipoygenase reaction. *Photobiochemistry and Photobiophysics*, 1(3), 175–182.
- Brenner, E. D., Stahlberg, R., Mancuso, S., Vivanco, J., Baluška, F., & Van Volkenburgh, E. (2006). Plant neurobiology: an integrated view of plant signaling. *Trends in Plant Science*, 11(8), 413–419. <https://doi.org/10.1016/j.tplants.2006.06.009>
- Brilli, F., Ruuskanen, T. M., Schnitzhofer, R., Müller, M., Breitenlechner, M., Bittner, V., ... Hansel, A. (2011). Detection of plant volatiles after leaf wounding and darkening by proton transfer reaction “time-of-flight” mass spectrometry (PTR-TOF). *PLoS ONE*, 6(5). <https://doi.org/10.1371/journal.pone.0020419>
- Buttler, W. L. (1962). Effects of red and far-red light on the fluorescence yield of chlorophyll in vivo. *Biochimica et Biophysica Acta.*, 64(2), 309–317.
- Chen, J., Mcconnell, D. B., Henny, R. J., Everitt, K. C., & Anthurium, I. (2003). *Cultural guidelines for commercial production of interiorscape Spathiphyllum*. Document ENH958. Retrieved from <http://edis.ifas.ufl.edu/ep161>
- Cifra, M., & Pospíšil, P. (2014). Ultra-weak photon emission from biological samples: Definition, mechanisms, properties, detection and applications. *Journal of Photochemistry and Photobiology B : Biology*, 139, 2–10. <https://doi.org/10.1016/j.jphotobiol.2014.06.013>
- Colli, L., Facchini, U., & Guidotti, G. (1955). Further measurements on the bioluminescence of the seedlings. *Experientia*, 11(12), 479–481.
- Cordón, G. B., & Lagorio, M. G. (2006). Re-absorption of chlorophyll fluorescence in leaves revisited. A comparison of correction models. *Photochemical & Photobiological Sciences*, 5(8), 735–740. <https://doi.org/10.1039/B517610G>

- Creath, K. (2008). A look at some systemic properties of self-bioluminescent emission. In *Proceedings of SPIE* (Vol. 7057, p. 705708 1–11). <https://doi.org/10.1117/12.800667>
- Creath, K., & Schwartz, G. E. (2005). Biophoton interaction in biological systems: evidence of photonic info-energy transfer? *Proceedings of SPIE*, 5866, 338–347. <https://doi.org/10.1117/12.620846>
- Evans, J. R., von Caemmerer, S. (2018). *Light use and leaf gas exchange: Chapter 1*, In R. Munns, S. Schmidt, & C. Beveridge (Eds.), *Plants in Action*. (2d ed.). New Zealand: Australian Society of Plant Scientists. Retrieved from <http://plantsinaction.science.uq.edu.au>
- Fall, R., Hansel, A., Jordan, A., & Lindinger, W. (1999). Volatile organic compounds emitted after leaf wounding: On-line analysis by proton-transfer-reaction mass spectrometry. *Journal of Geophysical Research*, 104(D13), 15,963-15,974. <https://doi.org/10.1029/1999JD900144>
- Flor-Henry, M., McCabe, T. C., de Bruxelles, G. L., & Roberts, M. R. (2004). Use of a highly sensitive two-dimensional luminescence imaging system to monitor endogenous bioluminescence in plant leaves. *BMC Plant Biology*, 4, 19. <https://doi.org/10.1186/1471-2229-4-19>
- Floridi, L. (2017). Semantic conceptions of information. In E. N. Zalta (Ed.), *The Stanford Encyclopedia of Philosophy* (Spring 2017 Edition), Retrieved from <https://plato.stanford.edu/archives/spr2017/entries/information-semantic/>
- Flors, C., Fryer, M. J., Waring, J., Reeder, B., Bechtold, U., Mullineaux, P. M., ... Baker, N. R. (2006). Imaging the production of singlet oxygen in vivo using a new fluorescent sensor, Singlet Oxygen Sensor Green®. *Journal of Experimental Botany*, 57(8), 1725–1734. <https://doi.org/10.1093/jxb/erj181>
- Frické, M. (2009). The knowledge pyramid: A critique of the DIKW hierarchy. *Journal of Information Science*, 35(2), 131–142. <https://doi.org/10.1177/0165551508094050>
- Frohlich, H. (1970). Long range coherence and the action of enzymes imprint: *Nature*, 228(5276), 1093.
- Garfield, E. (1986). The metaphor-science connection. *Essays of an Information Scientist: Current Comments*, 9(42), 316–323. Retrieved from <http://garfield.library.upenn.edu/essays/v9p316y1986.pdf>
- Gasanov, R. A., Mamedov, T. G., Tarusov, B. N. (1963). Spontaneous induction of luminescence in plants under aerobic and anaerobic conditions. *Soviet Physics.Doklady*, 8, 619–621. <https://doi.org/10.1002/mus.25389>

- Godfrey-Smith, P. (2007). Information in biology. In D. Hull and M. Ruse (Eds.), *The Cambridge Companion to the Philosophy of Biology* (pp. 103–119). Cambridge University Press.
- Godfrey-Smith, P., & Sterelny, K. (2016). Biological Information. In E. N. Zalta (Ed.) *The Stanford Encyclopedia of Philosophy*. (Summer 2016 Edition), Retrieved from <https://plato.stanford.edu/archives/sum2016/entries/information-biological/>
- Gurwitch, A. (1925). The mitogenetic rays. *Botanical Gazette*, 80(2), 224–226. Retrieved from <http://www.jstor.org/stable/2470608> .
- Gurwitsch, A. A. (1988). A historical review of the problem of mitogenetic radiation. *Experientia*, 44(7), 545–550.
- Hamamatsu Photonics. (2018a). Metal package PMT with cooler: Photosensor modules H7422 series. Retrieved from <https://www.hamamatsu.com/resources/pdf/etd/m-h7422e.pdf>
- Hamamatsu Photonics. (2018b). Photon counter: USB interface compatible counting unit C8855-01. Retrieved from [https://www.hamamatsu.com/resources/pdf/etd/C8855-01\\_TACC1078E.pdf](https://www.hamamatsu.com/resources/pdf/etd/C8855-01_TACC1078E.pdf)
- Hamamatsu Photonics. (2005). H7422/H7422P series photo sensor module instruction manual. Hamamatsu Photonics K. K., Electron Tube Center, JA
- Hameroff, S. R., & Penrose, R. (2014). Consciousness in the universe: A review of the “Orch OR” theory. *Physics of Life Reviews*, 11(1), 39–78. <https://doi.org/10.1016/j.plrev.2013.08.002>
- Hameroff, S. R. (1988). Coherence in the Cytoskeleton: Implications for biological information processing. In H. Fröhlich (Ed), *Biological coherence and response to external stimuli*, (pp. 242–265). Berlin-Heidelberg. [https://doi.org/https://doi.org/10.1007/978-3-642-73309-3\\_14](https://doi.org/https://doi.org/10.1007/978-3-642-73309-3_14)
- Hideg, É., Juhász, M., Bornman, J. F., & Asada, K. (2002). The distribution and possible origin of blue–green fluorescence in control and stressed barley leaves. *Photochemical & Photobiological Sciences*, 1(12), 934–941. <https://doi.org/10.1039/B201916G>
- Hideg, É., Scott, R. Q., & Inaba, H. (1989). High resolution emission spectra of one second delayed fluorescence from chloroplasts. *Federation of European Biochemical Societies Letters*, 250(2), 275–279. [https://doi.org/10.1016/0014-5793\(89\)80737-9](https://doi.org/10.1016/0014-5793(89)80737-9)
- Inform, (n.d.). In Oxford English Dictionary. Retrieved from <http://www.oed.com/view/Entry/95559?rskey=sM2Hfo&result=1&isAdvanced=true>

- Information, (n.d.). In Oxford English Dictionary. Oxford University Press. Retrieved from <http://www.oed.com/view/Entry/95568?redirectedFrom=information&>
- International Laboratory of Plant Neurobiology. (n.d.). Retrieved from <http://www.linv.org/about-us/>
- Ives, J. A., van Wijk, E. P. A., Bat, N., Crawford, C., Walter, A., Jonas, W. B., ... van der Greef, J. (2014). Ultraweak photon emission as a non-invasive health assessment: A systematic review. *PLoS ONE*, *9*(2). <https://doi.org/10.1371/journal.pone.0087401>
- Kato, K., Iyozumi, H., Kageyama, C., Inagaki, H., & Yamaguchi, A. (2014). Application of ultra-weak photon emission measurements in agriculture. *Journal of Photochemistry & Photobiology, B: Biology*, *139*, 54–62. <https://doi.org/10.1016/j.jphotobiol.2014.06.010>
- Knight, K. R., & Collins, P. (2011, July). The Face of a Frog : Time-lapse Video Reveals Never-Before-Seen Bioelectric Pattern. *TuftsNow*. Retrieved from <https://now.tufts.edu/news-releases/face-frog-time-lapse-video-reveals-never-seen>
- Kuhn, T. (1993). Metaphor in Science. In A. Ortony (Ed.), *Metaphor and Thought* (2d ed., pp. 533–542). Cambridge, UK: Cambridge University Press.
- Lagorio, M. G., Cordon, G. B., & Iriel, A. (2015). Reviewing the relevance of fluorescence in biological systems. *Photochemical & Photobiological Sciences*, *14*(9), 1538–1559. <https://doi.org/10.1039/C5PP00122F>
- Li, K. H., Popp, F. A., Nagl, W., & Klima, H. (1983). Indications of Optical Coherence in Biological Systems and Its Possible Significance. In H. Fröhlich and F. Kremer (Eds.), *Coherent excitations in biological systems I* (pp. 117–122). Berlin Heidelberg: Springer-Verlag.
- Lichtenthaler, H. K., Langsdorf, G., Lenk, S., & Buschmann, C. (2005). Chlorophyll fluorescence imaging of photosynthetic activity with the flash-lamp fluorescence imaging system. *Photosynthetica*, *43*(3), 355–369. Retrieved from <http://www.scopus.com/inward/record.url?eid=2-s2.0-26444522224&partnerID=40&md5=03efb0600d43176815c70c95fcc94e6a>
- Lichtenthaler, H. K., & Miede, J. A. (1997). Fluorescence imaging as a diagnostic tool for plant stress. *Trends in Plant Science*, *2*(8), 316–320. [https://doi.org/10.1016/S1360-1385\(97\)89954-2](https://doi.org/10.1016/S1360-1385(97)89954-2)
- Loreto, F., Barta, C., Brilli, F., & Nogues, I. (2006). On the induction of volatile organic compound emissions by plants as consequence of wounding or fluctuations of light and temperature. *Plant, Cell and Environment*, *29*(9), 1820–1828. <https://doi.org/10.1111/j.1365-3040.2006.01561.x>

- Machlup, F. (1983). Semantic Quirks in Studies of Information. In F. Machlup and U. Mansfield (Eds.), *The study of information: Interdisciplinary messages* (pp. 641–671). New York, NY: John Wiley & Sons.
- Matsui, K., Sugimoto, K., Mano, J., Ozawa, R., & Takabayashi, J. (2012). Differential metabolisms of green leaf volatiles in injured and intact parts of a wounded leaf meet distinct ecophysiological requirements. *PLoS ONE*, 7(4), 1–10. <https://doi.org/10.1371/journal.pone.0036433>
- Miller, J. G. (1978). *Living systems*. New York, NY: McGraw Hill.
- Misra, A. N., Misra, M., & Singh, R. (2012). *Chlorophyll fluorescence in plant biology*. (A. N. Misra, Ed.). InTech. <https://doi.org/10.5772/35111>
- Mochizuki, S., Sugimoto, K., Koeduka, T., & Matsui, K. (2016). Arabidopsis lipoxygenase 2 is essential for formation of green leaf volatiles and five-carbon volatiles. *Federation of European Biochemical Societies Letters*, 590(7), 1017–1027. <https://doi.org/10.1002/1873-3468.12133>
- Morker, K. H., & Roberts, M. R. (2011). Light as both an input and an output of wound-induced reactive oxygen formation in Arabidopsis leaves. *Plant Signaling & Behavior*, 6(8), 1087–1089. <https://doi.org/10.4161/psb.6.8.15823>
- Mukerji, I., & Sauer, K. (1993). Energy transfer dynamics of an isolated light harvesting complex of Photosystem I from spinach: time-resolved fluorescence measurements at 295 K and 7. *Biochimica et Biophysica Acta.*, 1142(3), 311–320.
- Oros, C. L., Alves, F. (2018). Leaf wound induced ultraweak photon emission is suppressed under anoxic stress: Observations of *Spathiphyllum* under aerobic and anaerobic conditions using novel *in vivo* methodology. *PLoS ONE* 13(6): e0198962. <https://doi.org/10.1371/journal.pone.0198962>
- Parker, E., & United States. National Commission on Libraries and Information Science. (1973). *Information and society: A report to the national commission on libraries and information science* (Ed 073 776). Washington, D.C: National Commission on Libraries and Information Science; prepared by ERIC Document Reproduction Service, Bethesda, Md. (1973).
- Pedrós, R., Moya, I., Goulas, Y., & Jacquemoud, S. (2008). Chlorophyll fluorescence emission spectrum inside a leaf. *Photochemical & Photobiological Sciences*, 7(4), 498. <https://doi.org/10.1039/b719506k>
- Pokorny, J. (2009). Frohlich's coherent vibrations in healthy and cancer cells. *Neural Network World*, 4(9), 369–378.
- Popp, F. A., Li, K. H., Mei, W. P., Galle, M., Neurohr, R. (1988). Physical aspects of biophotons. *Experientia*, 44, 576–585.

- Popp, F. A., Gurwitsch, A. A., Inaba, H., Slawinski, J., Cilento, G., Van Wijk, R., Schamhart, D. (1988). Biophoton emission: A multi-author review. *Experientia*, 44(7), 543–600.
- Popp, F. A. (2003a). Biophotons - background, experimental results. Theoretical approach and application. In F. A. Popp & L. Belousov (Eds.), *Integrative Biophysics: Biophotonics* (3d ed., pp. 387–438). Netherlands: Kluwer Academic Publishers.
- Popp, F. A. (2003b). Properties of biophotons and their theoretical implications. *Indian Journal of Experimental Biology*, 41(May), 391–402.
- Popp, F. A., Gu, Q., & Li, K.-H. (1994). *Biophoton emission: Experimental background and theoretical approaches*. *Modern Physics Letters B* (Vol. 08). <https://doi.org/10.1142/S0217984994001266>
- Popp, F. A., Ruth, B., Bahr, W., Bohm, J., Grass, P., Grolig, G., ... Wulle, P. (1981). Emission of visible and ultraviolet radiation by active biological systems. *Collective Phenomena.*, 3, 187–214.
- Pospíšil, P., Prasad, A., & Rác, M. (2014). Role of reactive oxygen species in ultra-weak photon emission in biological systems. *Journal of Photochemistry and Photobiology B: Biology*, 139, 11–23. <https://doi.org/10.1016/j.jphotobiol.2014.02.008>
- Prasad, A., & Pospíšil, P. (2011). Linoleic acid-induced ultra-weak photon emission from *Chlamydomonas reinhardtii* as a tool for monitoring of lipid peroxidation in the cell membranes. *PLoS ONE*, 6(7). <https://doi.org/10.1371/journal.pone.0022345>
- Prasad, A., Sedlářová, M., Kale, R. S., & Pospíšil, P. (2017). Lipoxygenase in singlet oxygen generation as a response to wounding: In vivo imaging in *Arabidopsis thaliana*. *Scientific Reports*, 7(1), 9831. <https://doi.org/10.1038/s41598-017-09758-1>
- Racine, D., Rastogi, A., & Bajpai, R. P. (2013). Hints at quantum characteristics of light signals measured from a human subject, 2013(September). <https://doi.org/10.4236/cm.2013.43>
- Radotic, K., Radenovic, C., & Jeremic, M. (1998). Spontaneous ultraweak bioluminescence in plants: Origin, mechanisms and properties. *General Physiology Biophysics*, 17, 289–308. Retrieved from <http://www.pubmedcentral.nih.gov/articlerender.fcgi?artid=3260698&tool=pmcentrez&rendertype=abstract>
- Roschger, P., Devaraj, B., Scott, R. Q., & Inaba, H. (1992). Induction of a transient enhancement of low level chemiluminescence in intact leaves by anaerobic treatment. *Photochemistry and Photobiology*, 56(2), 281–284.

- Rowley, J. (2007). The wisdom hierarchy: Representations of the DIKW hierarchy. *Journal of Information Science*, 33(2), 163–180. <https://doi.org/10.1177/0165551506070706>
- Rubik, B. (2002). The biofield hypothesis: Its biophysical basis and role in medicine. *Journal of Alternative And Complementary Medicine*, 8(6), 703–717. <https://doi.org/10.1089/10755530260511711>
- Sauermann, G., Mei, P. W., Hoppe, U., & Stab, F. (1999). Ultraweak photon emission of human skin in vivo: Influence of topically applied antioxidants on human skin. *Methods In- Enzymology*, 300, 419–428.
- Schneider, T. D. (2006). Claude Shannon: Biologist. *IEEE Engineering in Medicine and Biology Magazine*, (January/February), 30–33.
- Schneider, T. D., & Mastrorarde, D. N. (1996). Fast multiple alignment of ungapped DNA sequences using information theory and a relaxation method. *Discrete Applied Mathematics*, 71(1–3), 259–268. [https://doi.org/10.1016/S0166-218X\(96\)00068-6](https://doi.org/10.1016/S0166-218X(96)00068-6)
- Schwabl, H., & Klima, H. (2005). Spontaneous ultraweak photon emission from biological systems and the endogenous light field. *Forsch Komplementarmed Klass Natureheilkd*, 12(2), 84–89. <https://doi.org/DOI: 10.1159/000083960>
- Shannon, C. E. (1948). A mathematical theory of communication. *The Bell System Technical Journal*, 27, 379–423, 623–656, Jul, Oct. <https://doi.org/10.1002/j.1538-7305.1948.tb01338.x>
- Shannon, C. E., & Weaver, W. (1963). *The mathematical theory of communication*. Urbana and Chicago: University of Illinois Press.
- Shen, X., Liu, F., Li, X. Y. (1993). Experimental study on photocount statistics of the ultraweak photon emission from some living organisms. *Experientia*, 49(4), 291–295.
- Shen, X. (2003). Detection of photon emission from biological systems. In F. A Popp and L. Belousov (Eds.), *Integrative Biophysics* (pp. 287–305). Netherlands: Kluwer Academic Publishers.
- Slawinska, D., & Slawinski, J. (1983). Biological chemiluminescence. *Photochemistry and Photobiology*, 37(6), 709–771. <https://doi.org/10.1111/j.1751-1097.1983.tb04544.x>
- Tuomi, I. (1999). Data is more than knowledge: Implications of the reversed knowledge hierarchy for knowledge management and organizational memory. *Journal of Management Information Systems*, 16(3), 103–117.

- ul Hassan, M. N., Zainal, Z., & Ismail, I. (2015). Green leaf volatiles: Biosynthesis, biological functions and their applications in biotechnology. *Plant Biotechnology Journal*, 13(6), 727–739. <https://doi.org/10.1111/pbi.12368>
- Unlocking the bioelectric code. (2013). Retrieved from [http://www.whatayear.org/06\\_13.php](http://www.whatayear.org/06_13.php)
- Van Wijk, R. (2001). Bio-photons and bio-communication. *Journal of Scientific Exploration*, 15(2), 183–197.
- Vandenberg, L. N., Morrie, R. D., & Adams, D. S. (2011). V-ATPase-dependent ectodermal voltage and Ph regionalization are required for craniofacial morphogenesis. *Developmental Dynamics*, 240(8), 1889–1904. <https://doi.org/10.1002/dvdy.22685>
- Vartapetian, B. B. (2005). Plant anaerobic stress as a novel trend in ecological physiology, biochemistry, and molecular biology: 1. Establishment of a new scientific discipline. *Russian Journal of Plant Physiology*, 52(6), 826–844. <https://doi.org/10.1007/s11183-005-0122-6>
- Vartapetian, B. B. (2015). Plant anaerobic stress as a novel avenue of research in ecological biology and biotechnology. In I. I. Norkin (Ed.) (pp. 1–130). Moscow.
- Vartapetian, B. B., Agapova, L. P., Averianov, A. A., & Veselovsky, V. (1974). New approach to study of oxygen transport in plants using chemiluminescent method. *Nature*, (454), 269.
- Vartapetian, B. B., & Jackson, M. B. (1997). Plant adaptations to anaerobic stress. *Annals of Botany*, 79(suppl 1), 3–20. <https://doi.org/10.1093/oxfordjournals.aob.a010303>
- Veselovskii, V. A., Sekamova, E. N., Tarusov, V. N. (1963). Mechanism of ultra weak spontaneous luminescence of organisms. *Biofizika*, 8(1), 125–127.
- Voeikov, V. L., & Belousov, L. V. (2007). From mitogenetic rays to biophotons. In L. Belousov, V. L. Voeikov, & V. S. Martynyuk (Eds.), *Biophotonics and Coherent Systems in Biology*. New York, NY: Springer Science+Business Media, LLC.
- von Bertalanffy, L. (1969). *General systems theory: Foundations, development, applications*. New York, NY: George Braziller, Inc.
- Wei, J., Wang, L., Zhu, J., Zhang, S., Nandi, O. I., & Kang, L. (2007). Plants attract parasitic wasps to defend themselves against insect pests by releasing hexenol. *PLoS ONE*, 2(9), 1–7. <https://doi.org/10.1371/journal.pone.0000852>
- Winkler, R., Guttenberger, H., & Klima, H. (2009). Ultraweak and induced photon emission after wounding of plants. *Photochemistry and Photobiology*, 85(4), 962–965. <https://doi.org/10.1111/j.1751-1097.2009.00537.x>



- Wu, P., & He, X. (2009). Research on the ultraweak photon emission from anti-cancer plants. *Journal of Biomedical Science & Engineering*, (June), 155–157.  
<https://doi.org/10.4236/jbise.2009.23026>
- Yang, D. S., Son, K. C., & Kays, S. J. (2009). Volatile organic compounds emanating from indoor ornamental plants. *American Society for Horticultural Science*, 44(2), 396–400.

## INITIAL DISTRIBUTION LIST

1. Defense Technical Information Center  
Ft. Belvoir, Virginia
2. Dudley Knox Library  
Naval Postgraduate School  
Monterey, California